

DTIC FILE COPY

4

NSWC TR 86-108

# PROTOTYPE RECHARGEABLE LITHIUM BATTERIES

BY W. B. EBNER AND H. W. LIN  
(HONEYWELL POWER SOURCES CENTER)

EDITED AND REVIEWED BY DR. P. H. SMITH AND DR. S. D. JAMES (NSWC)

FOR NAVAL SURFACE WARFARE CENTER  
RESEARCH AND TECHNOLOGY DEPARTMENT

JUNE 1987

AD-A199 463

Approved for public release; distribution is unlimited.

DTIC  
ELECTE  
SEP 27 1988  
S D  
H



## NAVAL SURFACE WARFARE CENTER

Dahlgren, Virginia 22448-5000 • Silver Spring, Maryland 20903-5000

88 9 26 207

UNCLASSIFIED

SECURITY CLASSIFICATION OF THIS PAGE

REPORT DOCUMENTATION PAGE				
1a. REPORT SECURITY CLASSIFICATION UNCLASSIFIED		1b. RESTRICTIVE MARKINGS		
2a. SECURITY CLASSIFICATION AUTHORITY		3. DISTRIBUTION/AVAILABILITY OF REPORT Approved for public release; distribution is unlimited.		
2b. DECLASSIFICATION/DOWNGRADING SCHEDULE				
4. PERFORMING ORGANIZATION REPORT NUMBER(S)		5. MONITORING ORGANIZATION REPORT NUMBER(S) NSWC TR 86-108		
6a. NAME OF PERFORMING ORGANIZATION Honeywell Power Sources Center	6b. OFFICE SYMBOL (If applicable)	7a. NAME OF MONITORING ORGANIZATION Naval Surfaces Warfare Center (Code R33)		
6c. ADDRESS (City, State, and ZIP Code) 104 Rock Road Horsham, PA 19044		7b. ADDRESS (City, State, and ZIP Code) 10901 New Hampshire Avenue Silver Spring, MD 20903-5000		
8a. NAME OF FUNDING/SPONSORING ORGANIZATION	8b. OFFICE SYMBOL (If applicable)	9. PROCUREMENT INSTRUMENT IDENTIFICATION NUMBER N60921-84-C-0029		
8c. ADDRESS (City, State, and ZIP Code)		10. SOURCE OF FUNDING NUMBERS		
		PROGRAM ELEMENT NO. 62314N	PROJECT NO. 0	TASK NO. RJ14Y41
11. TITLE (Include Security Classification) Prototype Rechargeable Lithium Batteries				
12. PERSONAL AUTHOR(S) Ebner, W.B. and Lin, H.W.				
13a. TYPE OF REPORT Final - Phase I	13b. TIME COVERED FROM 8/84 TO 1/86	14. DATE OF REPORT (Year, Month, Day) 1987 June	15. PAGE COUNT 145	
16. SUPPLEMENTARY NOTATION Edited and reviewed by Dr. P. H. Smith and Dr. S. D. James (NSWC)				
17. COSATI CODES			18. SUBJECT TERMS (Continue on reverse if necessary and identify by block number)	
FIELD	GROUP	SUB-GROUP	Rechargeable Lithium Cells      Organic Electrolyte Solutions	
07	04		Ester Solvents                      Low Temperature	
			Insertion Cathode Materials      High Rate Capabilities	
19. ABSTRACT (Continue on reverse if necessary and identify by block number)				
<p>This report details the work performed on Phase I of an overall two-phase program. The aim of Phase I is to select a room-temperature lithium (Li) rechargeable couple that offers high energy density (60-90 Wh/lb), good rate capability (C/6-C/1), and low temperature operability.</p> <p>Among the four cathode systems investigated - <math>V_2O_5</math>, <math>TiS_2</math>, <math>V_2S_5</math> and <math>Li_xCoO_2</math> - the <math>Li/V_2O_5</math> couple emerged as the best performer capable of meeting the performance goals described above. The other three cathode systems were dropped from further development during the course of the program because of their general instability with ester-based electrolytes, especially the methyl formate (MF)-based electrolyte. The MF-based electrolyte was selected because of its superior conductivity which is essential for rate capability and low temperature operability.</p> <p style="text-align: right;">(Cont.)</p>				
20. DISTRIBUTION/AVAILABILITY OF ABSTRACT <input type="checkbox"/> UNCLASSIFIED/UNLIMITED <input checked="" type="checkbox"/> SAME AS RPT. <input type="checkbox"/> DTIC USERS		21. ABSTRACT SECURITY CLASSIFICATION UNCLASSIFIED		
22a. NAME OF RESPONSIBLE INDIVIDUAL Dr. Patricia Smith		22b. TELEPHONE (Include Area Code) (202) 394-2948	22c. OFFICE SYMBOL R33	

DD FORM 1473, 84 MAR

83 APR edition may be used until exhausted.  
All other editions are obsolete.

SECURITY CLASSIFICATION OF THIS PAGE

UNCLASSIFIED

**SECURITY CLASSIFICATION OF THIS PAGE**

19. (Cont.)

Specifically, the technical accomplishments of Phase I can be stated as follows:

- o An electrolyte formulation composed of 2M LiAsF<sub>6</sub> + 0.4 LiBF<sub>4</sub>/methyl formate saturated with CO<sub>2</sub> was successfully developed with the following demonstrated capabilities:
    - High Conductivity - 43 mmho/cm at room temperature and 13 mmho/cm at -40°C. This solution at -40°C is still three times more conductive than the more commonly used ether-based solution (e.g., LiAsF<sub>6</sub>/2-methyl tetrahydrofuran (THF)) at ambient temperature.
    - 93% Lithium Cycling Efficiency - this lithium efficiency enables the use of methyl formate-based solution in practical hardware. Li/V<sub>2</sub>O<sub>5</sub> cell cyclability up to 50 cycles can be projected at the 100% depth of discharge based on Li/V<sub>2</sub>O<sub>5</sub> ratio of 3:1.
  - o Li/V<sub>2</sub>O<sub>5</sub> cyclability surpassing 100 cycles in laboratory cells - cycled cell capacity can be held at a level corresponding to 80% cathode discharge efficiency. The ability to achieve this high level of cathode utilization is due to our focused development of the cathode processing technology. Particle size of the V<sub>2</sub>O<sub>5</sub> was found to be key to enhanced cell performance and electrode integrity was critical to achieving cyclability without degrading cell capacity.
- Li/V<sub>2</sub>O<sub>5</sub> laboratory cell produces 366 Wh/kg based on lithium and active cathode material (or 166 Wh/lb) at the 100th cycle when tested at room temperature. Using this value, practical energy densities of 50 Wh/lb and 60 Wh/lb can be projected for "D" cell and No. 6 size cell, respectively.
- o Discharge current density surpassing 5 mA/cm<sup>2</sup> - at average 55% cathode discharge efficiency for 205 cycles - this allows addressing application of the Li/V<sub>2</sub>O<sub>5</sub> technology in missions requiring rate capability up to C/1.3.

Phase I of this program, therefore, successfully selected a rechargeable technology (Li/V<sub>2</sub>O<sub>5</sub>) that is ready for transitioning to a hardware development phase. Phase I demonstrated overall performance capabilities of the Li/V<sub>2</sub>O<sub>5</sub> technology at the laboratory cell level, and the objective of Phase II is to further improve and demonstrate the stated capabilities of Li/V<sub>2</sub>O<sub>5</sub> cell at the hardware level via a 30 Ah cell.

<b>Accession For</b>	
NTIS GRA&I	<input checked="" type="checkbox"/>
DTIC TAB	<input type="checkbox"/>
Unannounced	<input type="checkbox"/>
Justification	
By _____	
Distribution/	
Availability Codes	
Dist	Avail and/or Special
A-1	

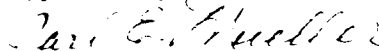


## FOREWORD

The development of a reliable rechargeable lithium battery technology having high rate capabilities and low temperature operability has become a major priority throughout the Department of Defense. In recent years, considerable progress has been made in ambient temperature lithium/secondary technology. However, this technology has not produced a practical Li/secondary cell nor have high rate or low temperature performance capabilities been demonstrated. To meet the demanding performance goals for naval applications, such as torpedo targets and seal delivery vehicles, significant advances are needed over the current state-of-the-art capabilities. To achieve these advances, Honeywell under the direction of the Electrochemistry Branch, R33, is developing an ester-based rechargeable technology that has the capability for both high rate and low temperature operations.

The authors acknowledge the assistance of P. Lensi in carrying out the cathode material syntheses, Dr. Wayne Worrell of The University of Pennsylvania for his consultation on cathode material structures, and Mrs. S.P.S. Yen of the Jet Propulsion Laboratory for her helpful discussions on  $TiS_2$ . The authors are also indebted to Dr. P. H. Smith and Dr. S.D. James of NSWC for their technical guidance, program direction, and continued support throughout the course of this work. This work was sponsored by the Office of Naval Technology under the Mine and Special Warfare Technology Block NS3B.

Approved by:



CARL E. MUELLER, Head  
Materials Division

## CONTENTS

<u>Chapter</u>		<u>Page</u>
1	INTRODUCTION.....	1-1
2	EXPERIMENTAL.....	2-1
	EXPERIMENTAL CELL DESCRIPTIONS.....	2-1
	CATHODE MANUFACTURING TECHNIQUES.....	2-1
	CATHODE MATERIAL SYNTHESIS AND CHARACTERIZATION.....	2-5
	ELECTROLYTE SOLUTIONS.....	2-9
	LITHIUM CYCLING EFFICIENCY MEASUREMENTS.....	2-10
	THERMAL STABILITY TESTS.....	2-10
3	RESULTS AND DISCUSSION.....	3-1
	CATHODE SELECTION STUDIES.....	3-1
	CATHODE MATERIAL CHARACTERIZATION TESTS.....	3-2
	CYCLE LIFE TESTS.....	3-29
	THERMAL STABILITY TESTS.....	3-53
	LITHIUM CYCLING EFFICIENCY MEASUREMENTS.....	3-56
	SCREENING STUDIES SUMMARY.....	3-88
	V <sub>2</sub> O <sub>5</sub> CATHODE PROCESSING STUDIES.....	3-91
	V <sub>2</sub> O <sub>5</sub> ROLL MILLED CATHODE OPTIMIZATION STUDIES.....	3-95
	V <sub>2</sub> O <sub>5</sub> PERFORMANCE DEMONSTRATION.....	3-104
4	CONCLUSIONS.....	4-1
	REFERENCES.....	5-1
	DISTRIBUTION.....	(1)

## ILLUSTRATIONS

<u>Figure</u>	<u>Page</u>
1-1 CONDUCTIVITY VERSUS TEMPERATURE DATA SHOWING SUPERIOR CONDUCTIVITIES OFFERED BY ESTER-BASED ELECTROLYTE SOLUTIONS.....	1-3
1-2 DISCHARGE PERFORMANCE OF Li/TiS <sub>2</sub> CELLS SHOWING THE DRAMATIC IMPROVEMENT IN RATE CAPABILITIES THAT CAN BE REALIZED USING HIGH CONDUCTIVITY ESTER-BASED SOLUTIONS OVER EXISTING STATE-OF-THE-ART SYSTEMS.....	1-4
1-3 DISCHARGE PERFORMANCE OF Li/V <sub>2</sub> O <sub>5</sub> AND Li/TiS <sub>2</sub> CELLS SHOWING THE EXCELLENT RATE CAPABILITIES THAT CAN BE ACHIEVED USING HIGH CONDUCTIVITY ESTER-BASED ELECTROLYTE SOLUTIONS WITH INSERTION-TYPE CATHODE MATERIALS.....	1-5
2-1 HALF-CELL ELECTRODE HOLDER.....	2-2
2-2 LABORATORY 2-PLATE WICK CELL HARDWARE .....	2-3
3-1 PARTICLE SIZE DISTRIBUTIONS FOR V <sub>2</sub> O <sub>5</sub> (LOTS CML-V2-001 AND CML-V2-003) .....	3-3
3-2 PARTICLE SIZE DISTRIBUTION FOR V <sub>2</sub> O <sub>5</sub> (LOT CML-V2-001) AND THE NH <sub>4</sub> VO <sub>3</sub> USED IN ITS PREPARATION.....	3-4
3-3 SCANNING ELECTRON MICROGRAPHS OF V <sub>2</sub> O <sub>5</sub> (LOT CML-V2-001).....	3-6
3-4 ELECTROCHEMICAL PERFORMANCE CHARACTERIZATION OF V <sub>2</sub> O <sub>5</sub> .....	3-10
3-5 PARTICLE SIZE DISTRIBUTION FOR TiS <sub>2</sub> (DEGUSSA, AS-RECEIVED).....	3-12
3-6 SCANNING ELECTRON MICROGRAPHS OF TiS <sub>2</sub> (DEGUSSA, AS-RECEIVED).....	3-13
3-7 ELECTROCHEMICAL PERFORMANCE CHARACTERIZATION OF DEGUSSA TiS <sub>2</sub> .....	3-15
3-8 SCANNING ELECTRON MICROGRAPHS OF (NH <sub>4</sub> ) <sub>3</sub> VS <sub>4</sub> AND THE V <sub>2</sub> S <sub>5</sub> PREPARED AT 260°C (LOT CML-VS-002).....	3-16
3-9 ELECTROCHEMICAL PERFORMANCE CHARACTERIZATION OF V <sub>2</sub> S <sub>5</sub> .....	3-18
3-10 PARTICLE SIZE DISTRIBUTION FOR Li <sub>x</sub> CoO <sub>2</sub> (LOT CML-CO-002).....	3-20
3-11 SCANNING ELECTRON MICROGRAPHS OF Li <sub>x</sub> CoO <sub>2</sub> (LOT CML-CO-002).....	3-21
3-12 ELECTROCHEMICAL PERFORMANCE CHARACTERIZATION OF Li <sub>x</sub> CoO <sub>2</sub> (LOT CML-CO-002, Li <sub>0.85</sub> Co <sub>0.97</sub> O <sub>2</sub> ).....	3-24
3-13 CHARGE-DISCHARGE PERFORMANCE OF A Li/Li <sub>x</sub> CoO <sub>2</sub> CELL WITH 2M LiAsF <sub>6</sub> + 0.4M LiBF <sub>4</sub> /MF SOLUTION (Li <sub>x</sub> CoO <sub>2</sub> = LOT CML-CO-002).....	3-26

## ILLUSTRATIONS (Cont.)

<u>Figure</u>	<u>Page</u>
3-14 CHARGE-DISCHARGE PERFORMANCE OF A Li/Li <sub>x</sub> CoO <sub>2</sub> CELL WITH 2M LiAsF <sub>6</sub> /MF SOLUTION (Li <sub>x</sub> CoO <sub>2</sub> = LOT CML-CO-002).....	3-27
3-15 CHARGE-DISCHARGE PERFORMANCE OF A Li/Li <sub>x</sub> CoO <sub>2</sub> CELL WITH 1.5M LiAsF <sub>6</sub> /MA SOLUTION (Li <sub>x</sub> CoO <sub>2</sub> = LOT CML-CO-002).....	3-28
3-16 V <sub>2</sub> O <sub>5</sub> SCREENING STUDIES: CYCLE LIFE PERFORMANCE WITH 2M LiAsF <sub>6</sub> + 0.4M LiBF <sub>4</sub> /MF SOLUTIONS.....	3-31
3-17 V <sub>2</sub> O <sub>5</sub> SCREENING STUDIES: CYCLE LIFE PERFORMANCE WITH 2M LiAsF <sub>6</sub> /MA SOLUTIONS.....	3-32
3-18 V <sub>2</sub> O <sub>5</sub> SCREENING STUDIES: CYCLE LIFE PERFORMANCE WITH 1M LiAsF <sub>6</sub> /DMSI SOLUTION.....	3-33
3-19 CHARGE/DISCHARGE BEHAVIOR OF Li/V <sub>2</sub> O <sub>5</sub> CELLS WITH 1.0M LiAsF <sub>6</sub> /DMSI SOLUTION AT AMBIENT (20-24°C) TEMPERATURE.....	3-34
3-20 TYPICAL DISCHARGE/CHARGE CURVE OF Li/V <sub>2</sub> O <sub>5</sub> LABORATORY CELLS IN 2M LiAsF <sub>6</sub> + 0.4M LiBF <sub>4</sub> /MF SOLUTIONS.....	3-35
3-21 TiS <sub>2</sub> SCREENING STUDIES: CYCLE LIFE PERFORMANCE WITH 2M LiAsF <sub>6</sub> + 0.4M LiBF <sub>4</sub> /MF SOLUTIONS.....	3-37
3-22 EXTENDED DISCHARGE PERFORMANCE OF A Li/TiS <sub>2</sub> CELL WITH A 2M LiAsF <sub>6</sub> + 0.4M LiBF <sub>4</sub> /MF ELECTROLYTE SOLUTION.....	3-38
3-23 CHARGE/DISCHARGE BEHAVIOR OF A Li/TiS <sub>2</sub> CELL WHEN CHARGED TO 3 VOLTS EMPLOYING A 2M LiAsF <sub>6</sub> + 0.4M LiBF <sub>4</sub> /MF ELECTROLYTE SOLUTION.....	3-39
3-24 X-RAY DIFFRACTION PATTERNS FOR TiS <sub>2</sub> CATHODES BEFORE AND AFTER EXTENDED CYCLING IN A 2M LiAsF <sub>6</sub> + 0.4M LiBF <sub>4</sub> /MF ELECTROLYTE SOLUTION (CHARGE/DISCHARGE RATE = 1.0 mA/cm <sup>2</sup> AT AMBIENT TEMPERATURE (20-24°C)).....	3-40
3-25 CHARGE/DISCHARGE BEHAVIOR OF A Li/TiS <sub>2</sub> CELL WHEN CHARGED TO 3 VOLTS EMPLOYING A 1.5M LiAsF <sub>6</sub> /MA ELECTROLYTE SOLUTION.....	3-41
3-26 TiS <sub>2</sub> SCREENING STUDIES: CYCLE LIFE PERFORMANCE IN METHYL ACETATE SOLUTIONS.....	3-42
3-27 TiS <sub>2</sub> SCREENING STUDIES: CYCLE LIFE PERFORMANCE IN METHYL ACETATE SOLUTIONS AS A FUNCTION OF LiAsF <sub>6</sub> CONCENTRATION.....	3-44
3-28 TiS <sub>2</sub> SCREENING STUDIES: CYCLE LIFE PERFORMANCE IN 3M LiAsF <sub>6</sub> /MA SOLUTIONS EMPLOYING EXTENDED VOLTAGE LIMITS.....	3-45

## ILLUSTRATIONS (CONT.)

<u>Figure</u>	<u>Page</u>
3-29 TiS <sub>2</sub> SCREENING STUDIES: EXTENDED CYCLE LIFE PERFORMANCE WITH 3M LiAsF <sub>6</sub> /MA SOLUTIONS.....	3-46
3-30 TiS <sub>2</sub> SCREENING STUDIES: CYCLE LIFE PERFORMANCE IN 2M LiAsF <sub>6</sub> /MA SOLUTIONS WITH AND WITHOUT 1,2-DIMETHOXYETHANE (DME) CO-SOLVENT.....	3-47
3-31 TiS <sub>2</sub> SCREENING STUDIES: CYCLE LIFE PERFORMANCE IN 2M LiAsF <sub>6</sub> /MA SOLUTIONS WITH AND WITHOUT TETRAHYDROFURAN (THF) CO-SOLVENT.....	3-48
3-32 TiS <sub>2</sub> SCREENING STUDIES: CYCLE LIFE PERFORMANCE WITH AND WITHOUT 2-METHYL THF CO-SOLVENT.....	3-49
3-33 Li <sub>2</sub> CoO <sub>2</sub> SCREENING STUDIES: CYCLE LIFE PERFORMANCE WITH 2M LiAsF <sub>6</sub> /MA SOLUTIONS AT A DISCHARGE RATE OF 1.0 mA/cm <sup>2</sup> .....	3-51
3-34 Li <sub>2</sub> CoO <sub>2</sub> SCREENING STUDIES: CYCLE LIFE PERFORMANCE WITH 2M LiAsF <sub>6</sub> /MA SOLUTIONS AT A DISCHARGE RATE OF 5 mA/cm <sup>2</sup> .....	3-52
3-35 LITHIUM CYCLABILITY TESTS: TYPICAL VOLTAGE PROFILES FOR METHYL FORMATE SOLUTIONS IN WICK CELLS (THIRD CYCLE).....	3-68
3-36 LITHIUM CYCLABILITY TESTS: TYPICAL VOLTAGE PROFILES FOR METHYL FORMATE SOLUTIONS IN WICK CELLS (TENTH CYCLE).....	3-69
3-37 LITHIUM CYCLABILITY TESTS: IR SPECTRUM OF SOLID PRODUCT FROM 2M LiAsF <sub>6</sub> /MF CELL.....	3-70
3-38 LITHIUM CYCLABILITY TESTS: IR SPECTRUM OF SOLID PRODUCT FROM 2M LiAsF <sub>6</sub> + 0.4M LiBF <sub>4</sub> /MF CELL.....	3-71
3-39 LITHIUM CYCLING EFFICIENCY VERSUS LiAsF <sub>6</sub> CONCENTRATION FOR METHYL FORMATE SOLUTIONS IN WICK CELLS.....	3-73
3-40 LITHIUM CYCLING EFFICIENCIES FOR XM LiAsF <sub>6</sub> + X/5M LiBF <sub>4</sub> /MF SOLUTIONS WITH AND WITHOUT CO <sub>2</sub> PRETREATMENT OF THE WORKING ELECTRODES.....	3-77
3-41 LITHIUM CYCLABILITY TESTS: TYPICAL VOLTAGE PROFILES FOR 2M LiAsF <sub>6</sub> + 0.4M LiBF <sub>4</sub> /MF SOLUTIONS IN WICK CELLS WITH AND WITHOUT CO <sub>2</sub> ADDED TO SOLUTION (THIRD CYCLE).....	3-78
3-42 LITHIUM CYCLABILITY TESTS: TYPICAL VOLTAGE PROFILES FOR 2M LiAsF <sub>6</sub> + 0.4M LiBF <sub>4</sub> /MF SOLUTIONS IN WICK CELLS WITH AND WITHOUT CO <sub>2</sub> ADDED TO SOLUTION (TENTH CYCLE).....	3-79
3-43 IR SPECTRUM OF SOLID REACTION PRODUCT FORMED ON LITHIUM CYCLED IN 2M LiAsF <sub>6</sub> /MA.....	3-81



## ILLUSTRATIONS (Cont.)

<u>Figure</u>	<u>Page</u>
3-44 LITHIUM CYCLING EFFICIENCY VERSUS $\text{LiAsF}_6$ CONCENTRATION FOR METHYL ACETATE SOLUTIONS.....	3-84
3-45 IR SPECTRUM OF SOLID REACTION PRODUCT FORMED ON LITHIUM CYCLED IN 1M $\text{LiAsF}_6$ /DMSI.....	3-87
3-46 LITHIUM CYCLING EFFICIENCY VERSUS $\text{LiAsF}_6$ CONCENTRATION FOR DIMETHYL SULFITE SOLUTIONS (HALF-CELL RESULTS).....	3-90
3-47 $\text{Li}/\text{V}_2\text{O}_5$ CELL CYCLE LIFE PERFORMANCE FOR VARIOUS CATHODE MANUFACTURING PROCESSES.....	3-94
3-48 EFFECTS OF CARBON TYPE ON THE PERFORMANCE OF ROLL MILLED $\text{V}_2\text{O}_5$ CATHODES.....	3-98
3-49 EFFECTS OF TEFLON BINDER CONTENT ON THE PERFORMANCE OF THE ROLL MILLED $\text{V}_2\text{O}_5$ CATHODES.....	3-100
3-50 EFFECTS OF CARBON CONTENT ON THE PERFORMANCE OF ROLL MILLED $\text{V}_2\text{O}_5$ CATHODES.....	3-101
3-51 PARTICLE SIZE DISTRIBUTIONS FOR THE METALLURG $\text{V}_2\text{O}_5$ VERSUS THAT FOR $\text{V}_2\text{O}_5$ MANUFACTURED FROM GROUND AMMONIUM METAVANADATE (LOT CML-V2-003).....	3-102
3-52 EFFECTS OF $\text{V}_2\text{O}_5$ PARTICLE SIZE ON THE PERFORMANCE OF ROLL MILLED CATHODES.....	3-103
3-53 DEMONSTRATION OF THE EXTENDED CYCLE LIFE CAPABILITIES OF THE RECHARGEABLE $\text{Li}/\text{V}_2\text{O}_5$ SYSTEM.....	3-105
3-54 EXTENDED CYCLE LIFE PERFORMANCE OF $\text{Li}/\text{V}_2\text{O}_5$ SYSTEM AT THE DISCHARGE RATE OF 5 $\text{mA}/\text{cm}^2$ .....	3-106

## TABLES

<u>Table</u>	<u>Page</u>
1-1 SUMMARY OF MATERIALS TO BE INVESTIGATED.....	1-2
2-1 METHODOLOGY OF CATHODE MATERIAL CHARACTERIZATIONS.....	2-6
2-2 CATHODE DESCRIPTION FOR $V_2O_5$ SCREENING STUDIES.....	2-12
2-3 TEST PARAMETERS FOR $V_2O_5$ CATHODE SCREENING STUDIES.....	2-12
3-1 SUMMARY OF SCREENING EVALUATIONS CONDUCTED IN THIS PROGRAM.....	3-2
3-2 X-RAY DIFFRACTION DATA FOR $V_2O_5$ (LOT CML-V2-001).....	3-7
3-3 X-RAY DIFFRACTION DATA FOR $V_2O_5$ (LOT CML-V2-002).....	3-8
3-4 X-RAY DIFFRACTION DATA FOR $V_2O_5$ (LOT CML-V2-003).....	3-9
3-5 X-RAY DIFFRACTION DATA FOR DEGUSSA $TiS_2$ (AS-RECEIVED).....	3-14
3-6 X-RAY DIFFRACTION DATA FOR $Li_xCoO_2$ (LOT CML-CO-002).....	3-22
3-7 X-RAY DIFFRACTION RESULTS FOR $Li_xCoO_2$ (LOT CML-CO-003).....	3-23
3-8 DISCHARGE RESULTS FOR $Li/Li_xCoO_2$ CELLS.....	3-29
3-9 AMPUL STORAGE TEST RESULTS FOR 2M $LiAsF_6$ + 0.4M $LiBF_4$ / MF SOLUTIONS (HISTORICAL DATA).....	3-53
3-10 AMPUL STORAGE TEST RESULTS FOR 1.0M $LiAsF_6$ /DMSI SOLUTIONS (HISTORICAL DATA).....	3-54
3-11 $V_2O_5$ THERMAL STABILITY TESTS--PHYSICAL APPEARANCE OF SAMPLES AFTER STORAGE INTERVAL.....	3-55
3-12 SOLUBILITY OF $V_2O_5$ IN LITHIUM BATTERY ELECTROLYTES--BY AA ANALYSIS...	3-55
3-13 X-RAY DIFFRACTION DATA FOR $V_2O_5$ STORED IN 2M $LiAsF_6$ + 0.4M $LiBF_4$ / MF AT AMBIENT TEMPERATURE (20-24°C).....	3-57
3-14 X-RAY DIFFRACTION DATA FOR $V_2O_5$ STORED IN 2M $LiAsF_6$ /MA AT AMBIENT TEMPERATURE (20-24°C).....	3-58
3-15 X-RAY DIFFRACTION DATA FOR $V_2O_5$ STORED IN 2M $LiAsF_6$ + 0.4M $LiBF_4$ /MF AT 71°C.....	3-59
3-16 X-RAY DIFFRACTION DATA FOR $V_2O_5$ STORED IN 2M $LiAsF_6$ /MA AT 71°C.....	3-60
3-17 $TiS_2$ THERMAL STABILITY TESTS--PHYSICAL APPEARANCE OF SAMPLES AFTER STORAGE INTERVAL.....	3-61

## TABLES (Cont.)

<u>Table</u>	<u>Page</u>
3-18 SOLUBILITY OF $TiS_2$ IN LITHIUM BATTERY ELECTROLYTES--BY AA ANALYSIS....	3-62
3-19 X-RAY DIFFRACTION DATA FOR $TiS_2$ STORED IN 2M $LiAsF_6$ /MA AT AMBIENT TEMPERATURE (20-24°C).....	3-63
3-20 X-RAY DIFFRACTION DATA FOR $TiS_2$ STORED IN 2M $LiAsF_6$ + 0.4M $LiBF_4$ /MF AT 71°C.....	3-64
3-21 X-RAY DIFFRACTION DATA FOR $TiS_2$ STORED IN 2M $LiAsF_6$ /MA AT 71°C.....	3-65
3-22 LITHIUM CYCLING RESULTS IN METHYL FORMATE SOLUTIONS--BASELINE EVALUATIONS.....	3-67
3-23 LITHIUM CYCLABILITY TESTS: SUMMARY OF IR RESULTS FOR SOLID PRODUCT FROM METHYL FORMATE SOLUTIONS.....	3-72
3-24 EFFECT OF $LiAsF_6$ CONCENTRATION ON LITHIUM CYCLING EFFICIENCY IN METHYL FORMATE (WICK CELL, NICKEL SUBSTRATE, DEAERATED).....	3-72
3-25 EFFECT OF ORGANIC ADDITIVES ON LITHIUM CYCLING EFFICIENCY IN METHYL FORMATE.....	3-75
3-26 EFFECT OF $CO_2$ ON LITHIUM CYCLING EFFICIENCY IN METHYL FORMATE (WICK CELL, NICKEL SUBSTRATE).....	3-76
3-27 LITHIUM CYCLING RESULTS IN METHYL ACETATE SOLUTIONS--BASELINE EVALUATIONS.....	3-80
3-28 LITHIUM CYCLABILITY TESTS: SUMMARY OF IR RESULTS FOR SOLID PRODUCT FROM 2M $LiAsF_6$ /MA SOLUTIONS.....	3-82
3-29 EFFECT OF $LiAsF_6$ CONCENTRATION ON LITHIUM CYCLING EFFICIENCY IN METHYL ACETATE.....	3-83
3-30 EFFECT OF ETHER CO-SOLVENTS ON LITHIUM CYCLING EFFICIENCY IN METHYL ACETATE.....	3-83
3-31 EFFECT OF ORGANIC ADDITIVES ON LITHIUM CYCLING EFFICIENCY IN METHYL ACETATE.....	3-85
3-32 EFFECT OF ELECTRODE PRETREATMENT WITH $CO_2$ ON LITHIUM CYCLING EFFICIENCY IN METHYL ACETATE.....	3-86
3-33 LITHIUM CYCLABILITY TESTS: SUMMARY OF IR RESULTS FOR SOLID PRODUCT FROM 1M $LiAsF_6$ /DMSI SOLUTIONS.....	3-88
3-34 EFFECT OF $LiAsF_6$ CONCENTRATION ON LITHIUM CYCLING EFFICIENCY IN DIMETHYL SULFITE (HALF-CELL, NO SOLUTION PRETREATMENT).....	3-89

TABLES (Cont.)

<u>Table</u>	<u>Page</u>
3-35 CATHODE DESCRIPTIONS FOR $V_2O_5$ CATHODE PROCESSING STUDIES.....	3-93
3-36 ROLL MILLED $V_2O_5$ CATHODE DESCRIPTIONS AND CYCLE PERFORMANCE SUMMARY.....	3-96
3-37 PERFORMANCE SUMMARY FOR $Li/V_2O_5$ LABORATORY CELLS TESTED UNDER EXTENDED CYCLE LIFE CONDITIONS.....	3-107

## CHAPTER 1

## INTRODUCTION

The development of a reliable rechargeable lithium (Li) technology having high rate capabilities and low temperature operability has become a major priority throughout the Department of Defense (DOD). In recent years, considerable progress has been made in ambient temperature Li/secondary technology. At low rates of discharge, good cycle performance has been demonstrated with a number of cathode materials. However, this technology has not produced a practical Li/secondary cell nor have high rate or low temperature performance capabilities been demonstrated. To meet the demanding performance goals for naval applications, such as torpedo targets and seal delivery vehicles, significant advances are needed over the current state-of-the-art capabilities. To achieve these advances, Honeywell under the direction of NSWC investigators offers the development of an ester-based rechargeable technology that has the capability for both high rate and low temperature operations.

The objective of this program, therefore, is to develop a lithium rechargeable cell technology capable of operating over a wide temperature range and offering good discharge rate capabilities. The specific program performance guidelines are:

- o Energy Density: 60 to 90 Wh/lb
- o Depth of Discharge: 75 percent
- o Rate Capabilities: C/6 to 2C
- o Cycle Life: 50 to 100 cycles at C/6 to 2C rates
- o Operating Temperature Range: -55°C to 75°C (generic applications)  
-2°C to 35°C (seawater applications)
- o Storage Temperature Range: -55°C to 75°C
- o Safety: Safe and resistant to abuse.

The approach adopted to achieve these performance capabilities is to employ insertion-type cathode materials (vanadium pentoxide [ $V_2O_5$ ], titanium disulfide [ $TiS_2$ ], vanadium (V) sulfide [ $V_2S_5$ ], and lithium cobalt oxide [ $LiCoO_2$ ]) with high conductivity, ester-based electrolyte solutions. Insertion cathode materials were selected based on their demonstrated long cycle life capabilities and excellent reversibility in various nonaqueous electrolyte systems. Ester-based solutions offer some of the highest conductivities achievable in organic solutions thus providing the intrinsic

properties needed to significantly enhance rate capabilities and low temperature operation. These solutions also exhibit good thermal, chemical, and electrochemical stability, as evidenced by their proven performance in primary lithium applications.

The present program is divided into two parts. Phase I involves selection of the electrochemical system offering the best performance capabilities, while Phase II will involve the development and testing of prototype hardware cells incorporating the selected technology. This report details the work conducted in Phase I.

The specific cathode materials and electrolyte solutions that have been investigated are summarized in Table 1-1. The superior conductivity offered by the ester-based solutions over the propylene carbonate- and 2-methyl THF-based solutions used in the current state-of-the-art rechargeable lithium cells is clearly illustrated in Figure 1-1. Figures 1-2 and 1-3 show the dramatic enhancements in rate capabilities that can be achieved with the ester-based solutions. Of the four cathode materials evaluated,  $V_2O_5$  and  $TiS_2$  are mature systems and therefore represented our primary candidates.  $V_2S_5$  and  $Li_xCoO_2$ , on the other hand, are new systems that could offer significant advantages in energy density if extended cycle life capabilities could be demonstrated.

TABLE 1-1. SUMMARY OF MATERIALS TO BE INVESTIGATED

<u>Cathode Materials</u>	<u>Solvents</u>	<u>Solutes</u>
$TiS_2$	Methyl Formate	$LiAsF_6$ (Lithium hexafluoroarsenate)
$Li_xCoO_2$	Methyl Acetate	$LiBF_4$ (Lithium tetrafluoroborate)
$V_2O_5$	Dimethyl Sulfite	
$V_2S_5$		

The major challenge at the outset of the program was to demonstrate cycle life capabilities with the ester-based solutions including both reversibility of the insertion cathode materials and efficient cycling of the lithium electrode. In addition, however, it was recognized at the start that cathode processing was a major factor in the successful development of a practical rechargeable cell technology and, therefore, cathode processing has been emphasized throughout our work.

In Phase I, we have successfully identified an electrochemical system possessing the intrinsic properties to greatly extend the state-of-the-art capabilities in rechargeable lithium technology and to meet the demanding performance goals for naval applications. This system consists of  $V_2O_5$  as the cathode material, methyl formate electrolyte solutions, and roll milled cathodes. Carbon dioxide ( $CO_2$ ) will be used as an electrolyte additive to provide high lithium cycling efficiencies in the methyl formate solutions.

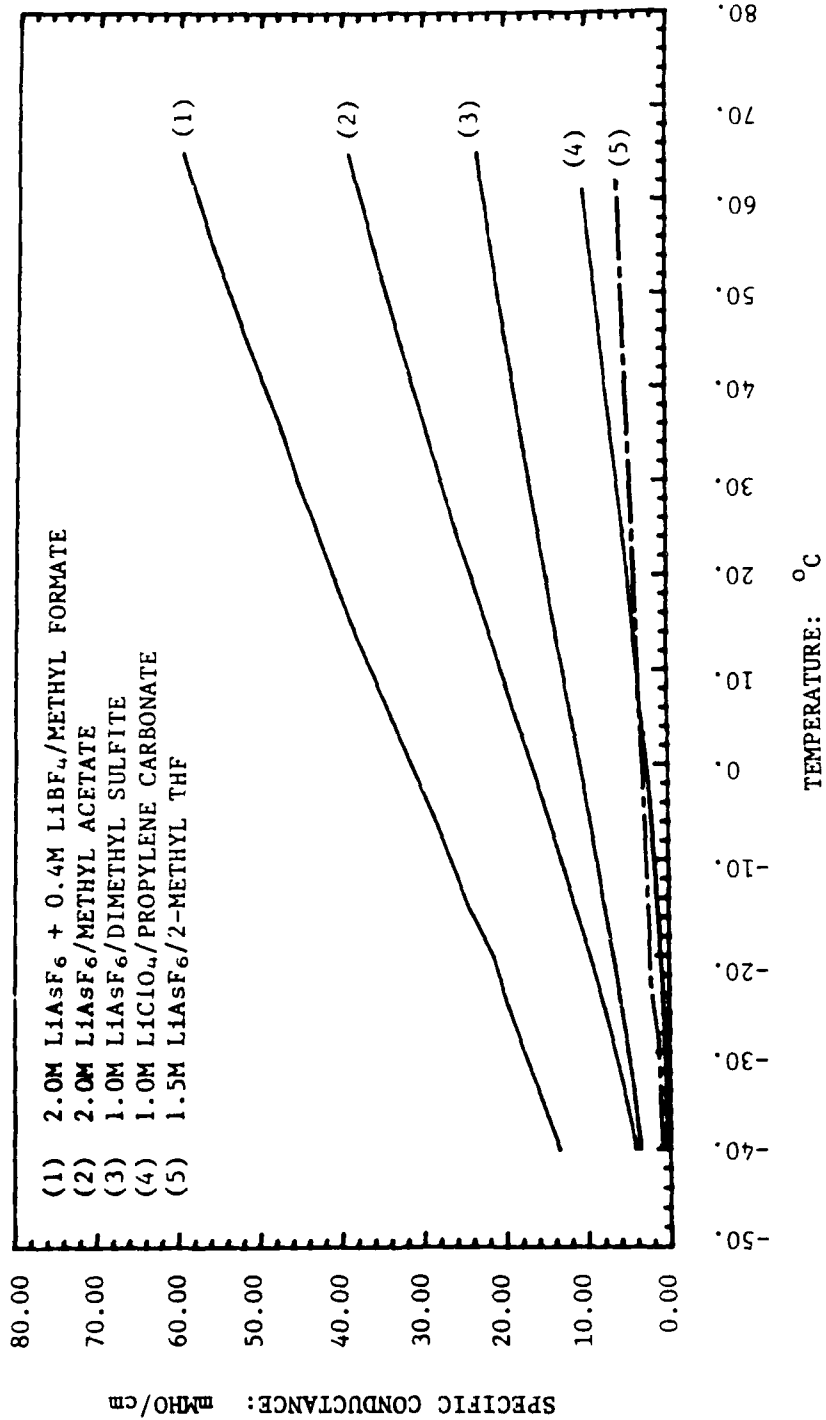


FIGURE 1-1. CONDUCTIVITY VERSUS TEMPERATURE DATA SHOWING SUPERIOR CONDUCTIVITIES OFFERED BY ESTER-BASED ELECTROLYTE SOLUTIONS

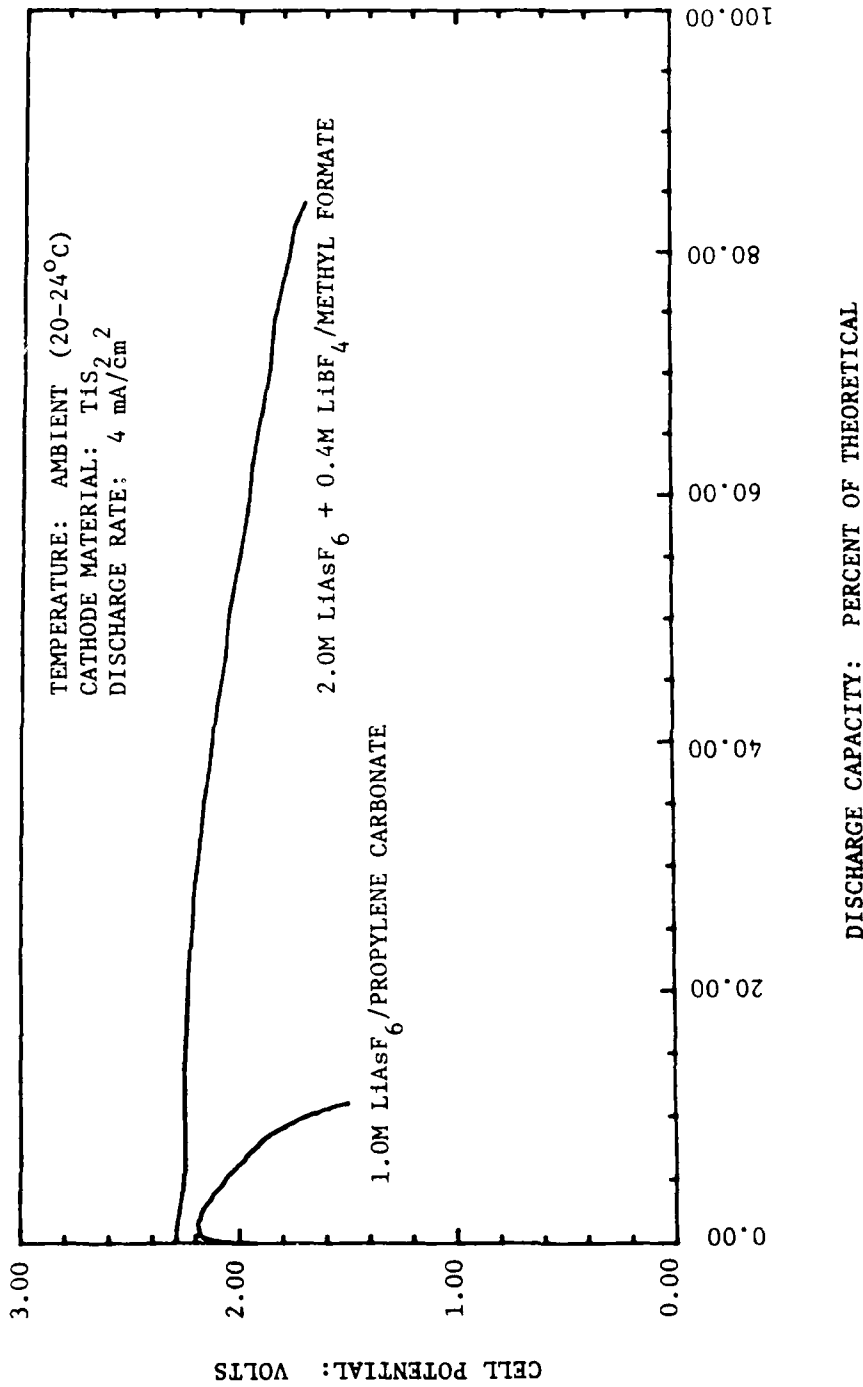


FIGURE 1-2. DISCHARGE PERFORMANCE OF Li/TiS<sub>2</sub> CELLS SHOWING THE DRAMATIC IMPROVEMENT IN RATE CAPABILITIES THAT CAN BE REALIZED USING HIGH CONDUCTIVITY ESTER-BASED SOLUTIONS OVER EXISTING STATE-OF-THE-ART SYSTEMS



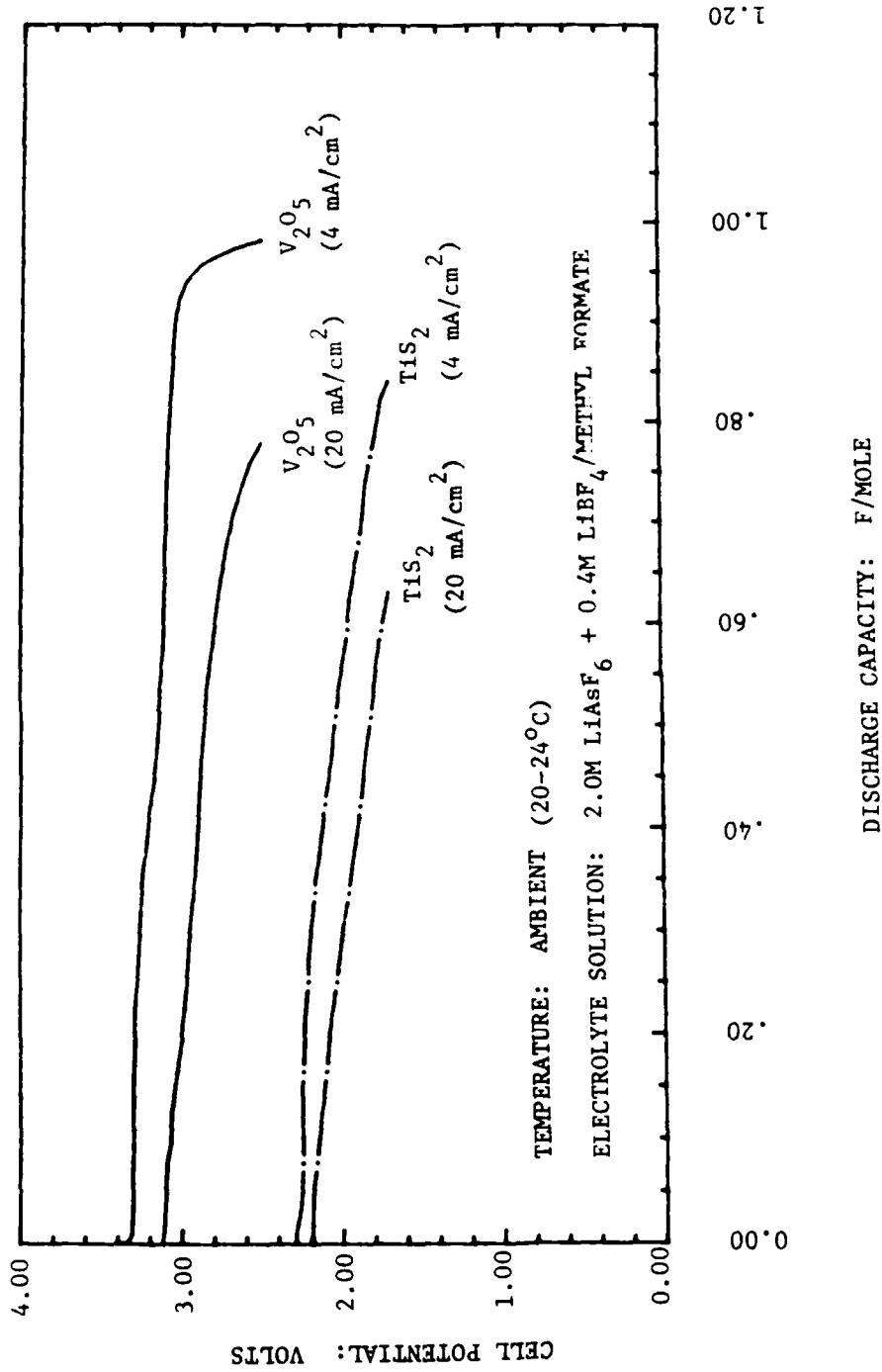


FIGURE 1-3. DISCHARGE PERFORMANCE OF Li/V<sub>2</sub>O<sub>5</sub> AND Li/TiS<sub>2</sub> CELLS SHOWING THE EXCELLENT RATE CAPABILITIES THAT CAN BE ACHIEVED USING HIGH CONDUCTIVITY ESTER-BASED ELECTROLYTE SOLUTIONS WITH INSERTION-TYPE CATHODE MATERIALS

CHAPTER 2  
EXPERIMENTAL

EXPERIMENTAL CELL DESCRIPTIONS

Half-Cell

The half-cell configuration, shown in Figure 2-1, incorporates three electrodes including a reference electrode. The anode and cathode each had a geometric surface area of 3.2 cm<sup>2</sup>. In cycle life tests, the anodes were sealed in a Celgard 2400 envelope while the cathodes were supported with porous glass disks to maintain good electrical contact with the expanded metal current collectors. Once assembled, the electrode holder was completely immersed in approximately 15 ml of electrolyte solution contained in a Fisher & Porter 3-ounce aerosol reaction vessel. The leads were brought out through Teflon compression seals mounted in the lid of the reaction vessel.

Wick Cell

The wick cells consisted of an electrode stack mounted between two glass slides held together with stainless steel wire and sealed in a Fisher & Porter 3-ounce aerosol reaction vessel. These cells employed approximately 1.5 ml of solution in the bottom of the reaction vessel with only the ends of the separator immersed in the electrolyte solution. Transport of the electrolyte solution to the electrode surfaces occurred through the wicking action of the separator. Two configurations of wick cells were employed in our investigations. The 2-plate cells, illustrated in Figure 2-2, consisted of one anode and one cathode separated by porous separator material. The 3-plate design incorporated two anodes connected in parallel, one on either side of the cathode. The separators used were either Celgard 2400 microporous polypropylene or Hollingsworth and Vose HV-932 glass fiber material.

CATHODE MANUFACTURING TECHNIQUES

Six cathode processes were evaluated in this program. A brief description of each process is given below.

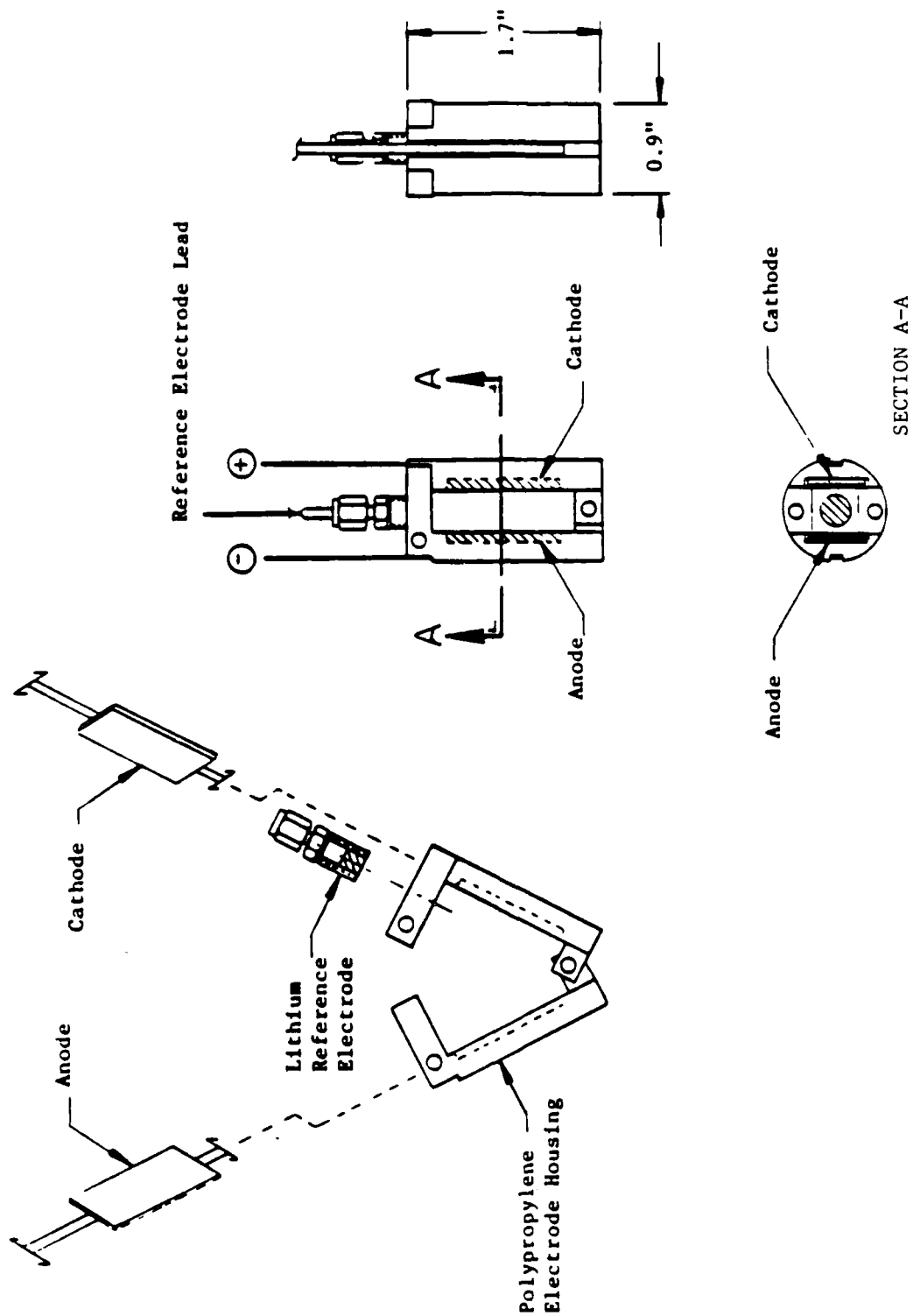


FIGURE 2-1. HALF-CELL ELECTRODE HOLDER

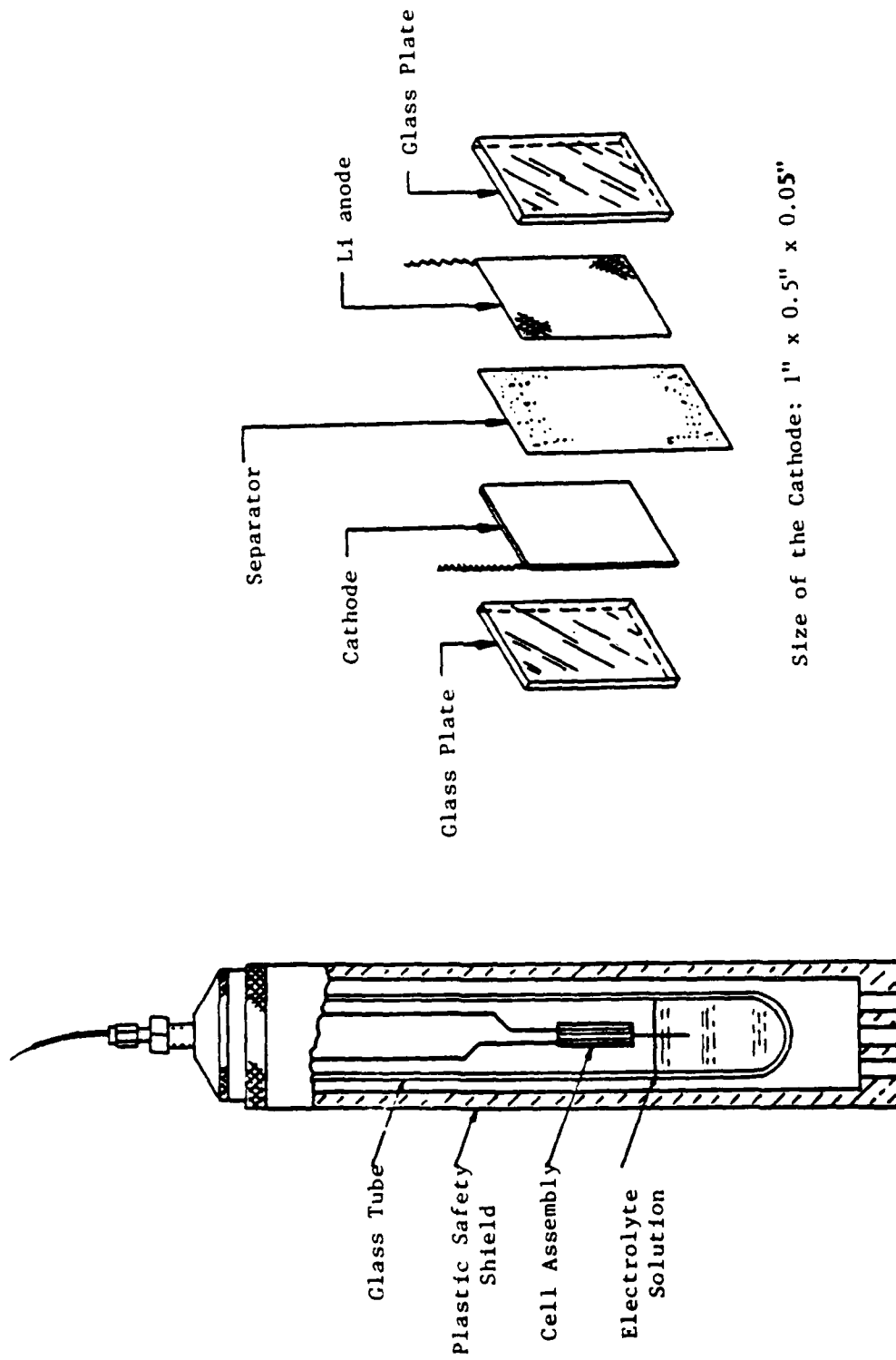


FIGURE 2-2. LABORATORY 2-PLATE WICK CELL HARDWARE

### Cold Pressing

Pressed powder electrodes were made by mixing dry powders of the active cathode material and conductive diluent in a high-speed blender and then pressing the resulting mixture onto both sides of an expanded metal grid at 6000 to 8000 psi. The thickness was controlled by the weight of cathode mix.

### Cold Pressing with Teflon Binder

These cathodes, containing active cathode material, conductive diluent and Teflon-6 powder (DuPont), were made in the same manner as described above.

### Cold Pressing With Microthene (Polyethylene)

These cathodes were made in the same manner as described above, except that the pressed electrodes are sintered under argon atmosphere at 100°C for one hour.

### Cold Pressing and Sintering with Teflon Binder

These cathodes were made in the same manner as described above except that the pressed electrodes are sintered under vacuum at 280°C to 300°C for one to two hours.

### Cold Pressing with Isotactic-Polypropylene Binder<sup>1</sup>

This cathode processing technique was developed by U.S. Army Laboratory Command (LABCOM) and involves dissolving isotactic-polypropylene powder near its crystalline melting point (100°C to 120°C) in a small volume of Decalin (decahydronaphthalene). The cathode material and conductive diluent are then added with vigorous stirring. Stirring is continued until the solution has cooled to room temperature. The resulting mixture is dried under vacuum at 150°C to remove the residual solvent and then ground to a fine powder in a high-speed grinder. Cathodes are then made by pressing the powder onto both sides of an expanded metal grid.

### Pasting with Ethylene Propylene Diene Terpolymer (EPDM) Binder

This process was developed at the Jet Propulsion Laboratory for use with  $TiS_2$  cathodes. Electrodes are prepared by mixing dry powders of cathode material and conductive diluent in a high-speed blender for 30 seconds. Cyclohexane containing one weight percent dissolved EPDM is then added in sufficient quantity to provide the required amount of binder. After stirring, the excess solvent is removed under vacuum until the mixture has achieved a paste-like consistency. The wet mixture is then pasted onto both sides of an expanded metal grid. The finished electrodes are vacuum dried at ambient temperature for several hours and then at 80°C for one hour.

Roll Milling with Telfon Binder<sup>1</sup>

In this process, the cathode mix was prepared by first blending Teflon-6 powder in the carrier solvent (mineral spirits) for 20 to 30 seconds using a high-speed blender. Next, the cathode material and conductive diluent were slowly added to the solution and blended for one minute. The mix was then vacuum filtered and kneaded in a polyethylene bag until it obtained a clay-like consistency. The material was then passed through a rolling mill approximately 12 times, being rotated 90 degrees after every two passes. This process produces a flexible sheet which was then air dried overnight and then vacuum dried for approximately three hours at 200°C. Cathodes were made by cutting out electrodes to the desired dimensions and pressing them onto expanded metal grids.

## CATHODE MATERIAL SYNTHESIS AND CHARACTERIZATION

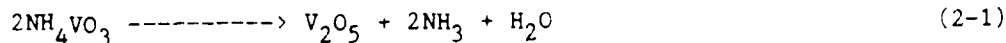
Of the four cathode materials evaluated,  $V_2O_5$ ,  $V_2S_5$ , and  $Li_xCoO_2$  were synthesized in-house while  $TiS_2$  was purchased from a commercial vendor (Degussa, battery grade). Before use, all cathode materials were characterized using the following series of analyses:

- o Stoichiometry
- o Particle Size Distribution
- o Purity
- o Morphology
- o Crystal Structure
- o Electrochemical Discharge Performance

The methodology for these analyses are summarized in Table 2-1.

Vanadium Pentoxide ( $V_2O_5$ )

Vanadium pentoxide was manufactured by the thermal decomposition of ammonium metavanadate ( $2NH_4VO_3$ ) at 380°C under flowing air per the following reaction:



Our extensive experience with  $V_2O_5$  in primary lithium cell applications has shown that the manufacturing conditions can have a significant influence on electrochemical performance of the prepared material. The key factor in producing  $V_2O_5$  is to rapidly remove ammonia as it is formed. If the residence time of ammonia becomes too long, reduction of  $V_2O_5$  will occur and the product will be contaminated with lower oxides of vanadium. Best results are achieved using thin layers of ammonium metavanadate and forced air flow.

Synthesis of  $V_2O_5$  was carried out in a tube furnace (Lindberg Model 55453) employing a 2.75-inch diameter by 48-inch long Pyrex glass tube. The ammonium metavanadate (Foote CP grade) starting material was spread out in a

TABLE 2-1. METHODOLOGY OF CATHODE MATERIAL CHARACTERIZATIONS

<u>Analysis</u>	<u>Technique</u>	<u>Instrumentation</u>
Stoichiometry	Wet chemical methods ( $V_2O_5$ ) Combustion ( $TiS_2$ , $V_2S_5$ ) Atomic Absorption Analysis ( $Li_xCoO_2$ )	
Particle Size Distribution	Sieve Analysis	Allen-Bradley Model L3P Sonic Sifter
Purity	EDAX*	Phillips Model PSEM 500 + EDAX* - scanning range of 0 to 18 KeV covering elements from Atomic Number 6 to Atomic Number 99
Morphology	SEM*	Phillips Model PSEM 500
Crystal Structure	X-Ray Diffraction	Phillips Model Mark I Powder Diffractometer - CuK $\alpha$ Radiation
Electrochemical Performance	Discharge at $0.5 \text{ mA/cm}^2$ using $2M LiAsF_6 + 0.4M LiBF_4/MF$ electrolyte solution at ambient temperature ( $20-24^\circ\text{C}$ )	

\* EDAX = Energy Dispersive Analysis  
SEM = Scanning Electron Microscope

uniform layer 0.6 to 0.8 inch thick on the inside wall of the glass tube. The tube was then slowly heated to 380°C and maintained at that temperature for a period of three hours employing a dry compressed air flow rate of 10 liters/minute. The product was then annealed at 560°C for 30 minutes at an air flow rate of 5 liters/minute after which the tube was slowly cooled to room temperature, maintaining the air flow at 5 liters/minute.

During the course of our evaluations, three lots of  $V_2O_5$  were manufactured, designated by lot numbers CML-V2-001 to CML-V2-003. Lots 001 and 002 employed as-received ammonium metavanadate while Lot 003 employed ammonium metavanadate which had been ground in a ball mill in an effort to reduce the particle size of the manufactured  $V_2O_5$ .

### Titanium Disulfide ( $TiS_2$ )

Extensive work has been done with titanium disulfide by other investigators, the results of which show that cycle life performance is strongly influenced by the stoichiometry of the starting cathode material.<sup>2-4</sup> If the  $TiS_2$  is metal rich, the excess metal atoms can occupy sites in the van der Waals gap effectively pinning the layers together. This can greatly impede the mobility of lithium ions and degrade rate capabilities. It also restricts the amount of lithium that can be incorporated, thus lowering capacity as well. Excess sulfur, on the other hand, can dissolve in the electrolyte solution and subsequently react with the lithium metal anode resulting in reduced lithium cycling efficiencies and increased polarization levels.

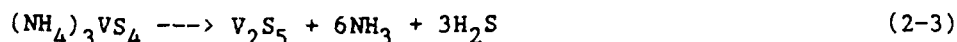
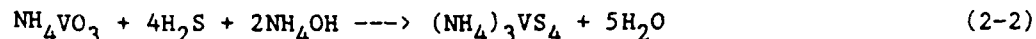
$TiS_2$  is costly and difficult to produce. At the outset of the program, we were convinced that without a commercial source of supply,  $TiS_2$  would never be a practical system, regardless of how well it performed.<sup>2</sup> Therefore, our approach was to purchase the best available grade of  $TiS_2$  for our evaluations rather than synthesize it in-house. In this way, we could be confident of a rapid development cycle into practical hardware if  $TiS_2$  emerged as the optimum cathode material for use with ester-based solutions.

The decision to purchase  $TiS_2$  was strongly influenced by the emergence of a new vendor, offering a high quality grade of material. This vendor is Degussa, who had earlier been selected by Exxon to be a large scale producer of  $TiS_2$  for their lithium/battery program. Exxon pioneered much of the early development of the  $TiS_2$  system and established the manufacturing methods and material specifications needed to achieve a high quality grade of  $TiS_2$ . Because of their ties with Exxon, we were confident that Degussa was knowledgeable in the material requirements for rechargeable lithium applications and could supply a high grade of material for our evaluations.



Vanadium (V) Sulfide ( $V_2S_5$ )

$V_2S_5$  was prepared in a two-step process involving the following reactions:



Ammonium thiovanadate ( $(NH_4)_3VS_4$ ) was prepared by reacting ammonium metavanadate ( $NH_4VO_3$ ) with hydrogen sulfide ( $H_2S$ ) in a solution of ammonium hydroxide ( $NH_4OH$ ). This was accomplished by slowly bubbling  $H_2S$  through a saturated solution of  $NH_4VO_3$  in  $NH_4OH$  with continuous stirring. The reaction flask was immersed in an ice-water bath to dissipate the heat from the exothermic reaction. Addition of  $H_2S$  was continued for 10 hours after which the fine brown precipitate that had formed was collected by filtration under a nitrogen blanket and washed with ethanol. The filter cake was vacuum dried at ambient temperature for 48 hours, crushed with a mortar and pestle, and then redried for another two hours under vacuum at ambient temperature.

$V_2S_5$  was then prepared by the thermal decomposition of  $(NH_4)_3VS_4$  in a tube furnace under argon flow. Two lots of material were prepared employing different temperatures to evaluate the effects of decomposition temperature on product quality.

The first lot of  $V_2S_5$  was prepared by slowly heating the  $(NH_4)_3VS_4$  to  $240^\circ C$  and holding it at that temperature for one hour. The temperature was then increased to  $250^\circ C$  for one hour and then to  $260^\circ C$  for 40 minutes. The tube was then allowed to cool to ambient temperature and the product collected under an argon atmosphere. This lot was designated as CML-VS-002.

The second lot of  $V_2S_5$  was prepared by slowly heating the  $(NH_4)_3VS_4$  to  $225^\circ C$  and maintaining it at that temperature for 3.5 hours. The tube was then allowed to cool to ambient temperature and the product collected under an argon atmosphere. This lot was designated as CML-VS-003.

Lithium Cobalt Oxide ( $Li_xCoO_2$ )

$Li_xCoO_2$  was prepared by the thermal decomposition of a pelletized mixture of lithium carbonate ( $Li_2CO_3$ ) and cobaltous carbonate ( $CoCO_3$ ) at  $900^\circ C$  in air. The synthesis was carried out by first mixing  $Li_2CO_3$  and  $CoCO_3$  together in a Li/Co mole ratio of 0.98 and then pressing the mixture into 1.55-inch diameter by 0.20-inch thick pellets at 10,000 psi employing a dwell time of one minute. The pellets were then heated at  $900^\circ C$  in a muffle furnace for 20 hours under an air flow rate of 1.8 L/minute. After cooling to room temperature, the pellets were ground in a mortar and pestle and twice reheated to  $900^\circ C$  for 20 hours under an air flow rate of approximately 0.6 liters/minute. Two lots of material were prepared in this manner, designated as CML-CO-002 and CML-CO-003.

## ELECTROLYTE SOLUTIONS

Purification

The general procedure employed for purifying ester solvents is to distill them from  $P_2O_5$ . This method was developed in the mid-1970's by Honeywell for purifying methyl formate and has been found to be extremely effective for removing water and methanol, the primary impurities found in commercial grades of methyl formate. E.M. Science (formerly MC/B) now uses this method to manufacture a special grade of methyl formate specifically for Honeywell for use in our lithium batteries.

Analysis of solvents was accomplished employing the Karl Fischer method for water and gas chromatography for other volatile impurities. Solutions were analyzed for water using the Karl Fischer technique.

Methyl Formate. Methyl formate was purchased from E.M. Science (special battery grade) and used as received. The only impurity detected in the purchased material was water at a concentration of 22 ppm.

Methyl Acetate. Methyl acetate was purchased from E.M. Science (Cat. No. MX0625; 99+ mol percent) and was purified by distillation from  $P_2O_5$ . Interestingly, the  $P_2O_5$  turned black after a short period of contact with methyl acetate. The reason for this color change is not known, but no degradation of the solvent or other adverse effects were observed, even after prolonged treatment with  $P_2O_5$ . As with methyl formate, distillation from  $P_2O_5$  was found to be an effective means of purifying methyl acetate.

Dimethyl Sulfoxide. Dimethyl sulfoxide (Eastman Kodak Cat. No. 5874) was found to form a gel with  $P_2O_5$  and thus could not be purified in the same manner as methyl formate and methyl acetate. Instead, this solvent was purified employing a double fractional distillation under reduced pressure.

Solution Manufacture

All solutions were manufactured in a glove box under an argon atmosphere. The purified solvents were prechilled to  $-10^{\circ}C$  to  $-20^{\circ}C$  to minimize heat buildup during the exothermic dissolution process. The salts used were:

- $LiAsF_6$  (Lithium hexafluoroarsenate): Electrochemical Grade, USS Agricultural -- used as received.
- $LiBF_4$  (Lithium tetrafluoroborate): Foote Mineral Co. -- used as received.

All solutions contained less than 50 ppm of water, as measured by the Karl Fischer method.

## LITHIUM CYCLING EFFICIENCY MEASUREMENTS

The lithium cycling efficiency tests were conducted by stripping and plating lithium between two lithium electrodes. This arrangement is designed to simulate the conditions in an actual cell under charge/discharge cycling and has been found to provide more reliable results than stripping and plating onto an inert substrate.

The working electrode was capacity limiting and consisted of 0.0035-inch thick lithium foil pressed onto a nickel or 304 stainless steel substrate with an expanded metal grid spot welded to it. The auxiliary electrode employed 0.020-inch thick lithium foil pressed onto nickel grid. Each electrode had a geometric surface area of 3.2 cm<sup>2</sup>. Tests were conducted with both 2-plate wick cells (Figure 2-2) and flooded half-cells (Figure 2-1). In the wick cell tests, 2-5 layers of Celgard 2400 were employed as the separator.

The tests were conducted employing a stripping/plating current density of 1.0 mA/cm<sup>2</sup> and cycling was continued until the lithium working electrode was completely consumed. Each half-cycle was three hours in duration which represented approximately 20 percent depth discharge based on the starting capacity of the working electrode. The cycling efficiency was determined using the following relationship:

$$E = \frac{C_i - \frac{C_o - C_i}{n}}{C_i} \times 100 \quad (2-4)$$

where:

- E = Cycling efficiency, percent
- C = Starting capacity of lithium working electrode, mAh
- C<sub>i</sub><sup>o</sup> = Capacity of lithium plated and stripped during each half-cycle, mAh
- n = Total number of cycles achieved

## THERMAL STABILITY TESTS

The thermal stability tests were designed to evaluate the compatibility of the cathode materials with the different electrolyte solutions. The samples consisted of approximately 0.5 g of cathode material immersed in electrolyte solution sealed in a glass ampul. Each sample also contained a strip of lithium metal in contact with the solutions. The lithium strips were enveloped in Celgard 2400 separator material to prevent direct contact with any particles of cathode material that may have been dispersed in the solution.

Each cathode material/electrolyte solution combination was evaluated under two storage conditions: Six months of ambient temperature (20-24°C) storage and one month storage at 71°C followed by five months storage at ambient temperature. After the storage intervals, the ampuls were opened in a glove

box under an argon atmosphere. The electrolyte solutions were carefully removed and analyzed by atomic absorption for either titanium or vanadium ion concentration to define the solubility level of the cathode material. The cathode materials were thoroughly rinsed with pure solvent to remove residual traces of the electrolyte salts and then investigated by x-ray diffraction analysis to determine if any gross changes in composition or structure had occurred.

#### Cycle Life Tests

Cycle life tests were conducted employing either half-cells (Figure 2-1) or 2-plate wick laboratory cells (Figure 2-2) at both room temperature and  $-20^{\circ}\text{C}$ . The separators used in laboratory cells consisted of two layers of 0.001 inch thick Celgard 2400. Discharge and charge cutoff voltages were varied in  $\text{Li}/\text{TiS}_2$  and  $\text{Li}/\text{Li}_x\text{CoO}_2$  cells as a part of evaluations.

In the case of  $\text{V}_2\text{O}_5$ , 3-plate wick laboratory cell was used with the utilized surface area of  $6.4\text{ cm}^2$ . Table 2-2 describes the cathodes used in these tests, while the test parameters are defined in Table 2-3. In these tests, the depth of discharge was limited to a maximum of 0.75 F/mole (i.e., 75 percent DOD). In this way, cells were discharged either 2.8 volts cutoff or 0.75 F/mole capacity limit, whichever was reached first.

TABLE 2-2. CATHODE DESCRIPTION FOR  $V_2O_5$  SCREENING STUDIES

Conductive Diluent:	Shawinigan Acetylene Black (50 percent compressed)
Binder:	isotactic-polypropylene
$V_2O_5$ Content:	86 weight percent
Conductive Diluent Content:	10 weight percent
Binder Content:	4 weight percent
Manufacturing Process:	cold pressed
Geometric Surface Area:	3.2 cm <sup>2</sup> /side
Nominal Thickness:	0.038 inch
Nominal Weight:	0.33 g
Nominal Density:	1.26 g/cc
Nominal Capacity:	49 mAh/F

TABLE 2-3. TEST PARAMETERS FOR  $V_2O_5$  CATHODE SCREENING STUDIES

Discharge Current Density:	1.0 mA/cm <sup>2</sup>
Discharge Voltage Cutoff:	2.8 volts
Maximum Discharge Capacity Limit:	0.75 F/mole
Charge Current Density:	1.0 mA/cm <sup>2</sup>
Charge Voltage Limit:	3.6 to 3.8 volts
Maximum Charge Capacity Limit:	0.75 F/mole

## CHAPTER 3

## RESULTS AND DISCUSSION

## CATHODE SELECTION STUDIES

Our overall objective in this work was to identify the cathode material/electrolyte solution combination offering the optimum capabilities toward meeting the performance goals of the program. Four cathode materials have been evaluated including  $TiS_2$ ,  $V_2O_5$ ,  $V_2S_5$ , and  $LiCoO_2$ . Our investigations of ester-based electrolyte solutions focused primarily on two solvents: methyl formate and methyl acetate. In addition, however, dimethyl sulfite (DMSI) was included in some of the evaluations. Dimethyl sulfite has been successfully used in primary lithium cells and has been reported to behave as a reversible liquid depolarizer at carbon electrodes. This latter quality could offer unique capabilities to rechargeable lithium applications, particularly with respect to providing protection against overdischarge, and it was therefore of interest to include dimethyl sulfite in our investigations.

All solutions employed  $LiAsF_6$  as the solute.  $LiAsF_6$  was selected based on its commercial availability in a high purity grade and its demonstrated performance in rechargeable lithium applications. Methyl formate solutions, however, also contained  $LiBF_4$  which is needed for solution stability at elevated temperatures.

To identify the best performing system, screening evaluations were conducted as summarized in Table 3-1. Before use, each cathode material was characterized using the methodology outlined in Table 2-1. Stoichiometry, particle size, and purity can all have a significant impact on electrochemical performance and cyclability of insertion-type cathode materials. The purpose of the characterization tests, therefore, was to ensure, to the best possible degree, that the cathode materials were of suitable quality before proceeding with the screening evaluations.

Once the electrochemical system had been selected, work focused on cathode processing, evaluating various manufacturing methods and then optimizing the cathode composition for performance. The effort under Phase I of the program culminated with a demonstration of the performance capabilities of the selected system under extended cycle life conditions.

TABLE 3-1. SUMMARY OF SCREENING EVALUATIONS CONDUCTED IN THIS PROGRAM

TEST	SOLVENT	CATHODE MATERIAL				
		NONE	TiS <sub>2</sub>	V <sub>2</sub> O <sub>5</sub>	V <sub>2</sub> S <sub>5</sub> **	Li <sub>x</sub> CoO <sub>2</sub>
Cycle Life Tests	Methyl Formate	-	X	X	-	X
Thermal Stability	Methyl Formate	*	X	X	-	-
Lithium Cyclability	Methyl Formate	X	-	-	-	-
Cycle Life Tests	Methyl Acetate	-	X	X	-	X
Thermal Stability	Methyl Acetate	-	X	X	-	-
Lithium Cyclability	Methyl Acetate	X	-	-	-	-
Cycle Life Tests	Dimethyl Sulfito	-	-	X	-	-
Thermal Stability	Dimethyl Sulfito	*	-	-	-	-
Lithium Cyclability	Dimethyl Sulfito	X	-	-	-	-

\* Specific tests were not conducted under this program. However, extensive data were available from previous work conducted by Honeywell in unrelated programs.

\*\* No work on V<sub>2</sub>S<sub>5</sub> due to its instability in ester-based electrolytes (see Vanadium (V) Sulfide section).

The following is a detailed discussion of the experimental results obtained during the selection, optimization, and demonstration of a rechargeable lithium technology as conducted in this program.

#### CATHODE MATERIAL CHARACTERIZATION TESTS

##### Vanadium Pentoxide (V<sub>2</sub>O<sub>5</sub>)

Particle Size. The particle size distribution for V<sub>2</sub>O<sub>5</sub> lots CML-V2-001 and CML-V2-003 are shown in Figure 3-1. It was found that the particle size distribution of the manufactured V<sub>2</sub>O<sub>5</sub> correlated well with that of the NH<sub>4</sub>VO<sub>3</sub> starting material, as illustrated in Figure 3-2.

The particle size distribution for Lot CML-V2-001, which employed as-received NH<sub>4</sub>VO<sub>3</sub>, had major population between 76 μ and 150 μ. In an effort to reduce the particle size of the manufactured V<sub>2</sub>O<sub>5</sub>, Lot CML-V2-003 employed NH<sub>4</sub>VO<sub>3</sub> which had been ball milled. As can be seen in Figure 3-1, this caused the percentage of fine particles (i.e., < 45 μ) to be significantly increased. However, a large portion of the population still fell in the 76-150 μ range.

### PARTICLE SIZE ANALYSIS OF V2O5

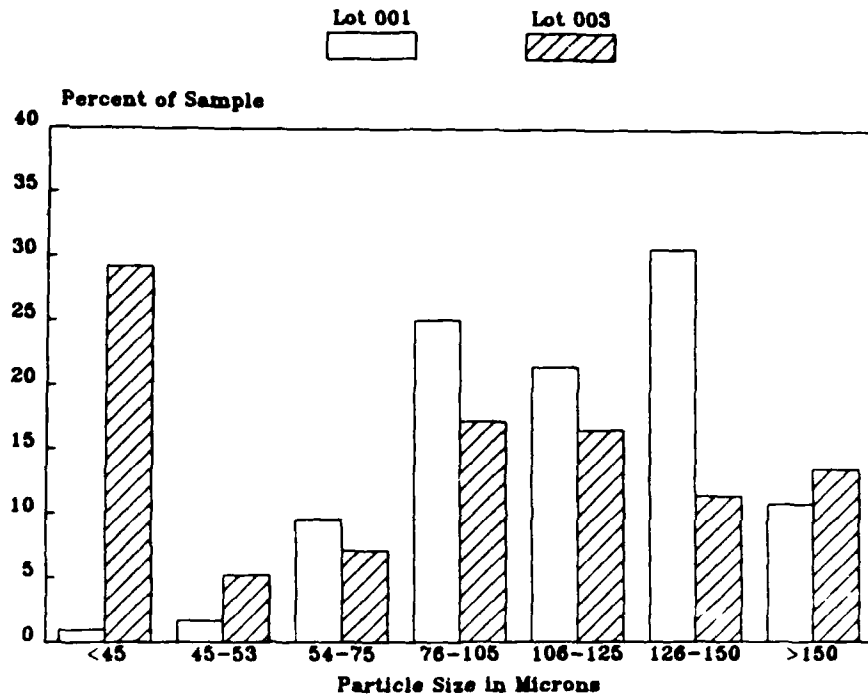


FIGURE 3-1. PARTICLE SIZE DISTRIBUTIONS FOR  $V_2O_5$   
(LOTS CML-V2-001 AND CML-V2-003)



### PARTICLE SIZE ANALYSIS

V2O5 vs. NH4VO3

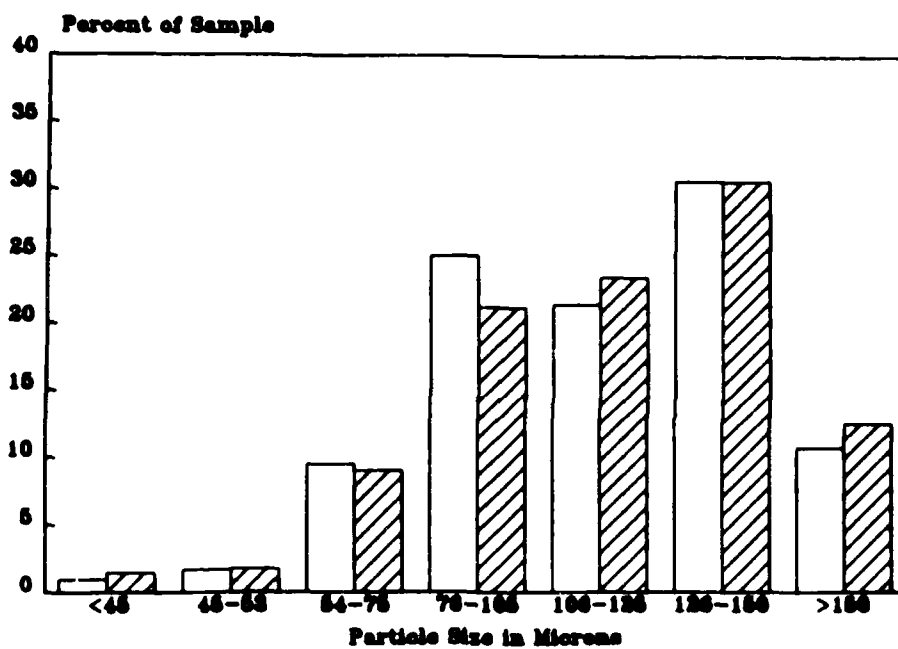


FIGURE 3-2. PARTICLE SIZE DISTRIBUTION FOR  $V_2O_5$  (LOT CML-V2-001) AND THE  $NH_4VO_3$  USED IN ITS PREPARATION

Morphology. Lot CML-V2-001 was used to characterize the morphology of the manufactured  $V_2O_5$ . Scanning electron micrographs for two sieve fractions are shown in Figure 3-3. As can be seen, the morphology changes with the particle size; the coarse particles (76-105  $\mu$ ) were observed to be ellipsoid in shape, while the fine particles (< 45  $\mu$ ) tended to be much more irregular.

Stoichiometry. The stoichiometry of the manufactured  $V_2O_5$  was determined through a wet chemical analysis for total vanadium involving a titration of 0.1N ferrous ammonium sulfate using a barium diphenylamine sulfonate indicator. The results for the three  $V_2O_5$  lots are as follows (theoretical =  $VO_{2.50}$ ):

Lot CML-V2-001:  $VO_{2.51}$   
 Lot CML-V2-002:  $VO_{2.58}$   
 Lot CML-V2-003:  $VO_{2.60}$

As can be seen, Lot CML-V2-001 was found to be in good agreement with the theoretical value while the other two lots are indicated to be oxygen rich.

Crystal Structure. The x-ray diffraction data for the three lots of  $V_2O_5$  are given in Tables 3-2 to 3-4. The results for all lots were found to be in good agreement with the Joint Committee on Powder Diffraction Standards (JCPDS).

Purity. The purity of the manufactured  $V_2O_5$  was assessed through an EDAX analysis of Lot CML-V2-001. The only impurity detected was a trace of silicon, present at an estimated concentration of 0.6 weight percent.

Electrochemical Performance. Discharge results for the three lots of  $V_2O_5$  are shown in Figure 3-4. The cathodes used in these tests were made by the cold pressing technique and contained 88 w/o  $V_2O_5$  + 10 w/o Dixon Graphite + 2 w/o Teflon for Lot 001 and 90 w/o  $V_2O_5$  + 10 w/o Dixon Graphite for Lots 002 and 003. The cells were discharged at 0.5 mA/cm<sup>2</sup> to a 2.5 volt cutoff using a 2M  $LiAsF_6$  + 0.4M  $LiBF_4$ /MF electrolyte solution. The separator consisted of one layer of 0.010" thick HV-932 glass separator. These tests employed 2-plate wick cells. Efficiencies of > 99 percent were achieved in all cases, based on a theoretical capacity of 1.0 F/mole. The average energy density was 459 Wh/kg based on active material.

Characterization Summary for  $V_2O_5$ . These characterization results show that the manufactured  $V_2O_5$  is a highly purified grade of material that can yield essentially 100 percent of theoretical capacity at low discharge rates. The particle size of  $V_2O_5$  is indicated to be determined by the particle size of the ammonium metavanadate from which it is manufactured and significant morphological differences were observed between fine and coarse particles that could influence the mechanical integrity of the finished electrodes and their cycle life performance. Although two lots of material were indicated to be oxygen rich, their discharge performance was excellent, demonstrating that the indicated variation in stoichiometry does not significantly affect electrochemical properties.

**SIEVE FRACTION ANALYZED: 76-105 $\mu$**



**SIEVE FRACTION ANALYZED: <44 $\mu$**



FIGURE 3-3. SCANNING ELECTRON MICROGRAPHS OF V<sub>2</sub>O<sub>5</sub> (LOT CML-V2-001)

TABLE 3-2. X-RAY DIFFRACTION DATA FOR  $V_2O_5$   
(LOT CML-V2-001)

hkl	d-spacing, Å		Relative Intensity, Percent	
	JCPDS Standard	Observed	JCPDS Standard	Observed
200	5.76	5.80	40	32
001	4.40	4.38	100	100
101	4.11	4.09	35	32
201	3.48	3.51	7	12
110	3.40	3.42	90	100
400	2.88	2.89	65	81
011	2.76	2.77	35	17
111	2.687	2.694	15	17
310	2.610	2.622	40	44
-	-	2.357	-	6
002	2.185	2.193	17	17
102	2.147	2.156	11	10
202	2.042	2.033	3	12
411	1.992	1.999	17	15
600	1.919	1.921	25	27
302	1.900	1.907	17	12
012	1.864	1.867	13	19
020	1.778	1.778	3	27
601	1.757	1.760	30	14
021	1.648	1.648	11	14
611	1.576	1.576	9	7
412	1.564	1.567	11	8
701	1.540	1.542	3	3
321	1.515	1.519	17	15
710	1.493	1.496	17	18
602	1.442	1.439	5	5
711	1.412	1.417	7	5

- NOTES: 1. Analysis conducted under helium flow.  
 2. Observed relative intensity based on peak height rather than on integrated peak area.  
 3. JCPDS Standard:  $a = 11.51\text{Å}$ ,  $b = 3.559\text{Å}$ ,  $c = 4.371\text{Å}$ , orthorhombic.

TABLE 3-3. X-RAY DIFFRACTION DATA FOR V<sub>2</sub>O<sub>5</sub>  
(LOT CML-V2-002)

hkl	d-spacing, Å		Relative Intensity, Percent	
	JCPDS Standard	Observed	JCPDS Standard	Observed
200	5.76	5.769	40	38
001	4.38	4.375	100	100
101	4.09	4.081	35	43
110	3.40	3.404	90	90
400	2.88	2.882	65	87
011	2.76	2.761	35	47
111	2.687	2.689	15	13
310	2.610	2.616	40	50
002	2.185	2.190	17	26
102	2.147	2.152	11	14
411	1.992	1.995	17	25
600	1.919	1.918	25	38
302	1.900	1.901	17	23
012	1.864	1.864	13	22
112	1.840	1.842	5	8
020	1.778	1.782	3	48
601	1.757	1.758	30	19
	-	1.702	-	5
021	1.648	1.651	11	20
121	1.632	1.635	7	11
611	1.576	1.576	9	11
412	1.564	1.566	11	20
701	1.540	1.540	3	10
321	1.515	1.516	17	24
710	1.493	1.495	17	27
602	1.442	1.444	5	12
711	1.412	1.414	7	15
022	1.380	1.379	5	10

- NOTES: 1. Analysis conducted in air.  
 2. Observed intensity based on peak height rather than integrated peak area.  
 3. JCPDS Standard:  $a = 11.51\text{Å}$ ,  $b = 3.559\text{Å}$ ,  $c = 4.371\text{Å}$ , orthorhombic.

TABLE 3-4. X-RAY DIFFRACTION DATA FOR  $V_2O_5$   
(LOT CML-V2-003)

hkl	d-spacing, Å		Relative Intensity, Percent	
	JCPDS Standard	Observed	JCPDS Standard	Observed
200	5.76	5.765	40	39
001	4.38	4.385	100	100
101	4.09	4.095	35	30
201	3.48	3.486	7	7
110	3.40	3.408	90	95
400	2.88	2.882	65	68
011	2.76	2.763	35	34
111	2.687	2.687	15	12
310	2.610	2.609	40	33
211	2.492	2.488	7	5
401	2.405	2.403	7	5
002	2.185	2.186	17	16
102	2.147	2.149	11	8
411	1.992	1.993	17	15
600	1.919	1.917	25	22
302	1.900	1.900	17	13
012	1.864	1.863	13	13
112	1.840	1.840	5	5
020	1.778	1.781	3	28
601	1.757	1.755	30	13
	-	1.701	-	4
021	1.648	1.649	11	13
121	1.632	1.634	7	5
611	1.576	1.575	9	8
412	1.564	1.563	11	9
701	1.540	1.538	3	5
321	1.515	1.514	17	14
710	1.493	1.492	17	17
602	1.442	1.443	5	5
711	1.412	1.413	7	6
022	1.380	1.380	5	5
303	1.363	1.362	5	5

- NOTES: 1. Analysis conducted under helium flow.  
 2. Observed intensity based on peak height rather than integrated peak area.  
 3. JCPDS Standard:  $a = 11.51\text{Å}$ ,  $b = 3.559\text{Å}$ ,  $c = 4.371\text{Å}$ , orthorhombic.

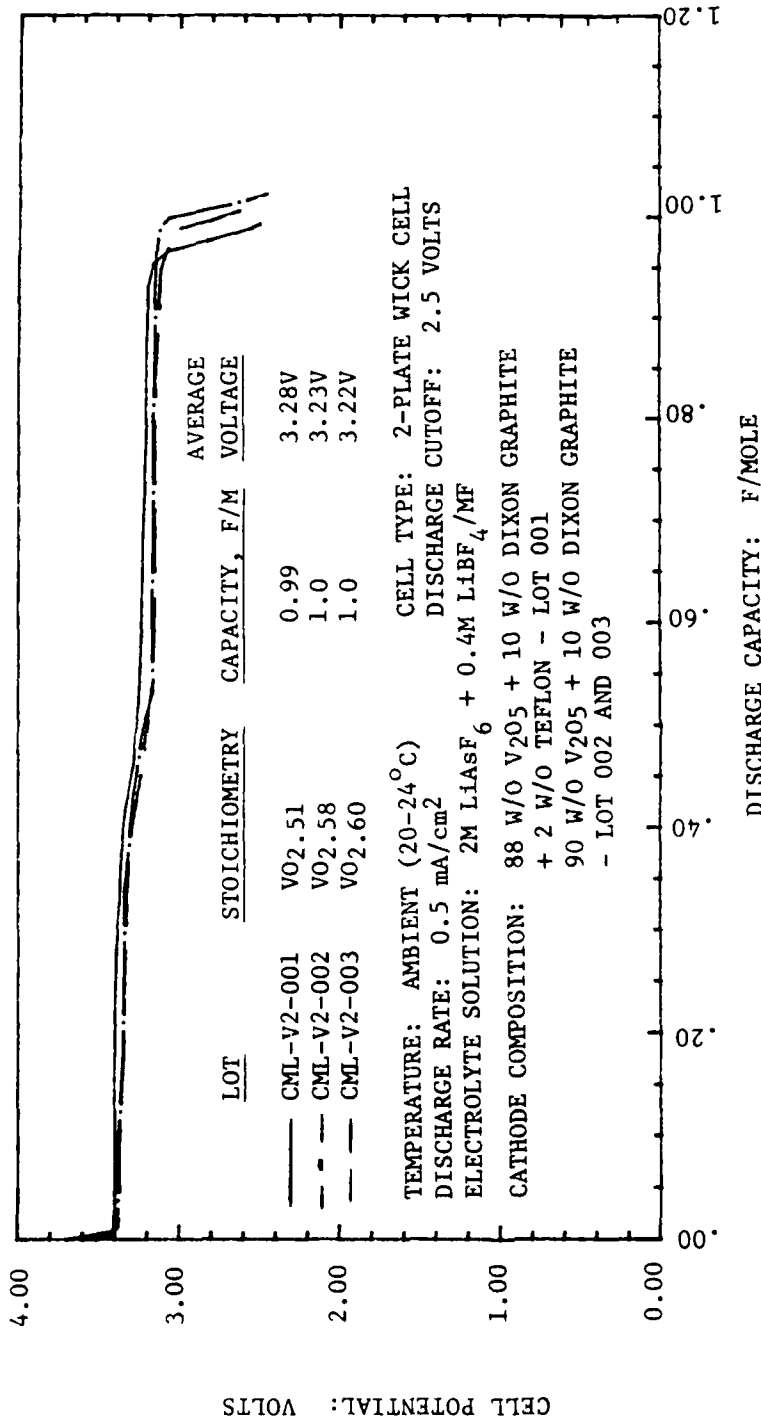


FIGURE 3-4. ELECTROCHEMICAL PERFORMANCE CHARACTERIZATION OF V<sub>2</sub>O<sub>5</sub>

Titanium Disulfide (TiS<sub>2</sub>)

Particle Size. The particle size distribution for the Degussa grade of TiS<sub>2</sub> is shown in Figure 3-5. Approximately 80 percent of the material fell at the extremes of the measured particle size range showing that the material consists primarily of a mixture of very large (>150μ) and very small (<45μ) particles.

Morphology. SEM analyses were conducted on two segregated particle size fractions; a coarse fraction (76-105μ) and a fine fraction (<45μ). The results, shown in Figure 3-6, show that both fractions are crystalline, but with significantly different particle morphology. The coarse particles are ellipsoid-shaped with some small, flake-like particles attached to the outer surface. The fine sieve fraction, however, consists almost entirely of the small flake-like particles.

Stoichiometry. The stoichiometry of TiS<sub>2</sub> was determined through combustion analysis at 900°C. The results indicate that the Degussa grade of TiS<sub>2</sub> is indeed stoichiometric, having a composition of Ti<sub>0.9992</sub>S<sub>2</sub>.

Crystal Structure. The x-ray powder diffraction pattern for TiS<sub>2</sub> is given in Table 3-5. The d-spacings are in good agreement with the JCPDS standard. The relative intensities in the observed pattern are also quite compatible with the standard except that the two strongest peaks are reversed. This discrepancy is believed to be due to preferred orientations in the sample.

Purity. EDAX analysis detected no impurities in the Degussa grade of TiS<sub>2</sub>.

Electrochemical Performance. This test was conducted in a 2-plate wick laboratory cell employing a 2M LiAsF<sub>6</sub> + 0.4M LiBF<sub>4</sub>/MF solution. The cathode contained 80 w/o TiS<sub>2</sub>, 10 w/o Dixon Graphite and 10 w/o Teflon and the cell was discharged at 0.5 mA/cm<sup>2</sup> to a 1.7V cutoff. The discharge curve is shown in Figure 3-7. The cell yielded an excellent capacity of 0.95 F/mole (theoretical = 1.0 F/mole) and the delivered energy density was 495 Wh/kg based on active material.

Characterization Summary For TiS<sub>2</sub>. The analytical results demonstrate that the Degussa grade of TiS<sub>2</sub> is of high purity and stoichiometric. The results also show that this grade of material consists primarily of very small and very large particles having significantly different morphologies.

Vanadium (V) Sulfide (V<sub>2</sub>S<sub>5</sub>)

Particle Size. No particle size analyses were conducted on the manufactured V<sub>2</sub>S<sub>5</sub>.

Morphology. The morphology of the manufactured V<sub>2</sub>S<sub>5</sub> was evaluated through SEM analysis of Lot CML-VS-002. The material was found to consist of large crystals with small crystallites dispersed over their surface. Furthermore, as illustrated in the micrograph shown in Figure 3-8, the morphology of the V<sub>2</sub>S<sub>5</sub> was found to be very similar to that of the (NH<sub>4</sub>)<sub>3</sub>VS<sub>4</sub> starting material.



### PARTICLE SIZE ANALYSIS TiS<sub>2</sub>

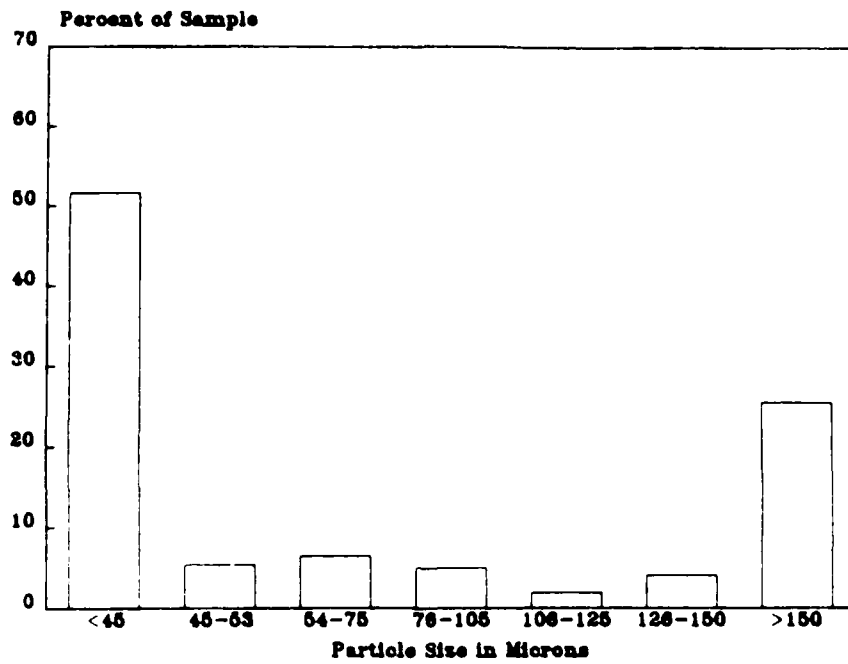


FIGURE 3-5. PARTICLE SIZE DISTRIBUTION FOR  
TiS<sub>2</sub> (DEGUSSA, AS-RECEIVED)

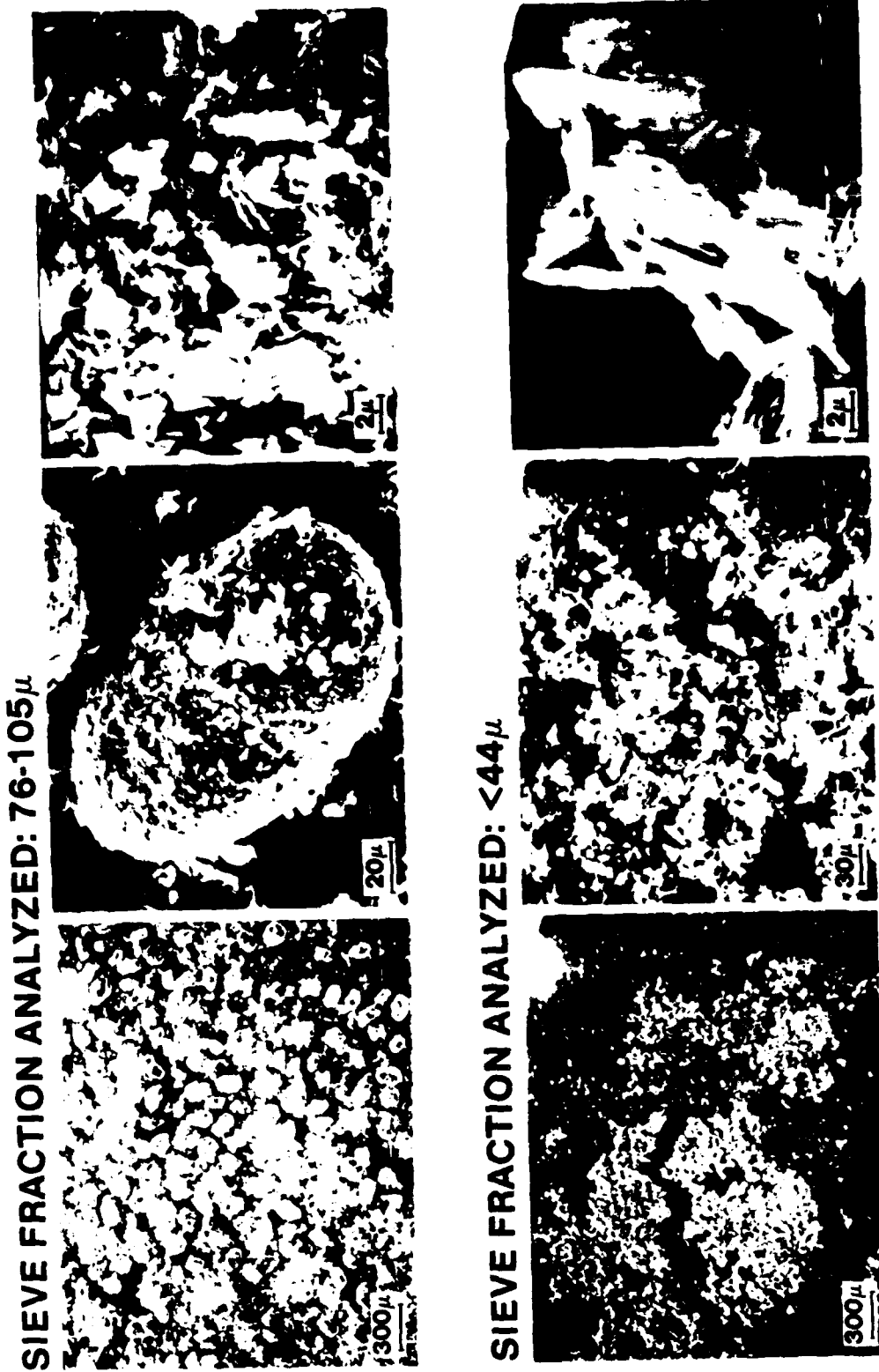


FIGURE 3-6. SCANNING ELECTRON MICROGRAPHS OF  $TiS_2$  (DECUSSA, AS-RECEIVED)

TABLE 3-5. X-RAY DIFFRACTION DATA FOR DEGUSSA TiS<sub>2</sub>  
(AS RECEIVED)

hkl	d-spacing, Å <sup>o</sup>		Relative Intensity, Percent	
	JCPDS Standard	Observed	JCPDS Standard	Observed
001	5.69	5.732	55	100
100	2.95	2.951	2	1
002	2.85	2.853	2	4
101	2.62	2.621	100	72
102	2.05	2.053	45	41
003	1.90	1.902	2	4
110	1.70	1.705	25	14
111	1.63	1.633	8	4
103	1.60	1.599	16	16
201	1.427	1.427	10	11
202	1.309	1.310	8	4
113	1.267	1.269	2	1
203	1.164	1.167	6	3
211	1.095	1.095	8	9

- NOTES: 1. Analysis conducted under helium flow.  
 2. Observed relative intensity based on peak height rather than on integrated peak area.  
 3. JCPDS Standard: a = 3.4049Å, c = 5.6912Å, hexagonal.

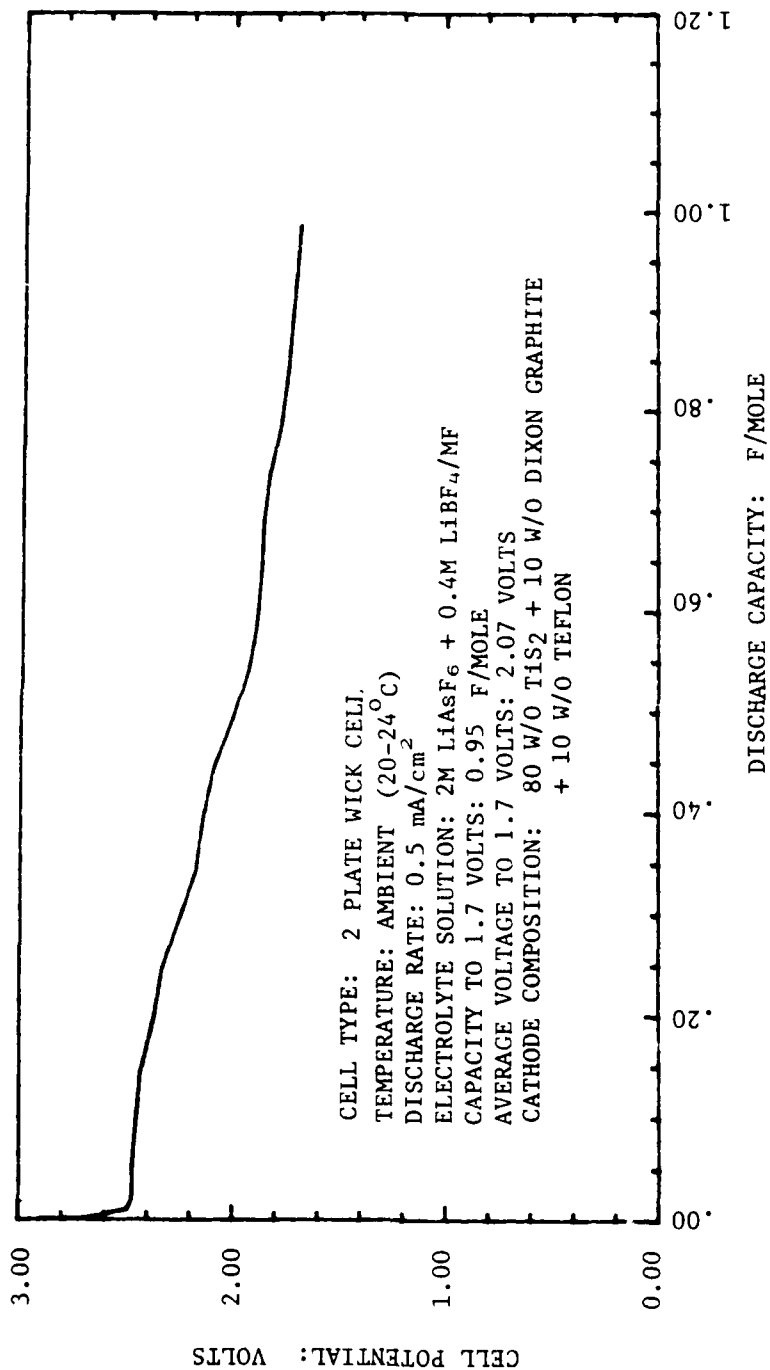


FIGURE 3-7. ELECTROCHEMICAL PERFORMANCE CHARACTERIZATION OF DEGUSSA TiS<sub>2</sub>

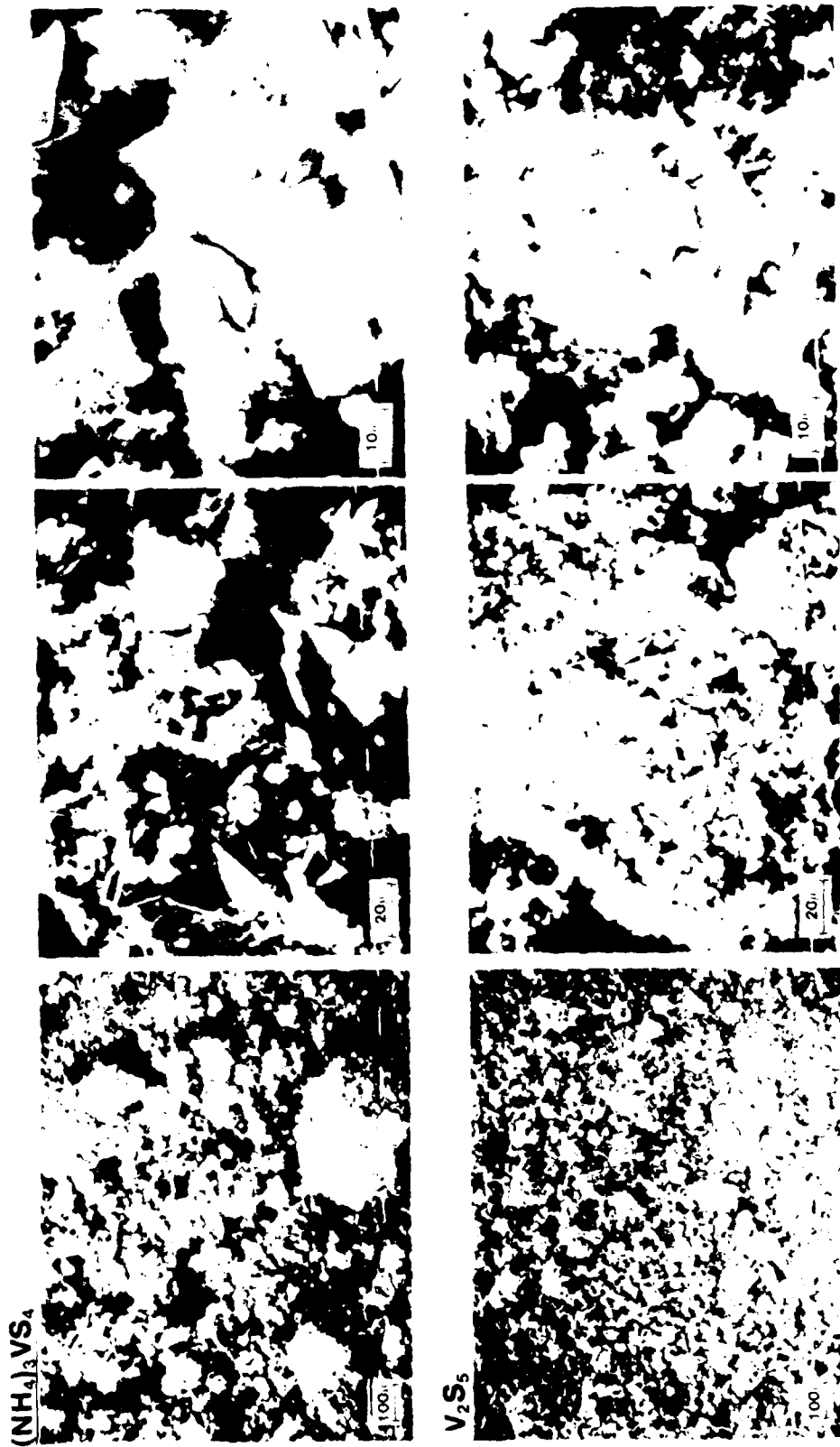


FIGURE 3-8. SCANNING ELECTRON MICROGRAPHS OF (NH<sub>4</sub>)<sub>3</sub>VS<sub>4</sub> AND THE V<sub>2</sub>S<sub>5</sub> PREPARED AT 260 °C (LOT CML-VS-002)

Stoichiometry. The stoichiometry of the manufactured  $V_2S_5$  was determined through combustion analysis in air at  $610^\circ C$  to form  $V_2O_5$ . The results were as follows:

Lot CML-VS-002:  $V_2S_{4.33}$   
 Lot CML-VS-003:  $V_2S_{4.91}$

Lot CML-VS-002, prepared at  $260^\circ C$ , is indicated to be sulfur deficient. The stoichiometry of Lot CML-VS-003, which was prepared at  $225^\circ C$ , was much closer to the theoretical value indicating that lower conversion temperatures are desirable in the manufacture of  $V_2S_5$ .

Crystal Structure. X-ray powder diffraction analysis of Lot CML-VS-002 yielded no sharp peaks confirming that the manufactured  $V_2S_5$  was amorphous.

Purity. No impurities were detected in Lot CML-VS-002 when analyzed by EDAX.

Electrochemical Discharge Performance. The cathodes used in these tests contained 80 w/o  $V_2S_5$ , 10 w/o Dixon Graphite and 10 w/o Teflon for Lot 2 and 90 w/o  $V_2S_5$  and 10 w/o Dixon Graphite for Lot 3. The cells were discharged at  $0.5 \text{ mA/cm}^2$  to a 1.5V cutoff using a 2M  $LiAsF_6$  + 0.4M  $LiBF_4$ /MF solution.

The tests yielded delivered capacities of less than 2 F/mole with both lots of  $V_2S_5$  (Figure 3-9). This output is significantly less than the 5 F/mole theoretical capacity. The average energy density was 426 Wh/Kg based on active material. The solution and separator were both observed to be discolored in the discharged cells.

Characterization Summary for  $V_2S_5$ . The results indicate that the temperature used to convert  $(NH_4)_3VS_4$  to  $V_2S_5$  can affect the stoichiometry of the product. At  $260^\circ C$ , the prepared material is indicated to be sulfur deficient while at  $225^\circ C$ , the product had a stoichiometry in reasonable agreement with the theoretical value.

The cell performance achieved with the two lots of  $V_2S_5$  is very similar to that reported by Jacobsen et al<sup>10</sup> for cells cycled approximately 10 times using  $LiClO_4$ /dioxolane electrolyte solution. They postulate that the observed capacity degradation may be due to the removal of edge sulfur atoms as lithium sulfide accompanied by polymerization to form amorphous  $VS_2$ . With ester-based solutions, we believe that similar compositional changes are occurring, but much more rapidly, being essentially complete by the end of the first discharge. The discoloration observed in the discharged cells further attests to compositional changes occurring in  $V_2S_5$ .

The compositional instability, apparently intrinsic to  $V_2S_5$ , indicates that, in practice, a  $Li/V_2S_5$  system should be treated as a  $Li/VS_2$  system. Assuming a reversible depth of discharge of 2.0 F/mole and an average voltage of 2.28 volts for  $VS_2$ ,<sup>10</sup> the theoretical energy density therefore decreases from 843 Wh/Kg to 443 Wh/Kg, thus offering no advantage over either

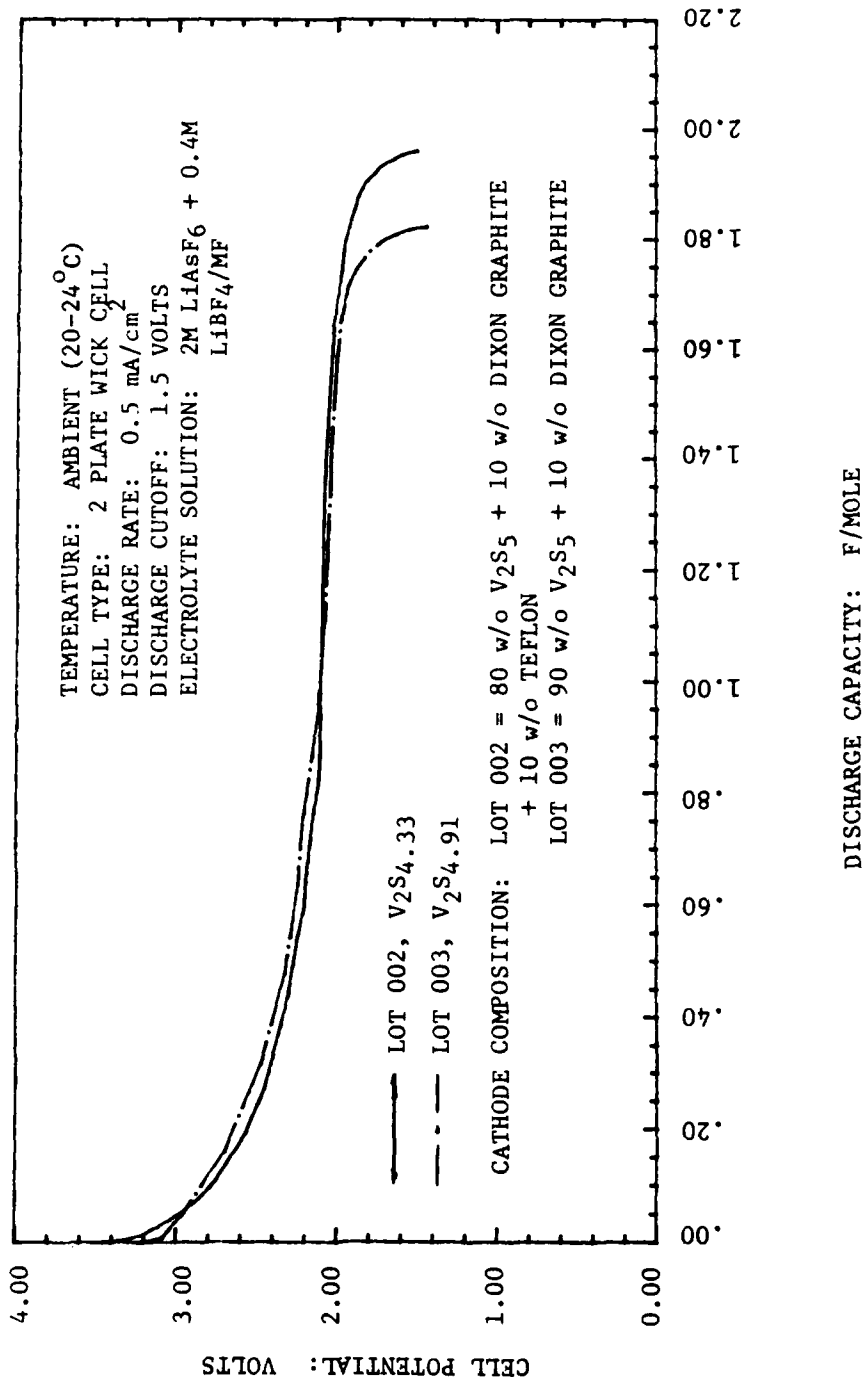


FIGURE 3-9. ELECTROCHEMICAL PERFORMANCE CHARACTERIZATION OF V<sub>2</sub>S<sub>5</sub>

$V_2O_5$  or  $TiS_2$ . This low energy density, combined with the difficulties in processing  $V_2S_5$  due to its extreme sensitivity to moisture and oxygen, significantly diminishes the attractiveness of  $V_2S_5$ . As a result, no further work was done with this cathode material.

### $Li_xCoO_2$

Particle Size. The particle size distribution for Lot CML-CO-002 is shown in Figure 3-10. The material was found to consist primarily of very large and very small particles with the major fraction falling in the  $> 150 \mu$  range.

Morphology. SEM micrographs for the manufactured  $Li_xCoO_2$ , Lot CML-CO-002, are shown in Figure 3-11. The material was found to be highly crystalline and the wide range of particle sizes are clearly shown.

Stoichiometry. The stoichiometry of  $Li_xCoO_2$  was determined through atomic absorption analysis for lithium and cobalt. The results were as follows:

Lot CML-CO-002:  $Li_{0.85}Co_{0.97}O_2$   
 Lot CML-CO-003:  $Li_{1.00}Co_{1.00}O_2$

Crystal Structure. The x-ray powder diffraction data for the two lots of  $Li_xCoO_2$  are given in Tables 3-6 and 3-7. The results for both lots are in good agreement with the JCPDS standard.

Purity. EDAX analysis of  $Li_xCoO_2$ , Lot CML-CO-002, detected no impurities in the manufactured material.

Electrochemical Performance.  $Li_xCoO_2$  is prepared in the discharged state, thus necessitating a cell to be charged before its electrochemical performance can be evaluated. The following paragraphs describe tests that were conducted as part of the characterization of Lot CML-CO-002 material. All cells employed aluminum current collectors in the cathode to prevent corrosion problems at the high oxidizing potentials present with this system.

Figure 3-12 shows the initial charge and discharge performance of a  $Li/Li_xCoO_2$  2-plate wick cell at  $0.5 \text{ mA/cm}^2$  employing a  $2M LiAsF_6 + 0.4M LiBF_4/MP$  solution. The cathode consisted of 80 w/o  $Li_xCoO_2$ , 10 w/o Shawinigan Acetylene Black (SAB, 50 percent compressed) and 10 w/o Teflon, and was prepared by the cold pressing technique. Charging was accomplished on a test station with the upper voltage limit set at 5.0 volts. However, no upward deflection in the voltage occurred to signal a fully charged state. As a result, the cell potential never reached 5 volts so the charge was manually terminated after a charge capacity of 1 F/mole. This represents approximately 15 percent overcharge based on the measured stoichiometry of the starting cathode material. At the end of the charge period, the electrolyte solution was observed to be dark amber in color, indicating that some decomposition of the solution had occurred. On the subsequent discharge, the cell delivered only 56 percent of the theoretical capacity, based on 1.0 F/mole.



**PARTICLE SIZE ANALYSIS OF  $\text{Li}_x\text{CoO}_2$**   
**Lot CML-CO-002**

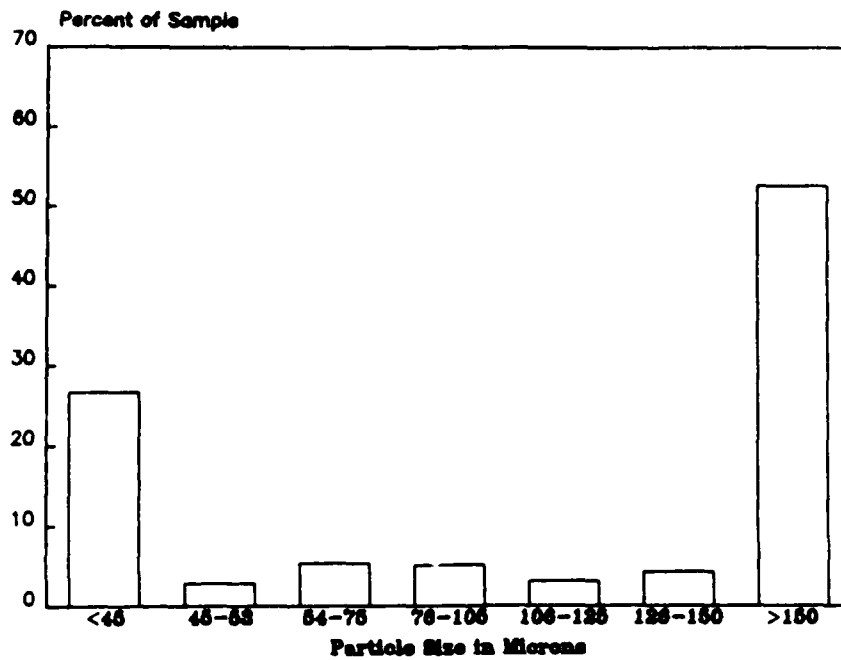


FIGURE 3-10. PARTICLE SIZE DISTRIBUTION FOR  $\text{Li}_x\text{CoO}_2$   
(LOT CML-CO-002)

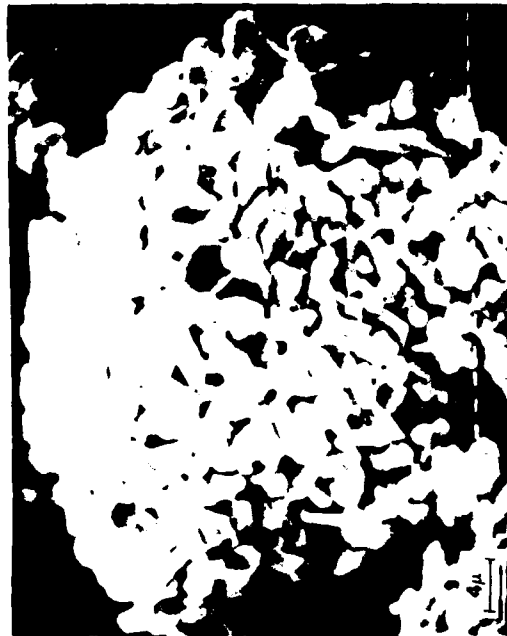
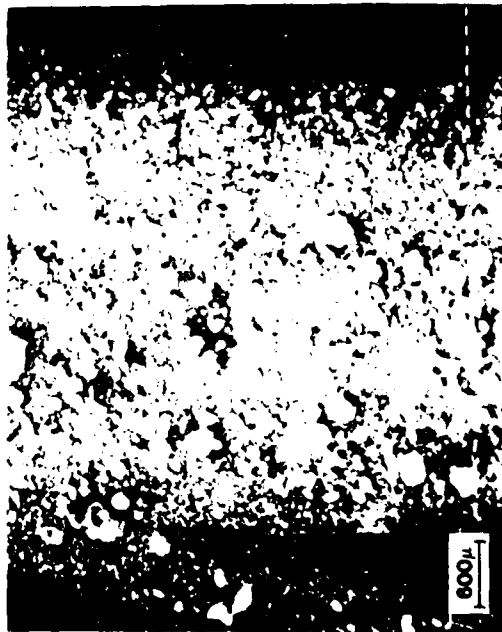
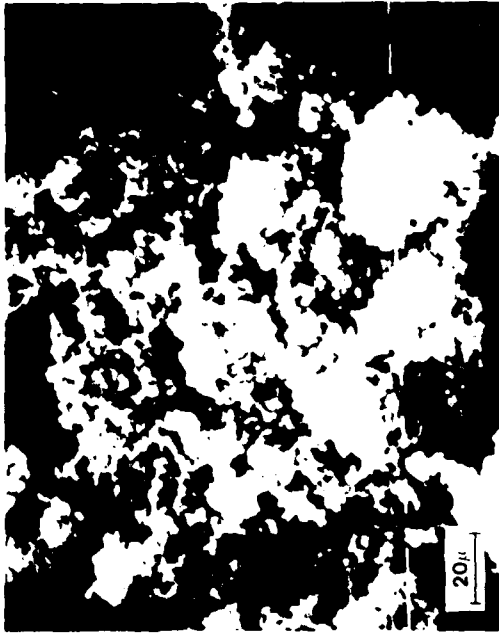


FIGURE 3-11. SCANNING ELECTRON MICROGRAPHS OF  $Li_xCoO_2$  (LOT CML-CO-002)

TABLE 3-6. X-RAY DIFFRACTION DATA FOR  $\text{Li}_x\text{CoO}_2$   
(LOT CML-CO-002)

<u>hkl</u>	<u>d-spacing, Å</u>		<u>Relative Intensity, Percent</u>	
	<u>JCPDS Standard</u>	<u>Observed</u>	<u>JCPDS Standard</u>	<u>Observed</u>
003	4.68	4.686	100	100
		2.435		14
101	2.401	2.404	16	52
006	2.346	2.344	4	16
012	2.302	2.304	4	19
104	2.001	2.003	35	95
015	1.841	1.840	6	18
107	1.549	1.551	10	20
018	1.424	1.426	10	24
110	1.407	1.409	8	28
113	1.348	1.349	6	18
<u>1010</u>	1.215	1.216	2	10
116	1.206	1.208	2	7
024	1.151	1.152	6	12
<u>0111</u>	1.130	1.132	4	7
119	1.045	1.046	2	5
027	1.041	1.043	4	6
208	1.001	1.003	6	7
<u>0210</u>	0.920	0.9204	2	6
<u>1112</u>	0.900	0.9010	4	9

- NOTES: 1. Analysis conducted under helium flow, sample was covered by scotch tape.
2. Observed relative intensity based on peak height rather than on integrated peak area.
3. JCPDS Standard:  $a = 2.8166\text{Å}$ ,  $c = 14.052\text{Å}$ , Hexagonal (rhombohedral). Observed:  $a = 2.818\text{Å}$ ,  $c = 14.050\text{Å}$ , Hexagonal (rhombohedral).

TABLE 3-7. X-RAY DIFFRACTION RESULTS FOR  $\text{Li}_x\text{CoO}_2$   
(LOT CML-CO-003)

<u>hkl</u>	<u>d-spacing, Å</u>		<u>Relative Intensity, Percent</u>	
	<u>JCPDS Standard</u>	<u>Observed</u>	<u>JCPDS Standard</u>	<u>Observed</u>
003	4.68	4.708	100	100
		2.439		9
101	2.401	2.405	16	42
006	2.346	2.344	4	6
012	2.302	2.305	4	13
104	2.001	2.007	35	77
015	1.841	1.859	6	6
107	1.549	1.554	10	17
018	1.424	1.428	10	23
110	1.407	1.412	8	21
		1.408 <sup>-1</sup>		13
113	1.348	1.352 <sup>-2</sup>	6	14
		1.349 <sup>-1</sup>		9
1010	1.215	1.220 <sup>-2</sup>	2	6
116	1.206	1.209	2	5
0012	1.169	1.172	4	3
024	1.151	1.154 <sup>-1</sup>	6	9
		1.150 <sup>-2</sup>		5
0111	1.130	1.134 <sup>-1</sup>	4	6
		1.130 <sup>-2</sup>		3
205	1.118	1.120 <sup>-2</sup>	2	3
		1.117 <sup>-1</sup>		2
027	1.041	1.044 <sup>-2</sup>	4	4

- NOTES: 1. Analysis conducted under helium flow.  
 2. Observed relative intensity based on peak height rather than on integrated peak area.  
 3. JCPDS Standard:  $a = 2.8166\text{Å}$ ,  $c = 14.052\text{Å}$ . Hexagonal (rhombohedral).

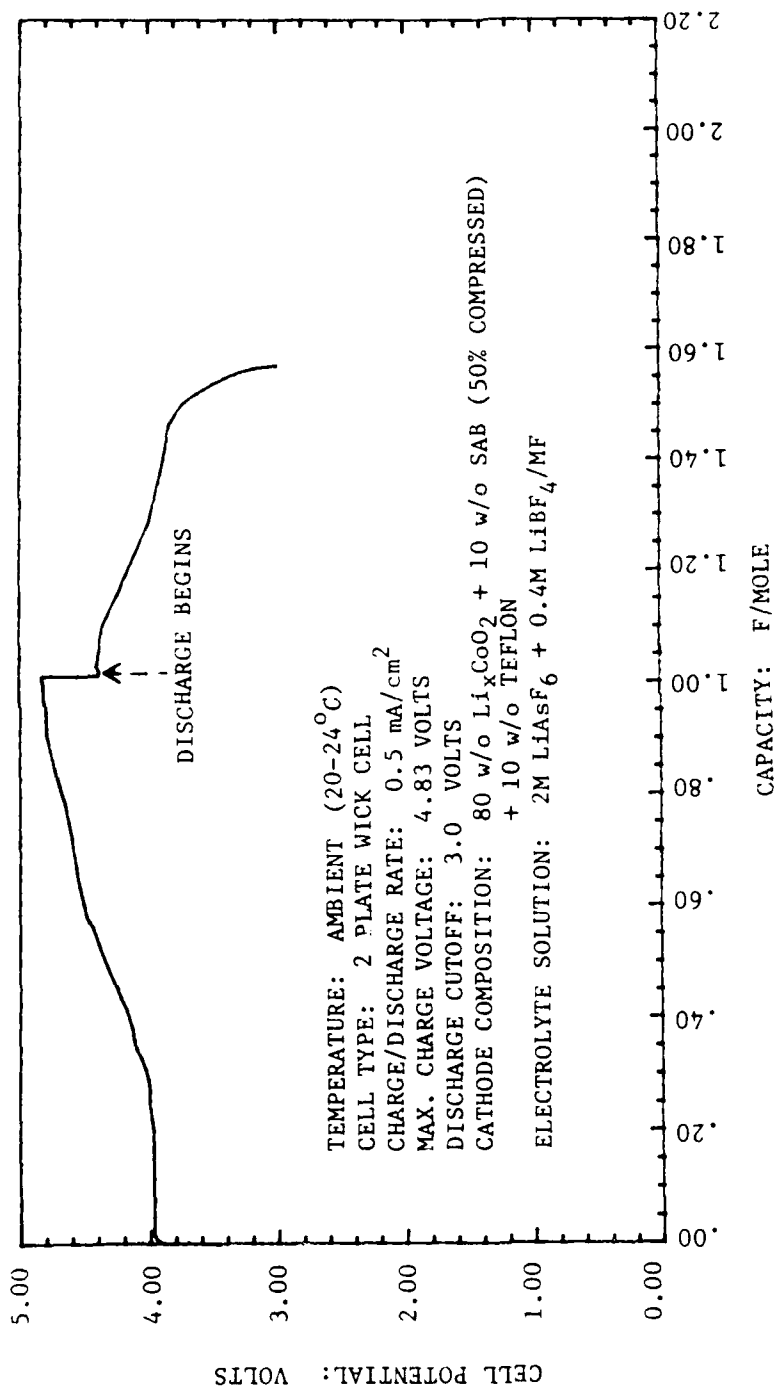


TABLE 3-12. ELECTROCHEMICAL PERFORMANCE CHARACTERIZATION OF Li<sub>x</sub>CoO<sub>2</sub>  
 (LOT CML-CO-002, Li<sub>0.85</sub>Co<sub>0.9702</sub>)

Since the low discharge capacity obtained in the first test could have been due to the observed electrolyte decomposition, additional tests were conducted to investigate the effects of solution composition on cell performance. The three solutions employed were:

2M LiAsF<sub>6</sub> + 0.4M LiBF<sub>4</sub>/MF (baseline solution)  
 2M LiAsF<sub>6</sub>/MF  
 1.5M LiAsF<sub>6</sub>/MA

These tests were designed to determine (1) whether or not LiBF<sub>4</sub> was the cause of the observed solution decomposition and (2) if methyl acetate solutions could offer better performance with Li<sub>x</sub>CoO<sub>2</sub>. The cold pressed cathodes used in these tests consisted of 90 w/o Li<sub>x</sub>CoO<sub>2</sub> and 10 w/o Teflon. No conductive diluent was employed in order to eliminate any possible carbon-catalyzed decomposition reactions. All testing was done at charge/discharge rate of 0.5 mA/cm<sup>2</sup>.

The initial charge/discharge curves for the three cells are shown in Figures 3-13 to 3-15. As with the first test, no upward deflection in voltage was observed in any of the cells during charging to indicate a fully charged condition. Therefore, charging was terminated at a capacity of approximately 1 F/mole. The following observations summarize the charging tests.

- o In general, the charging curves consisted initially of a relatively constant voltage (below 4.0 volts) for a duration dependent on the solvent medium. The cell employing the methyl acetate solution received the greatest charge in this region.
- o After charging to about 0.8 F/mole, the cells employing the methyl formate solutions both exhibited irregularities in the voltage/time curves indicating the possible onset of decomposition reactions due to overcharge. The amber color of the solutions at the end of charge confirm that some solution decomposition had occurred. Also, since decomposition was observed in both solutions, LiBF<sub>4</sub> is eliminated as the source of instability.
- o The cell employing the methyl acetate solution exhibited a smooth voltage profile throughout the charging process and the solution remained clear indicating that methyl acetate solutions may offer superior capabilities for use with Li<sub>x</sub>CoO<sub>2</sub>.

The discharge performance of the three cells is summarized in Table 3-8. Both cells employing methyl formate solutions yielded low capacities, apparently due to the observed solution decomposition during charge. The cell incorporating the methyl acetate solution yielded a much better efficiency along with an excellent energy density of 841 Wh/Kg (based on active components only). The fact that this latter cell delivered a capacity very close to the lithium content of the starting cathode material suggests that the maximum depth of discharge that can be achieved with Li<sub>x</sub>CoO<sub>2</sub> may be determined by the stoichiometry of the material when manufactured.

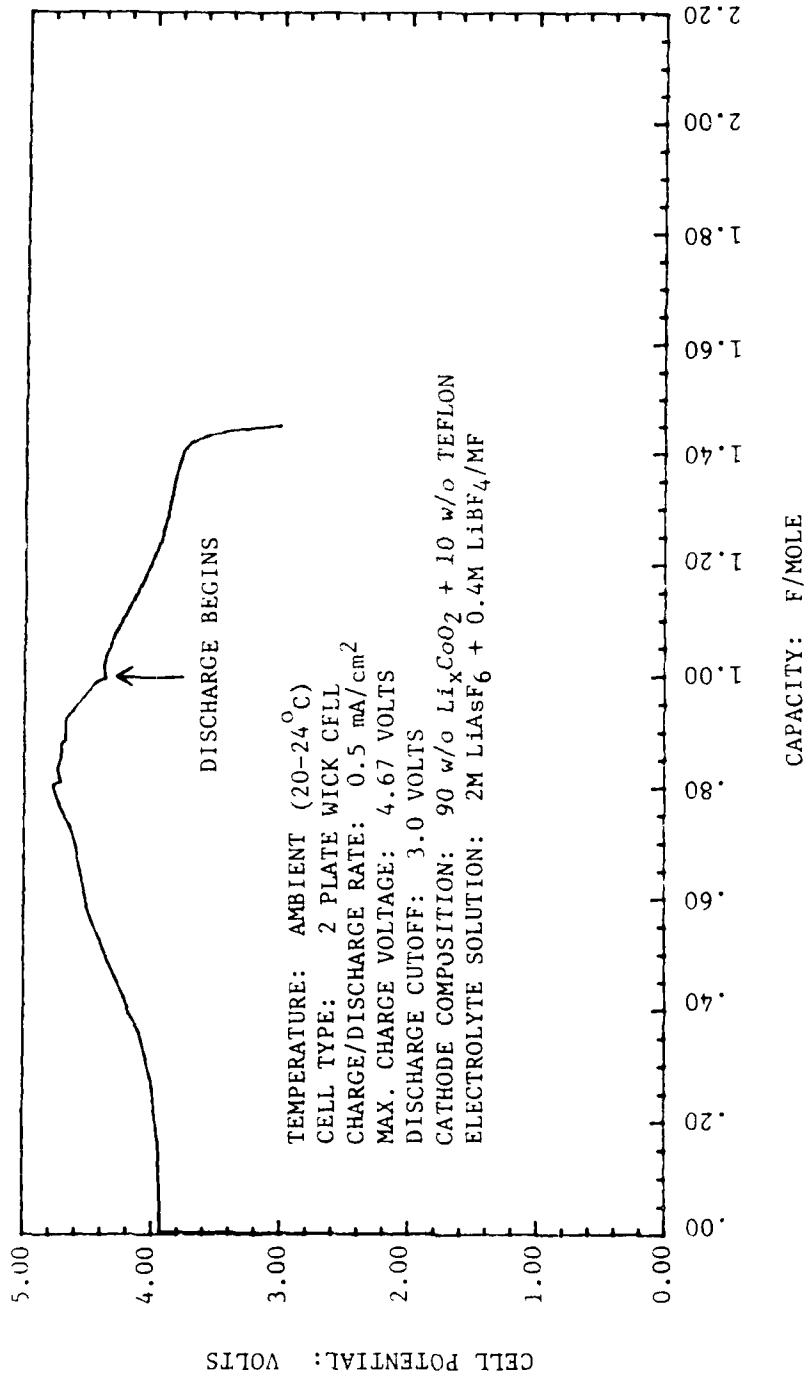


FIGURE 3-13. CHARGE-DISCHARGE PERFORMANCE OF A Li/Li<sub>x</sub>CoO<sub>2</sub> CELL WITH 2M LiAsF<sub>6</sub> + 0.4M LiBF<sub>4</sub>/MF SOLUTION (Li<sub>x</sub>CoO<sub>2</sub> = LOT CML-CO-002)

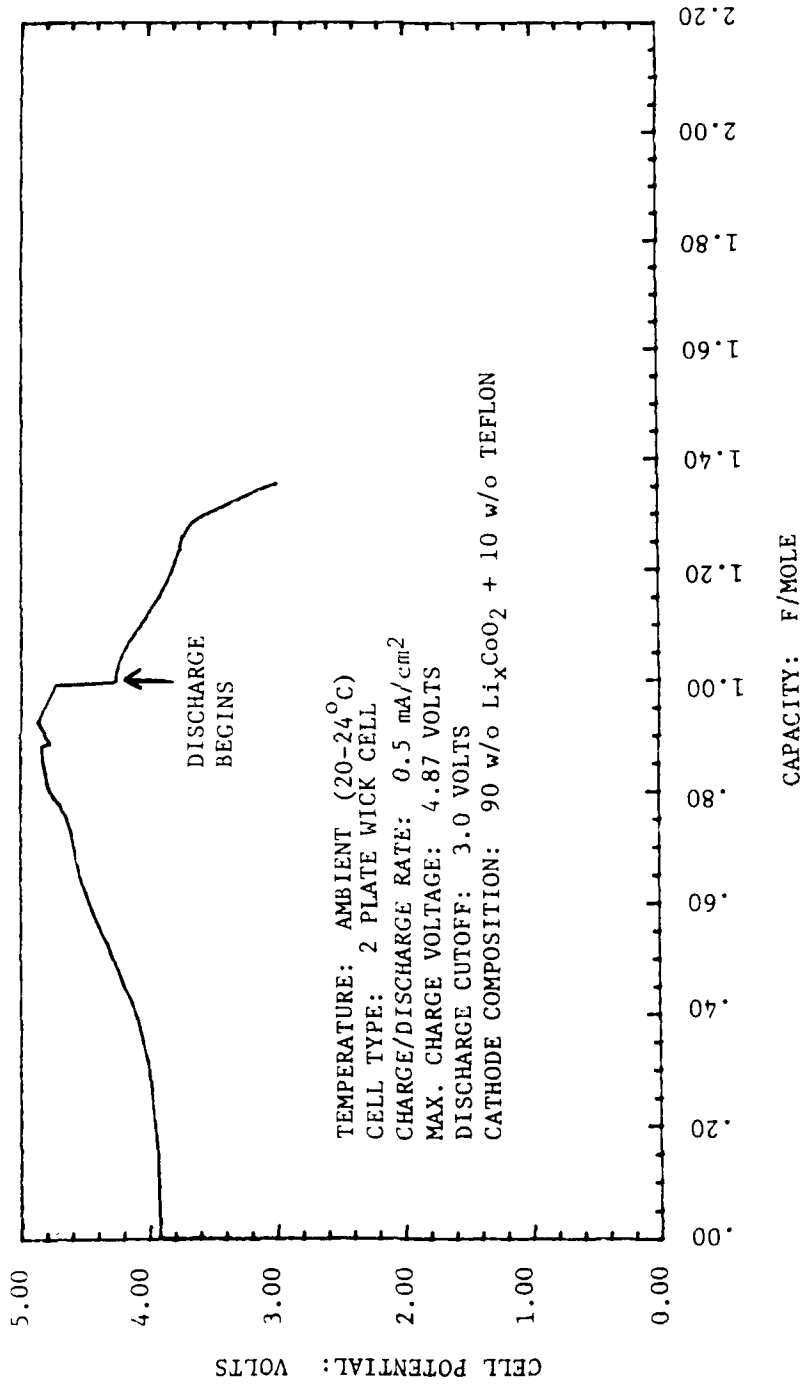


FIGURE 3-14. CHARGE-DISCHARGE PERFORMANCE OF A Li/Li<sub>x</sub>CoO<sub>2</sub> CELL WITH 2M LiAsF<sub>6</sub>/MF SOLUTION (Li<sub>x</sub>CoO<sub>2</sub> = LOT CML-CO-002)



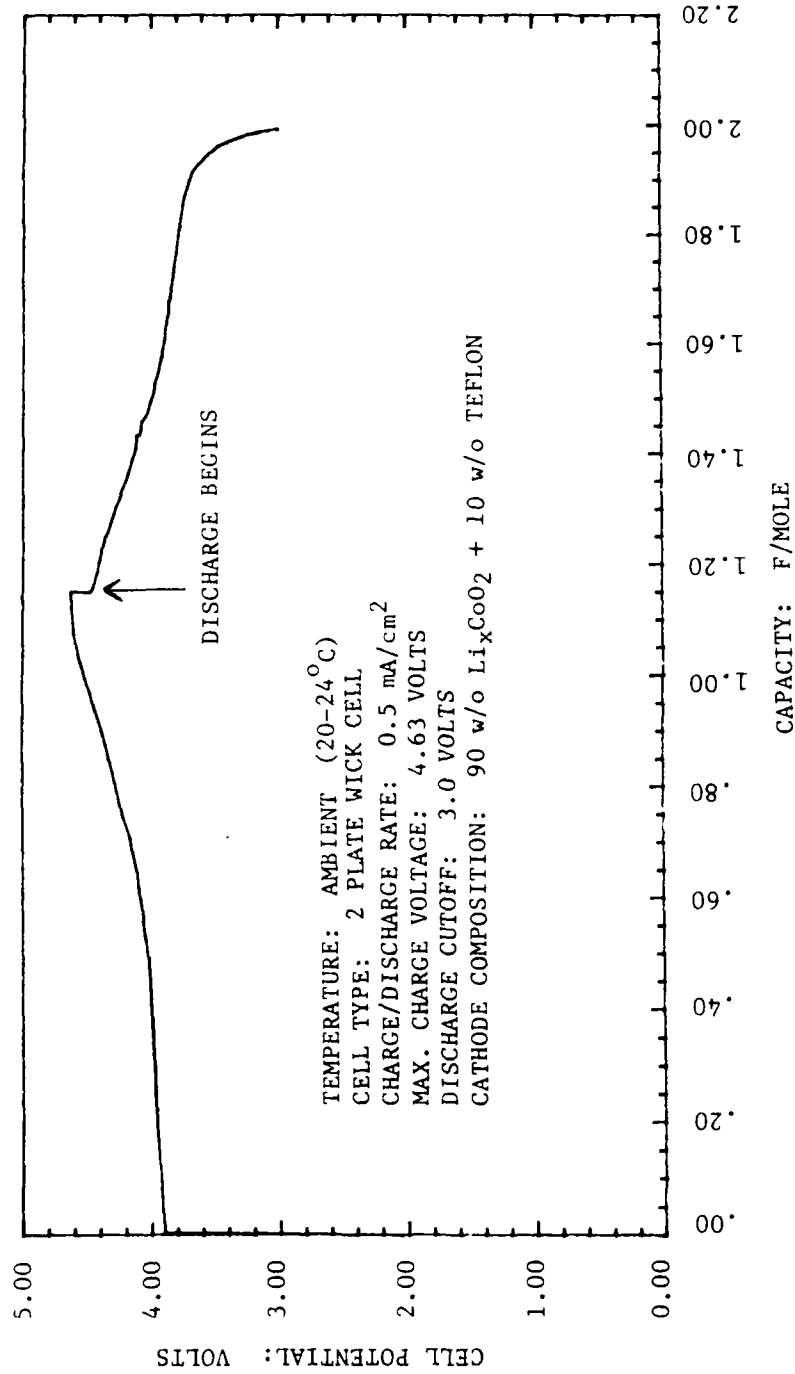


FIGURE 3-15. CHARGE-DISCHARGE PERFORMANCE OF A Li/Li<sub>x</sub>CoO<sub>2</sub> CELL WITH 1.5M LiAsF<sub>6</sub>/MA SOLUTION (Li<sub>x</sub>CoO<sub>2</sub> = LOT CML-CO-002)

TABLE 3-8. DISCHARGE RESULTS FOR Li/Li<sub>x</sub>CoO<sub>2</sub> CELLS

<u>Electrolyte Solution</u>	<u>Delivered Capacity, F/Mole</u>	<u>Average Voltage, V</u>	<u>Energy Density, Wh/Kg</u>
2M LiAsF <sub>6</sub> + 0.4M LiBF <sub>4</sub> /MF	0.46	4.01	521
2M LiAsF <sub>6</sub> /MF	0.36	3.84	366
1.5M LiAsF <sub>6</sub> /MA	0.84	3.96	841

NOTES: 1. The above performance values are based on a 3.0V cutoff.  
 2. The cathode composition was 90 w/o Li<sub>x</sub>CoO<sub>2</sub> + 10 w/o Teflon binder. (Li<sub>x</sub>CoO<sub>2</sub> = Lot CML-CO-002).  
 3. The energy density<sup>x</sup> is based on active material only.

Characterization Summary of Li<sub>x</sub>CoO<sub>2</sub>. The analytical results show that the manufactured Li<sub>x</sub>CoO<sub>2</sub> is of high purity. However, the reason for the difference in stoichiometry between the two lots of material is not clear. Evaluation of the electrochemical performance of the manufactured Li<sub>x</sub>CoO<sub>2</sub> was complicated by apparent electrolyte solution decomposition during charging. Although improved performance was achieved using methyl acetate solutions in place of methyl formate solutions, the absence of a voltage deflection at the end of charge indicates that a solution electrolysis reaction may still be accompanying the charging process. Therefore, the ability to charge this high voltage cathode material remains a key concern, even with the more electrochemically stable ester-based solutions. These initial results also indicate that the depth of discharge achievable with Li<sub>x</sub>CoO<sub>2</sub> may be determined by the stoichiometry of the starting cathode material.

#### CYCLE LIFE TESTS

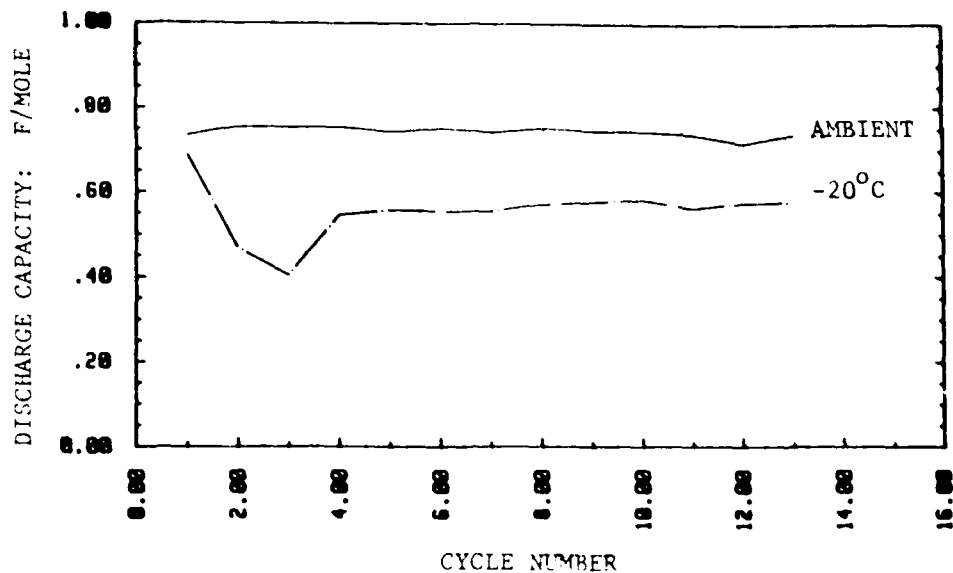
The objective of the cycle life tests was to define the reversibility of each cathode material in each of the electrolyte solutions. Due to the many cells involved, the tests were limited to the minimum number of cycles needed to reach a conclusion on each system. Generally, 10 to 40 cycles were sufficient for this purpose. Because at this point in the program, cathode composition and manufacturing processes had not been optimized for the various cathode materials.

V<sub>2</sub>O<sub>5</sub>

The cycle life performance for the V<sub>2</sub>O<sub>5</sub> laboratory cells is shown in Figures 3-16 to 3-18. At ambient temperature (20-24°C) the methyl formate solutions gave the best performance where the capacity remained constant at the 0.75 F/mole level. Cells employing methyl acetate and dimethyl sulfite solutions showed a sharp decline in capacity after 8 to 10 cycles. The loss in capacity with the dimethyl sulfite solutions appears to be caused by a loss of charging efficiency. Beginning with the fourth charge, a peak appeared in the charging voltage profile (Figure 3-19) and on the subsequent discharge the cell behaved as though it had only been partially charged, although the full charge capacity had been delivered to the cell. These results indicate that electrolysis of dimethyl sulfite may be occurring during the charging of V<sub>2</sub>O<sub>5</sub> cells.

At -20°C, all of the solvents exhibited a dip in capacity in the first 4 to 6 cycles. This dip is attributed to incomplete charging of the cells caused by the 3.6V limit. After the first few cycles, the charging cutoff voltage was increased to 3.8V, which greatly improved cell performance. Overall, the best performance was achieved with methyl formate solutions where the capacity leveled out at approximately 0.58 F/mole. Dimethyl sulfite also performed relatively well at the low temperature.

Based on these results, methyl formate is clearly shown to be the superior solvent for use with V<sub>2</sub>O<sub>5</sub>. A typical discharge-charge curve with the methyl formate solution is shown in Figure 3-20. Furthermore, when used with methyl formate solutions, V<sub>2</sub>O<sub>5</sub> has been demonstrated to offer good cycle life capabilities with no degradation in capacity observed in the limited cycle life tests conducted.



CHARGE/DISCHARGE RATE: 1.0 mA/cm<sup>2</sup>

DEPTH OF DISCHARGE: 0.75 F/mole

DISCHARGE VOLTAGE LIMIT: 2.8 Volts

CHARGE VOLTAGE LIMITS: AMBIENT TEMPERATURE (20-24°C)

Cycles 1-2 = 3.6V

Cycles 3-13 = 3.7V

-20°C

Cycles 1-3 = 3.6V

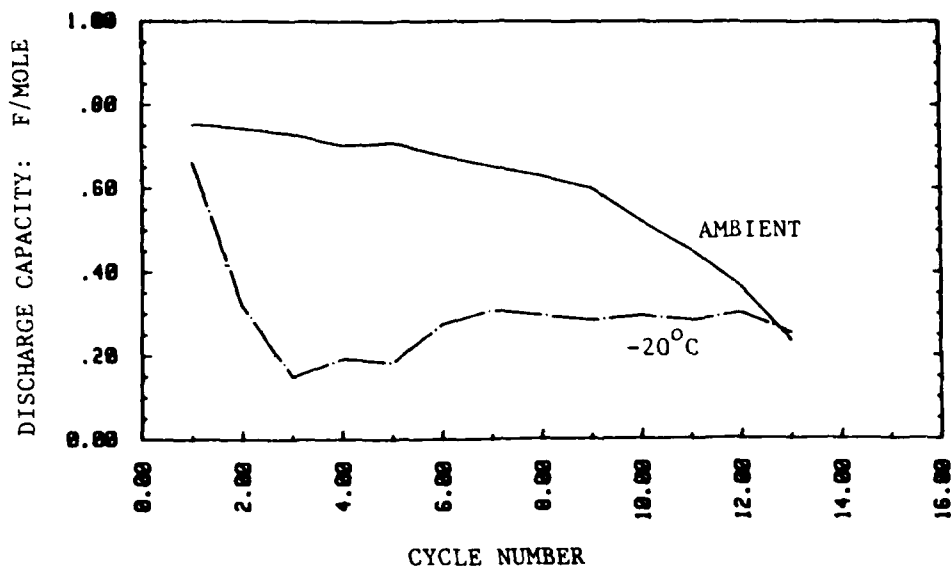
Cycles 4-13 = 3.8V

CELL TYPE: 3 PLATE WICK CELL

CATHODE COMPOSITION: 86 w/o V<sub>2</sub>O<sub>5</sub> + 10 w/o SAB (50% compressed) +  
4 w/o isotactic-polypropylene

SEPARATOR: 2 layers of Celgard 2400 (0.001" thick each)

FIGURE 3-16. V<sub>2</sub>O<sub>5</sub> SCREENING STUDIES: CYCLE LIFE PERFORMANCE WITH 2M LiAsF<sub>6</sub> + 0.4M LiBF<sub>4</sub>/MF SOLUTIONS



CHARGE/DISCHARGE RATE: 1.0 mA/cm<sup>2</sup>

DEPTH OF DISCHARGE: 0.75 F/Mole

DISCHARGE VOLTAGE LIMIT: 2.8V

CHARGE VOLTAGE LIMITS: Ambient Temperature (20-24°C)

Cycles 1-2 = 3.6V

Cycles 3-13 = 3.7V

-20°C

Cycles 1-4 = 3.6V

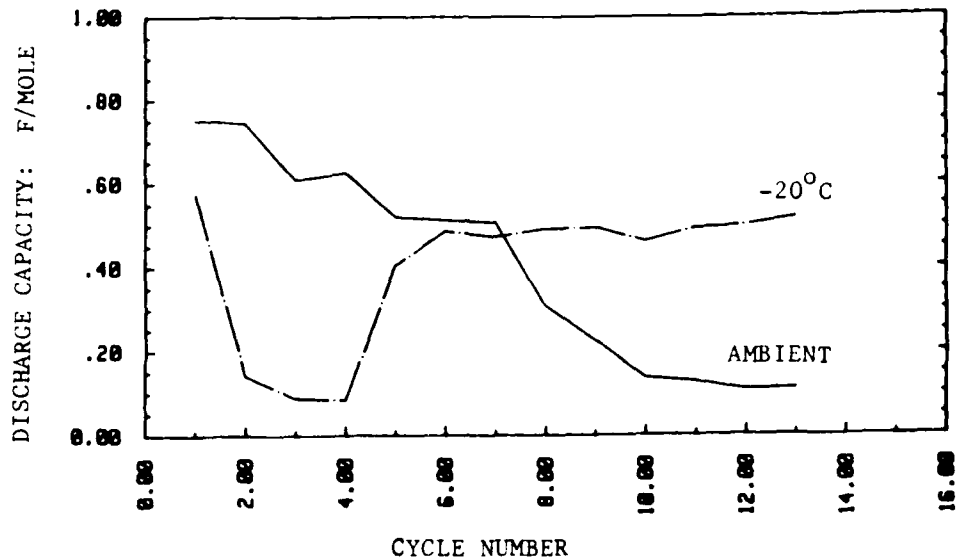
Cycles 5-13 = 3.8V

CELL TYPE: 3 PLATE WICK CELL

CATHODE COMPOSITION: 86 w/o V<sub>2</sub>O<sub>5</sub> + 10 w/o SAB (50% compressed) +  
4 w/o isotactic-polypropylene

SEPARATOR: 2 layers of Celgard 2400 (0.001" thick each)

FIGURE 3-17. V<sub>2</sub>O<sub>5</sub> SCREENING STUDIES: CYCLE LIFE PERFORMANCE WITH 2M LiAsF<sub>6</sub>/MA SOLUTIONS



CHARGE/DISCHARGE RATE:  $1.0 \text{ mA/cm}^2$

DEPTH OF DISCHARGE: 0.75 F/Mole

DISCHARGE VOLTAGE LIMIT: 2.8 Volts

CHARGE VOLTAGE LIMITS: Ambient Temperature (20-24°C)

Cycles 1-2 = 3.6V

Cycles 3-13 = 3.7V

-20°C

Cycles 1-5 = 3.6V

Cycles 6-13 = 3.8V

CELL TYPE: 3 PLATE WICK CELL

CATHODE COMPOSITION: 86 w/o  $\text{V}_2\text{O}_5$  + 10 w/o SAB (50% compressed) +  
4 w/o isotactic-polypropylene

SEPARATOR: 2 layers of Celgard 2400 (0.001" thick each)

FIGURE 3-18.  $\text{V}_2\text{O}_5$  SCREENING STUDIES: CYCLE LIFE PERFORMANCE WITH 1M  $\text{LiAsF}_6/\text{DMSI}$  SOLUTION

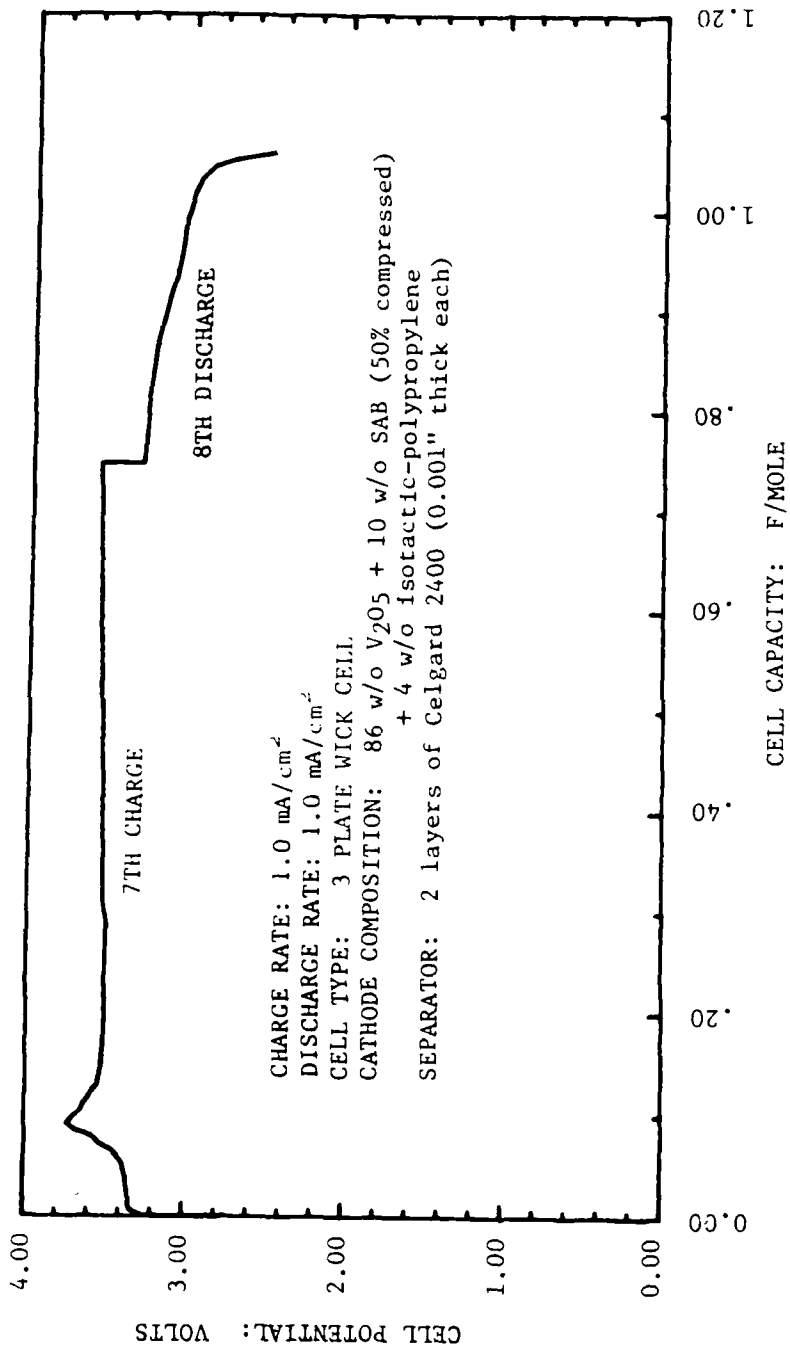


FIGURE 3-19. CHARGE/DISCHARGE BEHAVIOR OF Li/V<sub>2</sub>O<sub>5</sub> CELLS WITH 1.0M LiAsF<sub>6</sub>/DMSI SOLUTION AT AMBIENT (20-24°C) TEMPERATURE

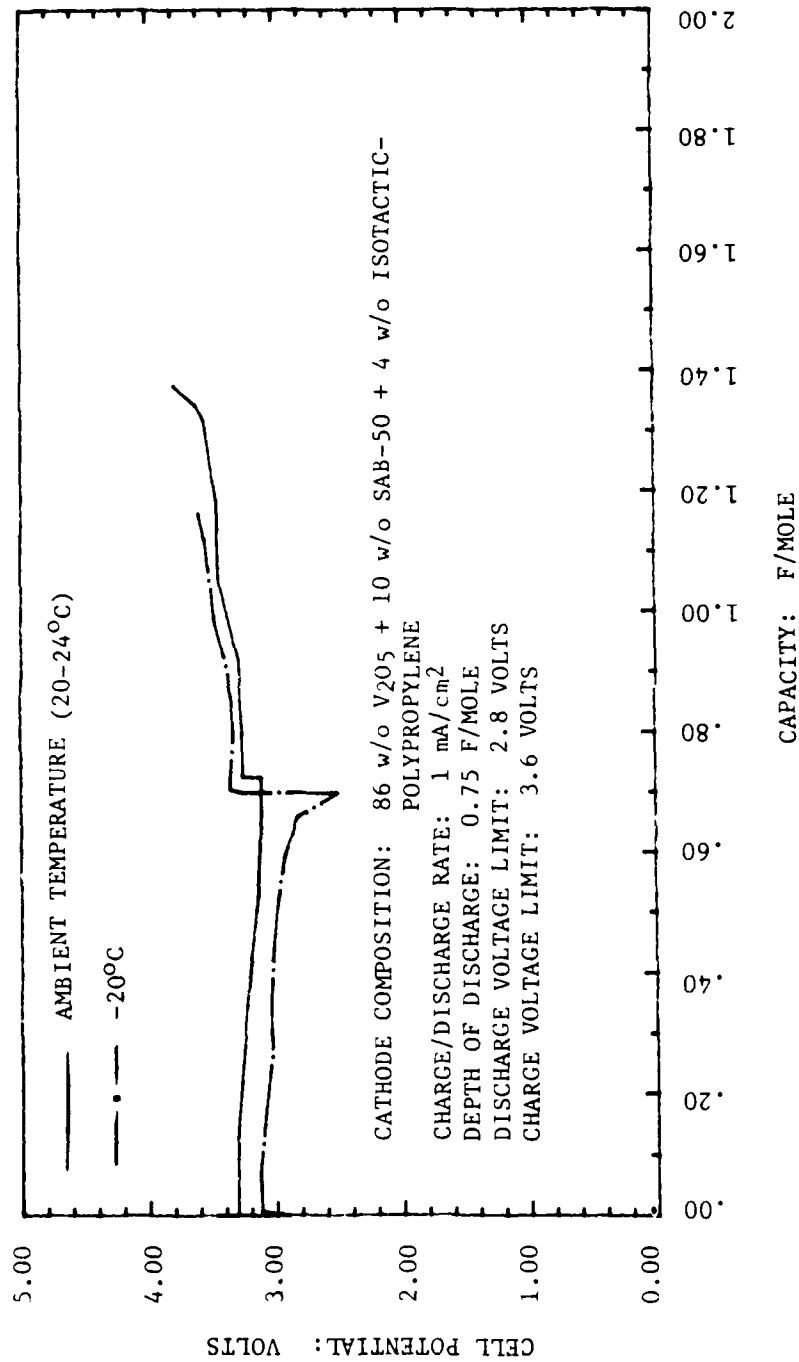


FIGURE 3-20. TYPICAL DISCHARGE/CHARGE CURVE OF Li/V<sub>2</sub>O<sub>5</sub> LABORATORY CELLS IN 2M LiAsF<sub>6</sub> + 0.4M LiBF<sub>4</sub>/MF SOLUTIONS



TiS<sub>2</sub>

Methyl Formate Solutions. Li/TiS<sub>2</sub> laboratory cell tests employing a 2M LiAsF<sub>6</sub> + 0.4M LiBF<sub>4</sub>/MF solution demonstrated a sharp decline in capacity in early cycle life. This capacity degradation was observed regardless of cathode process or cathode composition. Typical results are shown in Figure 3-21.

The charge/discharge voltage profiles observed with methyl formate solutions were unusual and suggested a mechanism more complex than merely inserting and removing lithium ions from the layered TiS<sub>2</sub> structure. During discharge, no "knee" was observed at the end, even after delivered capacities of up to 2 F/mole (Figure 3-22). During charge, distinct voltage plateaus were observed above about 2.6V with similar plateaus appearing in the next discharge (Figure 3-23). In addition, cathodes were observed to swell as much as 70 percent in methyl formate solutions as compared to approximately 5 percent in 2-methyl THF solutions under similar conditions.

To help elucidate the cause for the poor cycle life performance in methyl formate solutions, x-ray analyses were conducted on discharged and cycled cathodes. After the first discharge, a strong peak was observed having a d-spacing of 10Å indicative of significant lattice expansion. After extended cycling, cathodes exhibited only a few low intensity peaks indicating a major degradation of the structure of TiS<sub>2</sub> (Figure 3-24).

Based on these results, we believe that solvent cointercalation is occurring with methyl formate solutions, resulting in the observed capacity degradation. Therefore methyl formate solutions were deemed unsuitable for use with TiS<sub>2</sub> in long cycle life applications.

Methyl Acetate Solutions. Initial testing with methyl acetate solutions demonstrated significantly improved performance over that achieved with methyl formate. The voltage profiles were normal with distinct "knees" observed at the end of discharge and smooth s-shaped profiles observed during charge (Figure 3-25). With 1.5M and 2.0M LiAsF<sub>6</sub>/MA solutions, however, a gradual decline in capacity occurred throughout cycle life (Figure 3-26). The rate of this capacity degradation was still too great to meet the cycle life requirements of this program.

One approach evaluated to improve cycle life performance in methyl acetate solutions was to employ higher solute concentrations. The lithium cyclability studies discussed later in this chapter ("Lithium Cycling Efficiency Measurements") showed that, with methyl acetate, lithium cycling efficiencies increased with increasing solute concentration, suggesting that the salt may have some stabilizing effect on the solution.

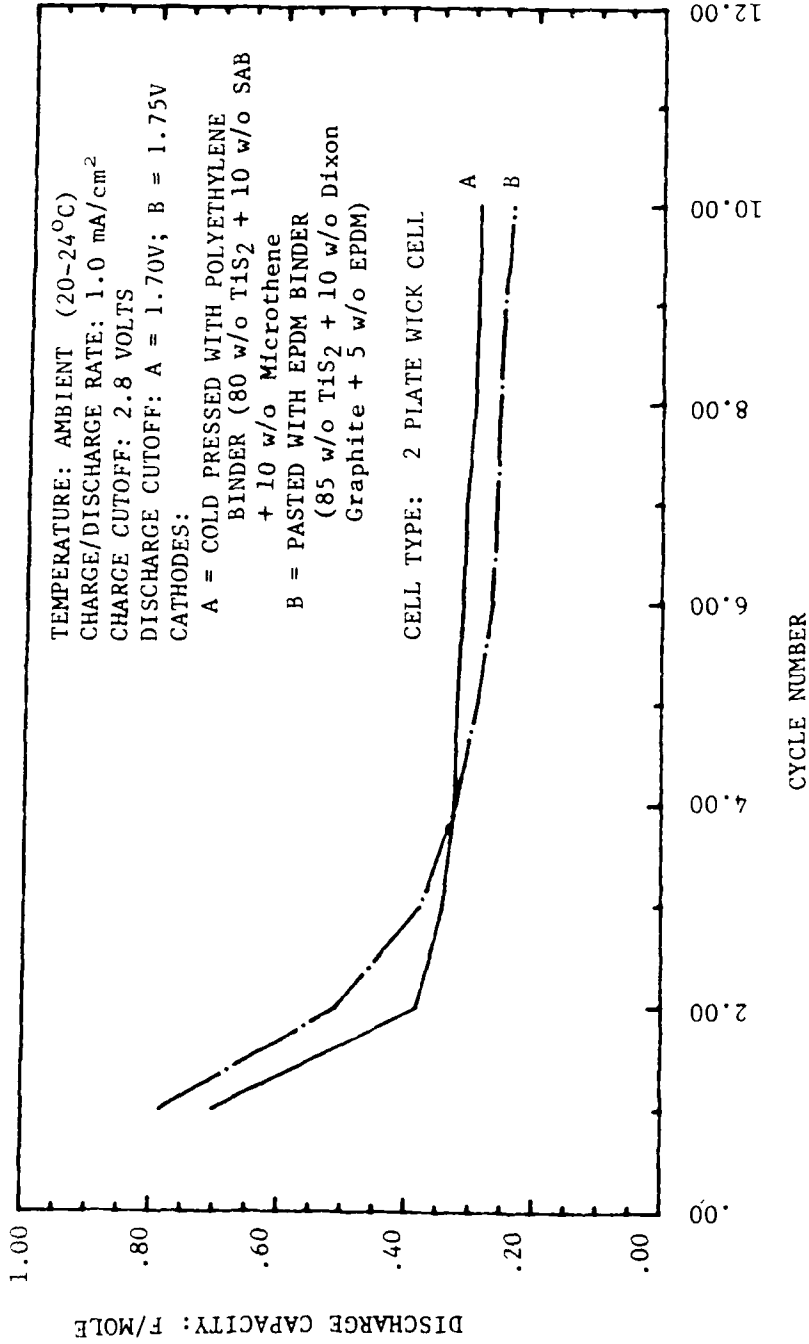


FIGURE 3-21. TiS<sub>2</sub> SCREENING STUDIES: CYCLE LIFE PERFORMANCE WITH 2M LiAsF<sub>6</sub> + 0.4M LiBF<sub>4</sub>/MF SOLUTIONS

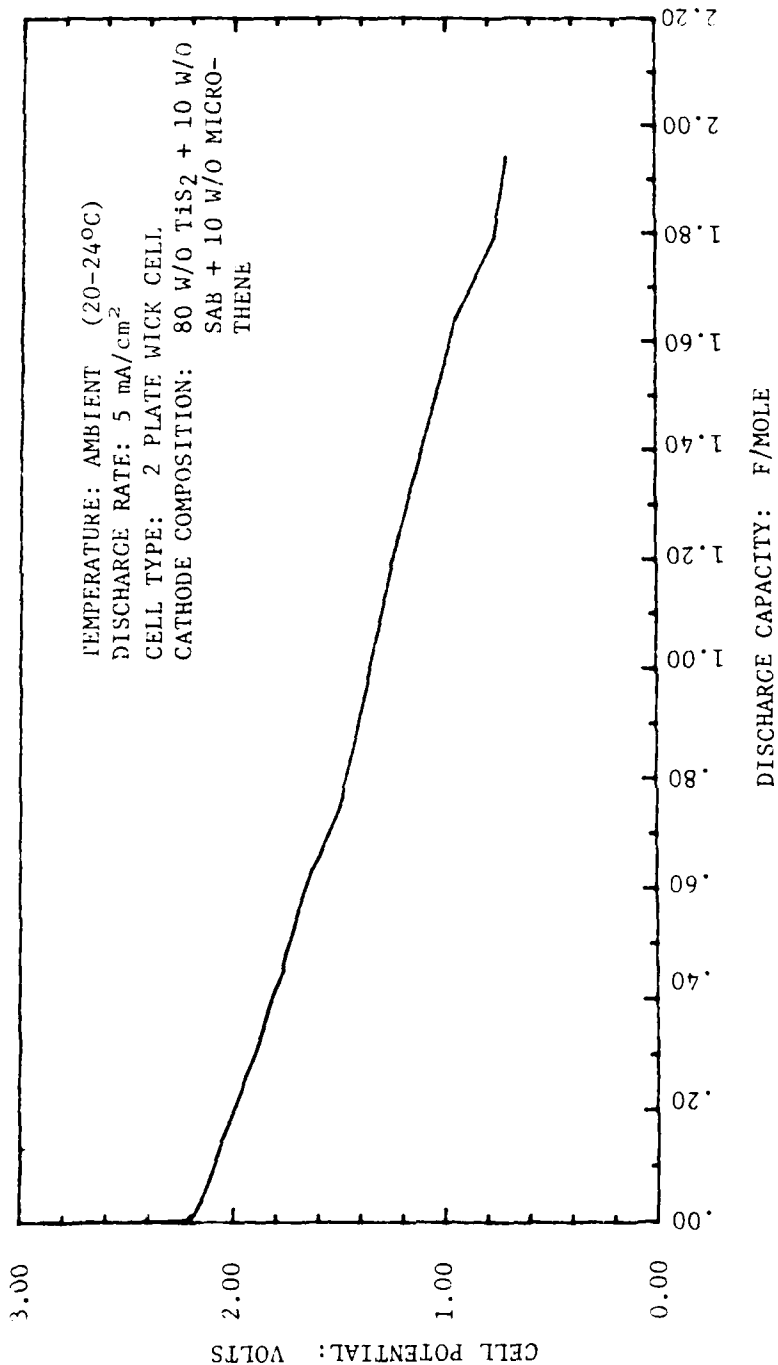


FIGURE 3-22. EXTENDED DISCHARGE PERFORMANCE OF A Li/TiS<sub>2</sub> CELL WITH A 2M LiAsF<sub>6</sub> + 0.4M LiBF<sub>4</sub>/MF ELECTROLYTE SOLUTION

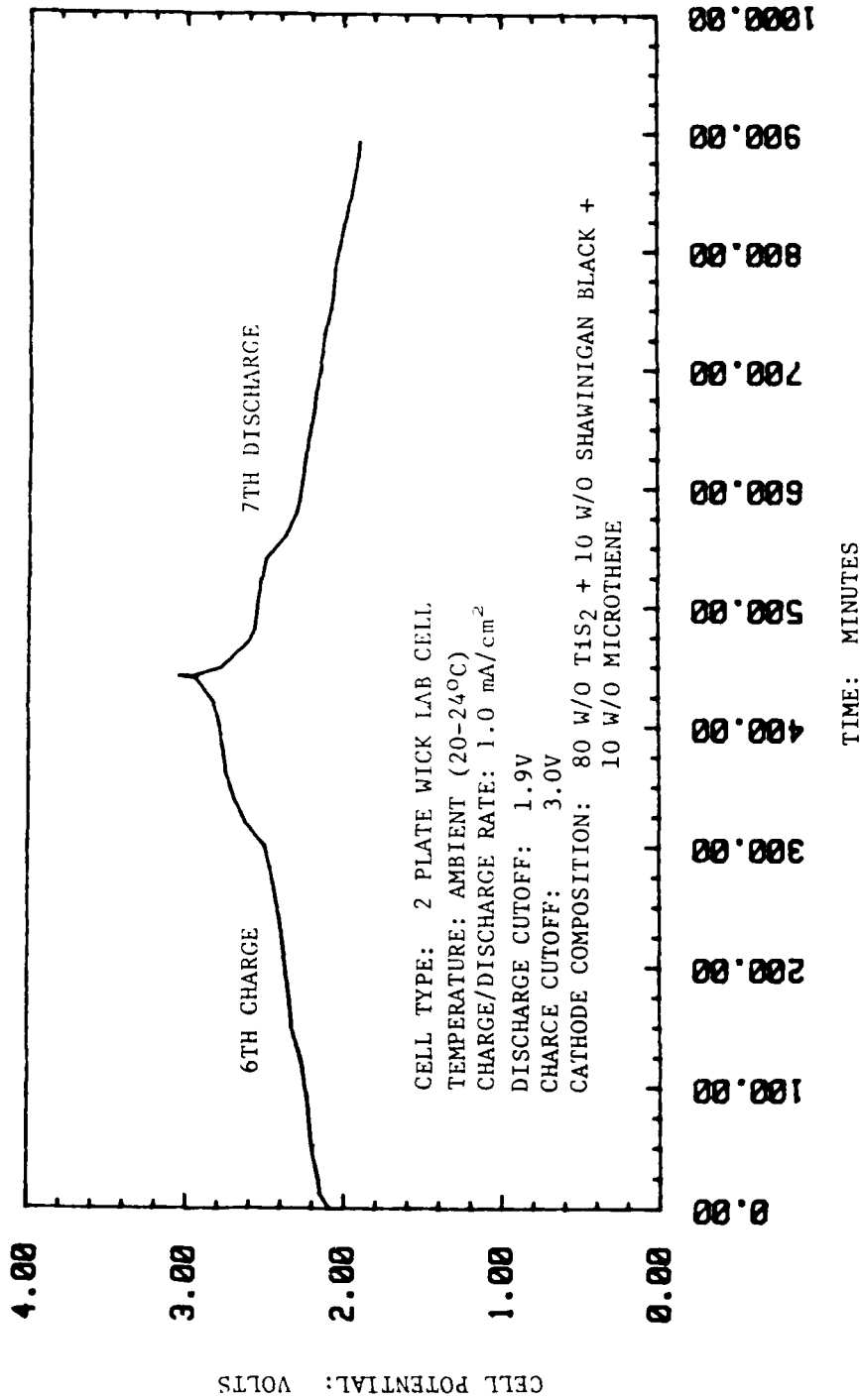


FIGURE 3-23. CHARGE/DISCHARGE BEHAVIOR OF A Li/TiS<sub>2</sub> CELL WHEN CHARGED TO 3 VOLTS EMPLOYING A 2M LiAsF<sub>6</sub> + 0.4M LiBF<sub>4</sub>/MF ELECTROLYTE SOLUTION

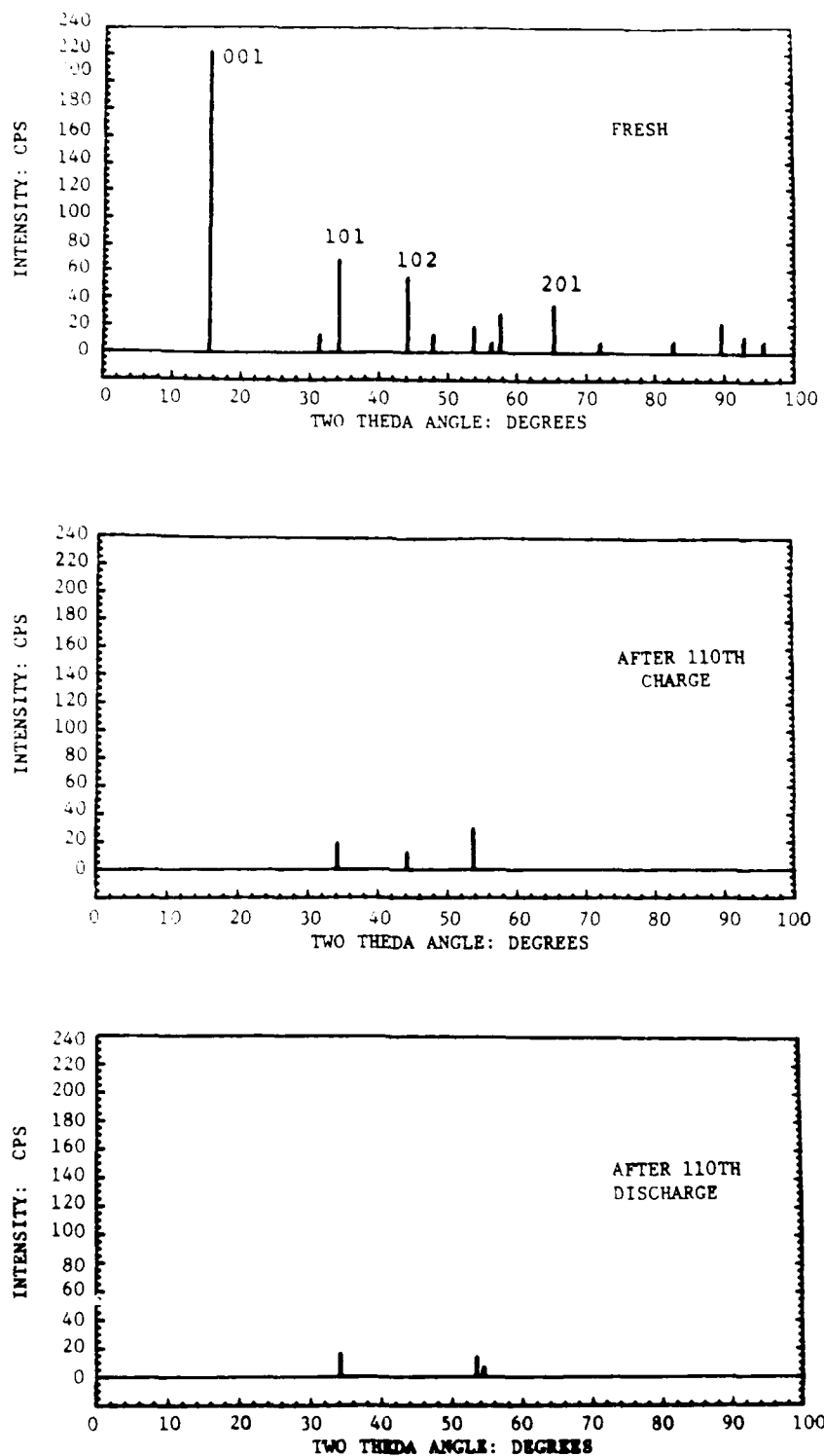


FIGURE 3-24. X-RAY DIFFRACTION PATTERNS FOR  $TiS_2$  CATHODES BEFORE AND AFTER EXTENDED CYCLING IN A  $2M LiAsF_6 + 0.4M LiBF_4/MF$  ELECTROLYTE SOLUTION (CHARGE/DISCHARGE RATE =  $1.0 mA/cm^2$  AT AMBIENT TEMPERATURE (20-24°C))

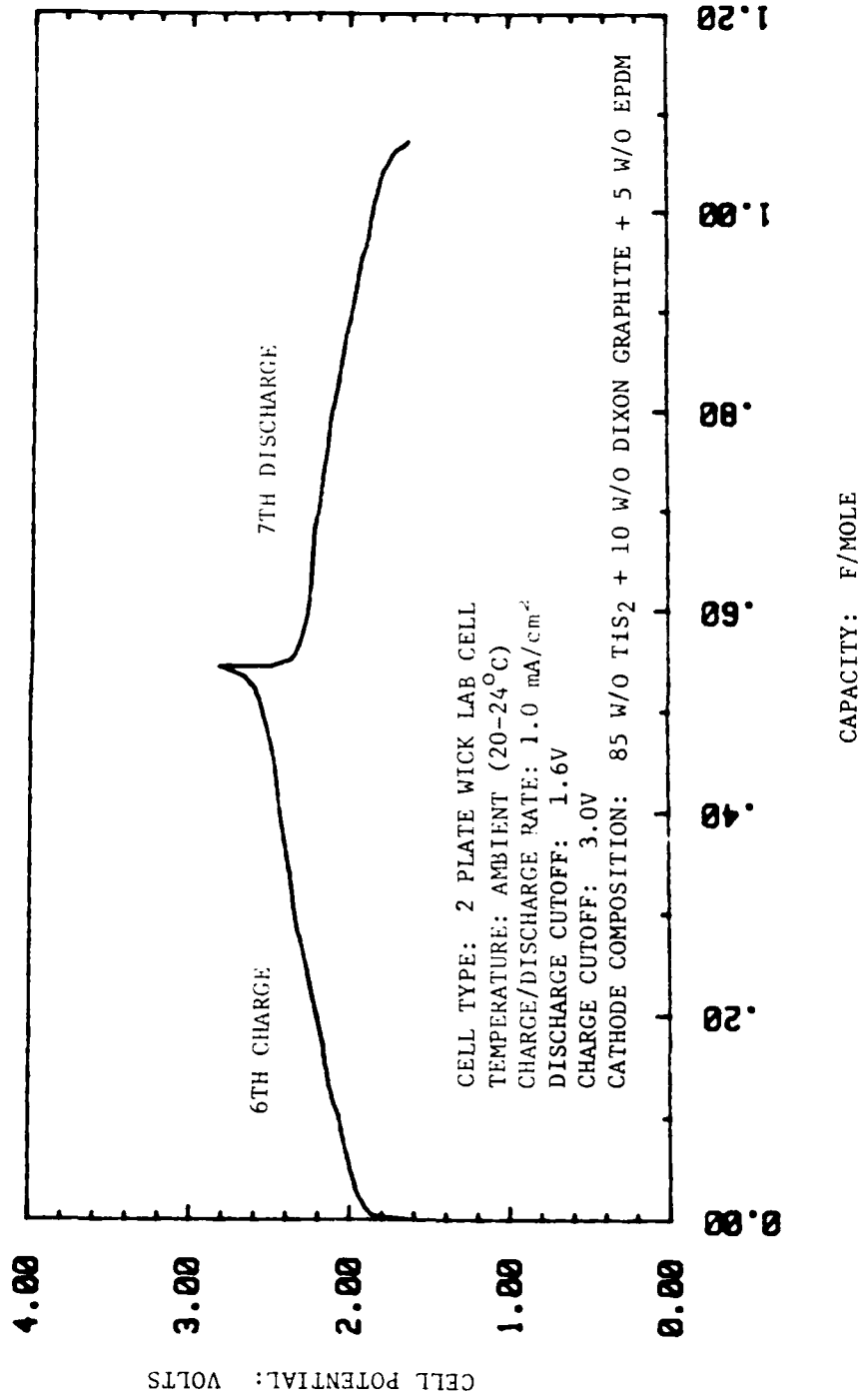


FIGURE 3-25. CHARGE/DISCHARGE BEHAVIOR OF A Li/TiS<sub>2</sub> CELL WHEN CHARGED TO 3 VOLTS EMPLOYING A 1.5M LiAsF<sub>6</sub>/MA ELECTROLYTE SOLUTION

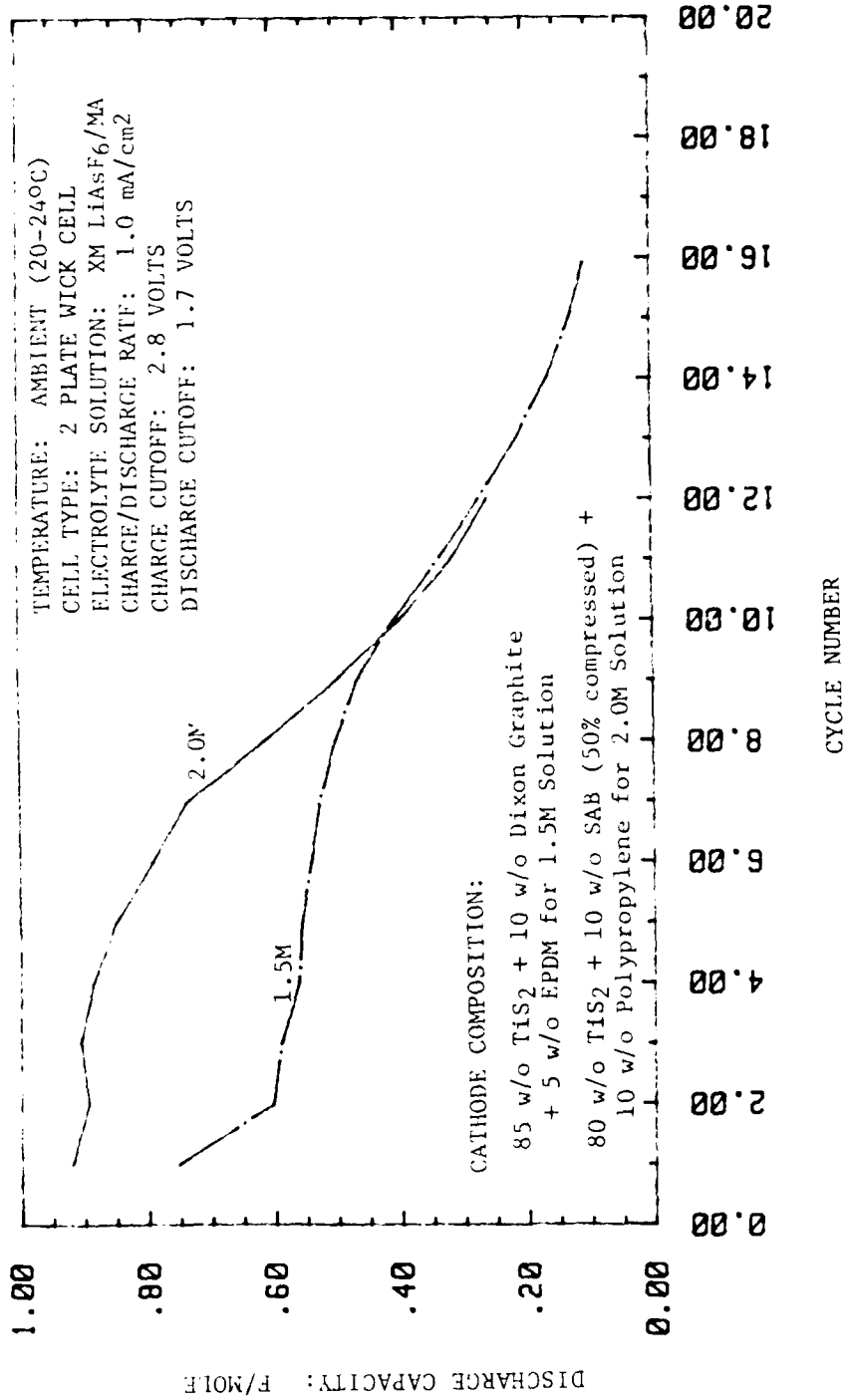


FIGURE 3-26. TiS<sub>2</sub> SCREENING STUDIES: CYCLE LIFE PERFORMANCE IN METHYL ACETATE SOLUTIONS

Figure 3-27 shows cycle life performance for Li/TiS<sub>2</sub> half-cells employing LiAsF<sub>6</sub> concentrations over the range of 2M to 3M. Half-cells were employed in these studies to ensure that anode effects were not contributing to the observed capacity degradation in the methyl acetate solutions. The cells were cycled between the limits of 2.8V and 1.7V based on cathode-to-reference voltage readings. The results show that improved performance was indeed achieved with the 2.5M solution, although capacity decline was still observed. The 3M solution delivered lower capacity, but significantly, showed no degradation in capacity over cycle life.

Because the 3M LiAsF<sub>6</sub>/MA solutions are highly viscous, polarization effects are more pronounced. Therefore, additional tests were conducted with the 3M solutions in which the voltage limits were extended to 3.0V and 1.4V. As can be seen in Figure 3-28, enhanced capacity was indeed achieved at ambient temperature (20-24°C) with little degradation in capacity over cycle life. At -20°C, however, the viscosity severely limits performance, even when employing the wider voltage limits.

Extended cycling results for the 3M solution tested at ambient temperature between the limits 2.8V and 1.7V are shown in Figure 3-29. Over 200 cycles have been achieved demonstrating that long cycle life capabilities can be realized with TiS<sub>2</sub> in ester-based solutions. The high viscosity of the 3M LiAsF<sub>6</sub>/MA solutions, however, severely limits low temperature performance and similar limitations would be expected for rate capabilities. Therefore, these solutions are not suited to meet the demanding performance requirements needed for this program.

A second approach investigated to improve the cycle life performance of TiS<sub>2</sub> in methyl acetate solutions was to employ ether co-solvents.<sup>9</sup> The co-solvents evaluated were 1,2-dimethoxyethane (DME), tetrahydrofuran (THF), and 2-methyl THF. These tests were also conducted in half-cells.

The cycle life results are shown in Figures 3-30 to 3-32. No beneficial effects were achieved with DME. Both THF and 2-methyl THF, however, improved cycle life performance demonstrating that ether co-solvents can indeed improve the performance of TiS<sub>2</sub> cathodes in methyl acetate solutions.

### Li<sub>x</sub>CoO<sub>2</sub>

The initial performance evaluations of Li<sub>x</sub>CoO<sub>2</sub> conducted as part of the material characterization studies demonstrated that decomposition of methyl formate solutions occurs during charging with subsequent degradation in discharge performance. Methyl acetate solutions, however, appeared to be more resistant to decomposition, thus offering encouragement for the continued evaluation of this system. Those initial tests also indicated that the maximum capacity obtainable with Li<sub>x</sub>CoO<sub>2</sub> may be limited by the stoichiometry of the starting material.



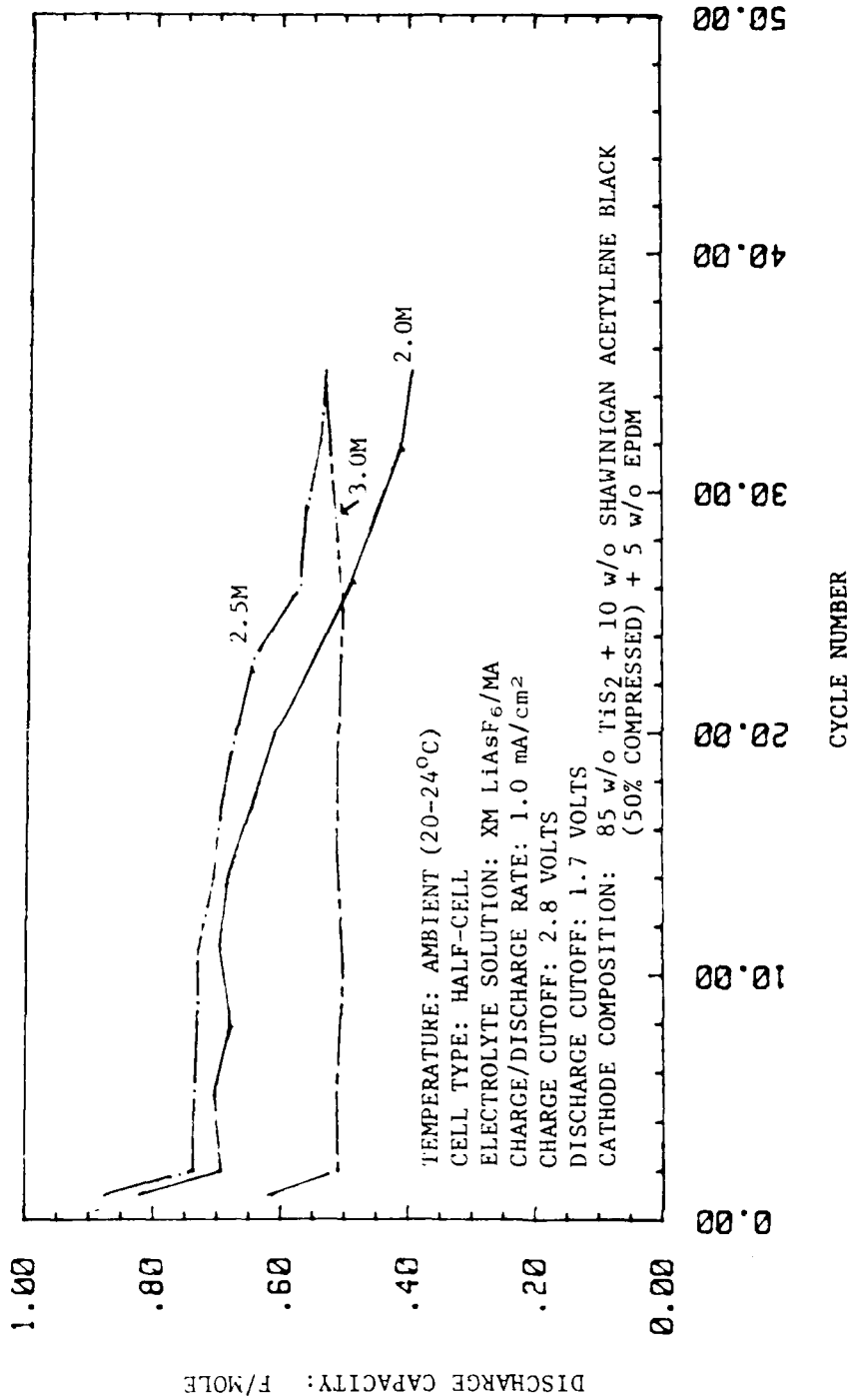


FIGURE 3-27. TiS<sub>2</sub> SCREENING STUDIES: CYCLE LIFE PERFORMANCE IN METHYL ACETATE SOLUTIONS AS A FUNCTION OF LiAsF<sub>6</sub> CONCENTRATION

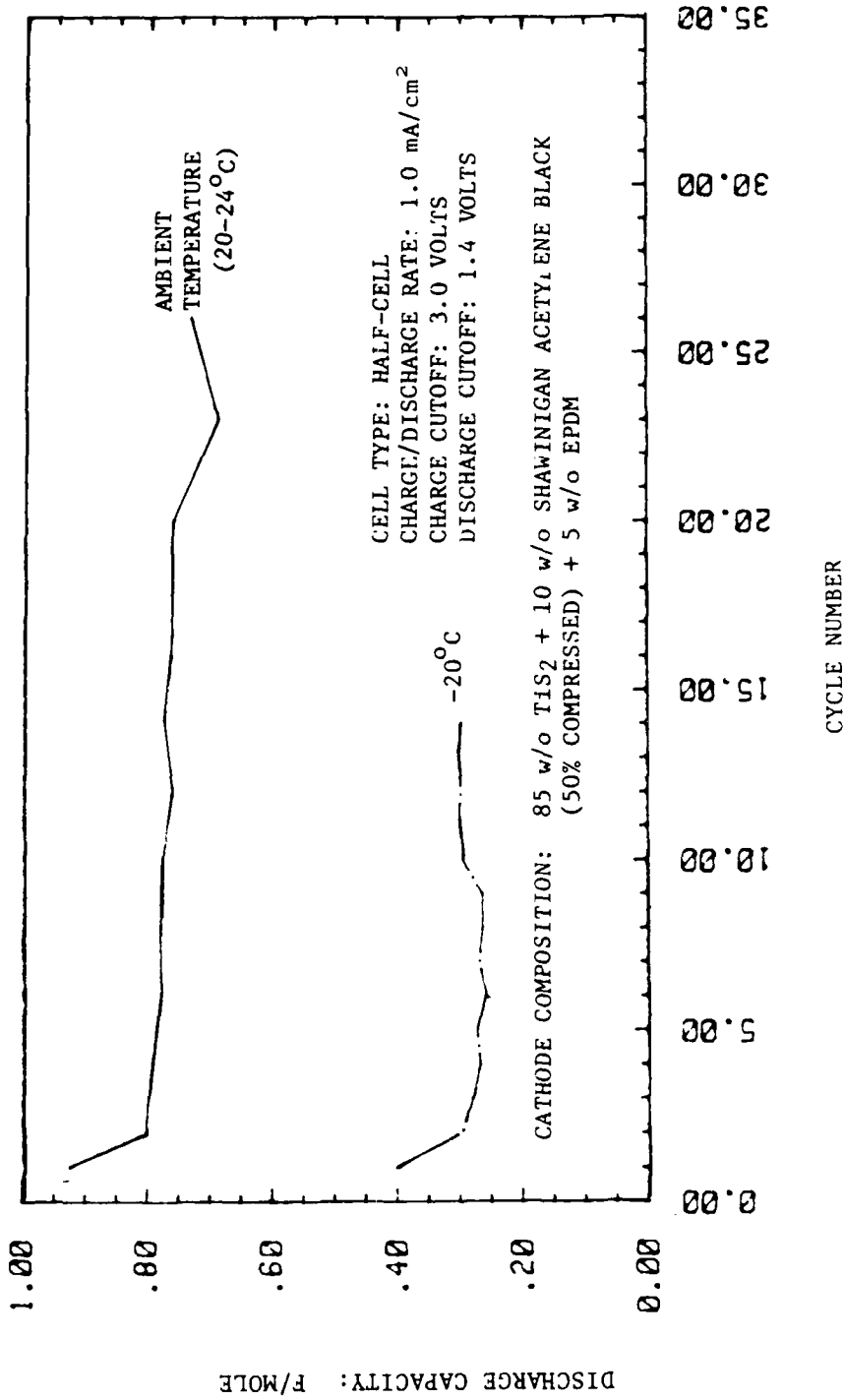


FIGURE 3-28. TiS<sub>2</sub> SCREENING STUDIES: CYCLE LIFE PERFORMANCE IN 3M LiAsF<sub>6</sub>/MA SOLUTIONS EMPLOYING EXTENDED VOLTAGE LIMITS

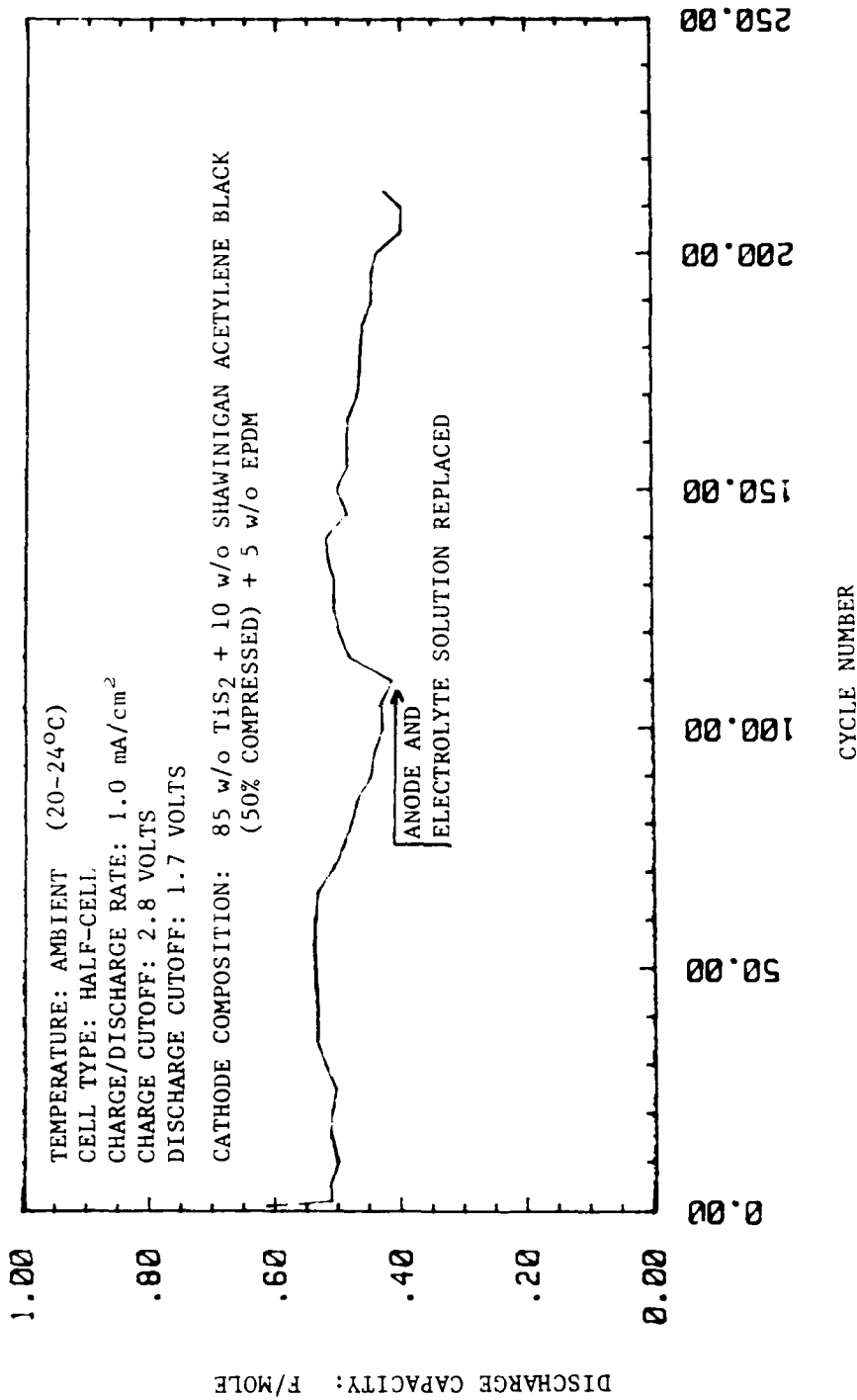


FIGURE 3-29. TiS<sub>2</sub> SCREENING STUDIES: EXTENDED CYCLE LIFE PERFORMANCE WITH 3M LiAsF<sub>6</sub>/MA SOLUTIONS

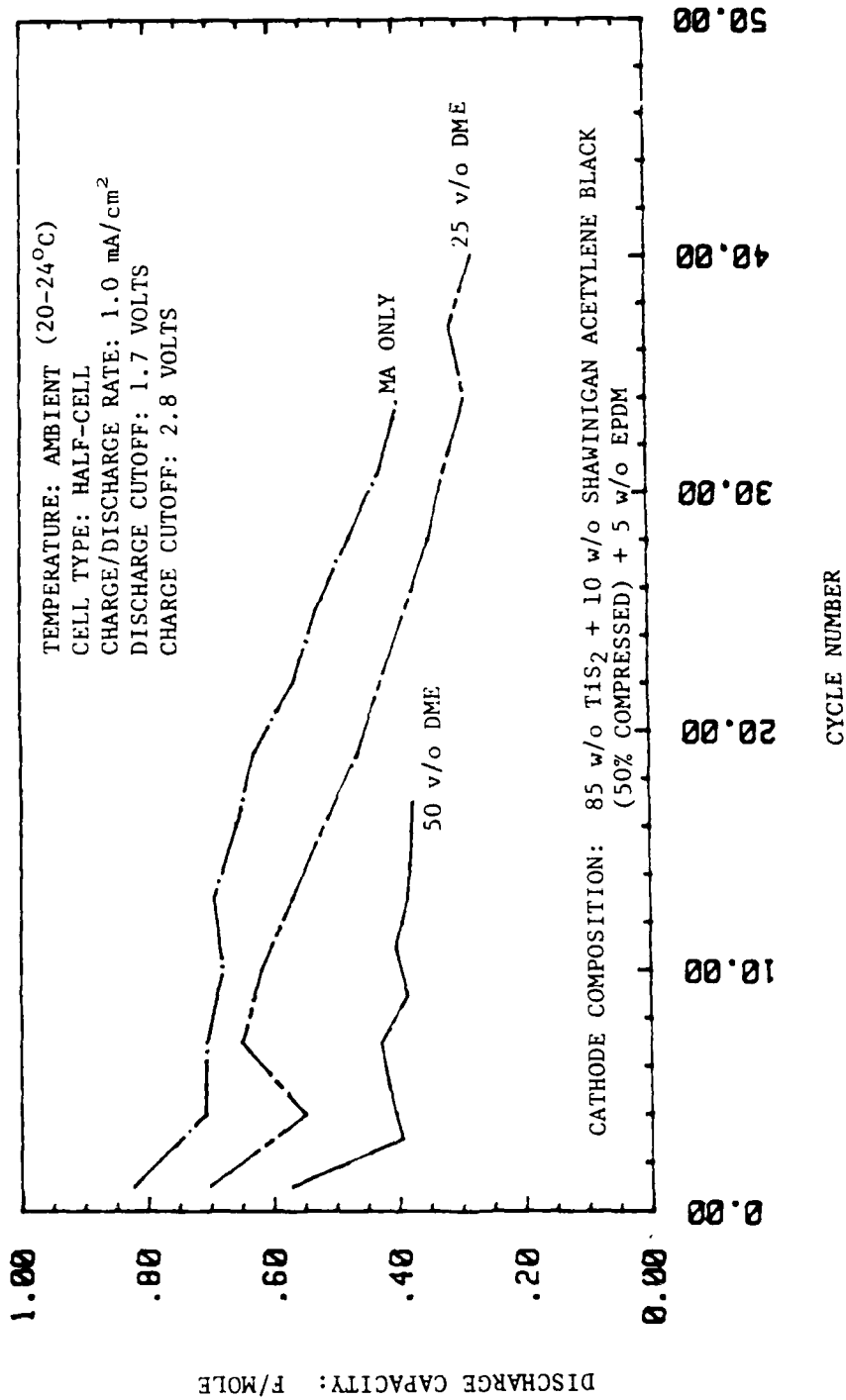


FIGURE 3-30. TIS<sub>2</sub> SCREENING STUDIES: CYCLE LIFE PERFORMANCE IN 2M LiAsF<sub>6</sub>/MA SOLUTIONS WITH AND WITHOUT 1,2-DIMETHOXYETHANE (DME) CO-SOLVENT

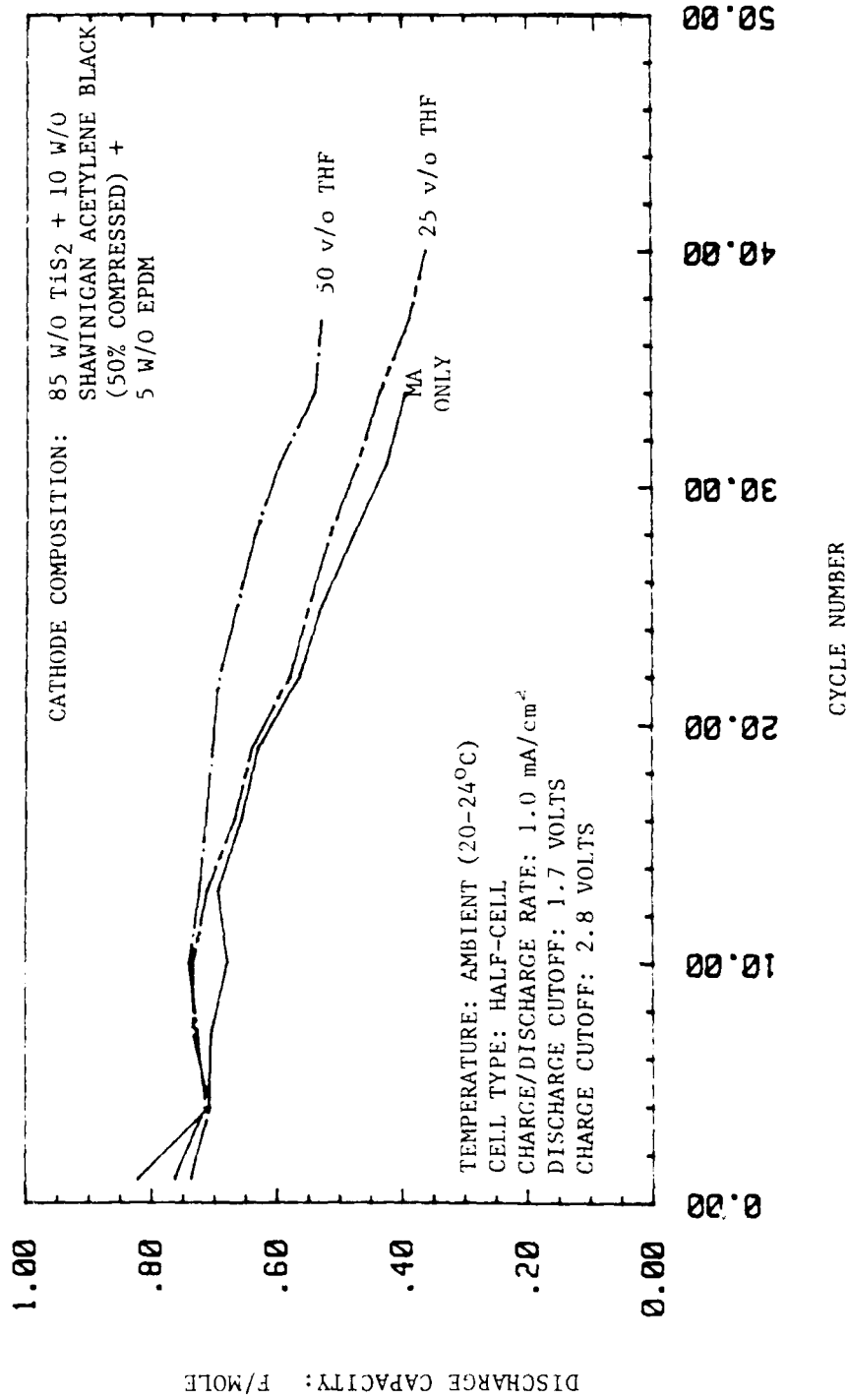


FIGURE 3-31. TiS<sub>2</sub> SCREENING STUDIES: CYCLE LIFE PERFORMANCE IN 2M LiAsF<sub>6</sub>/MA SOLUTIONS WITH AND WITHOUT TETRAHYDROFURAN (THF) CO-SOLVENT

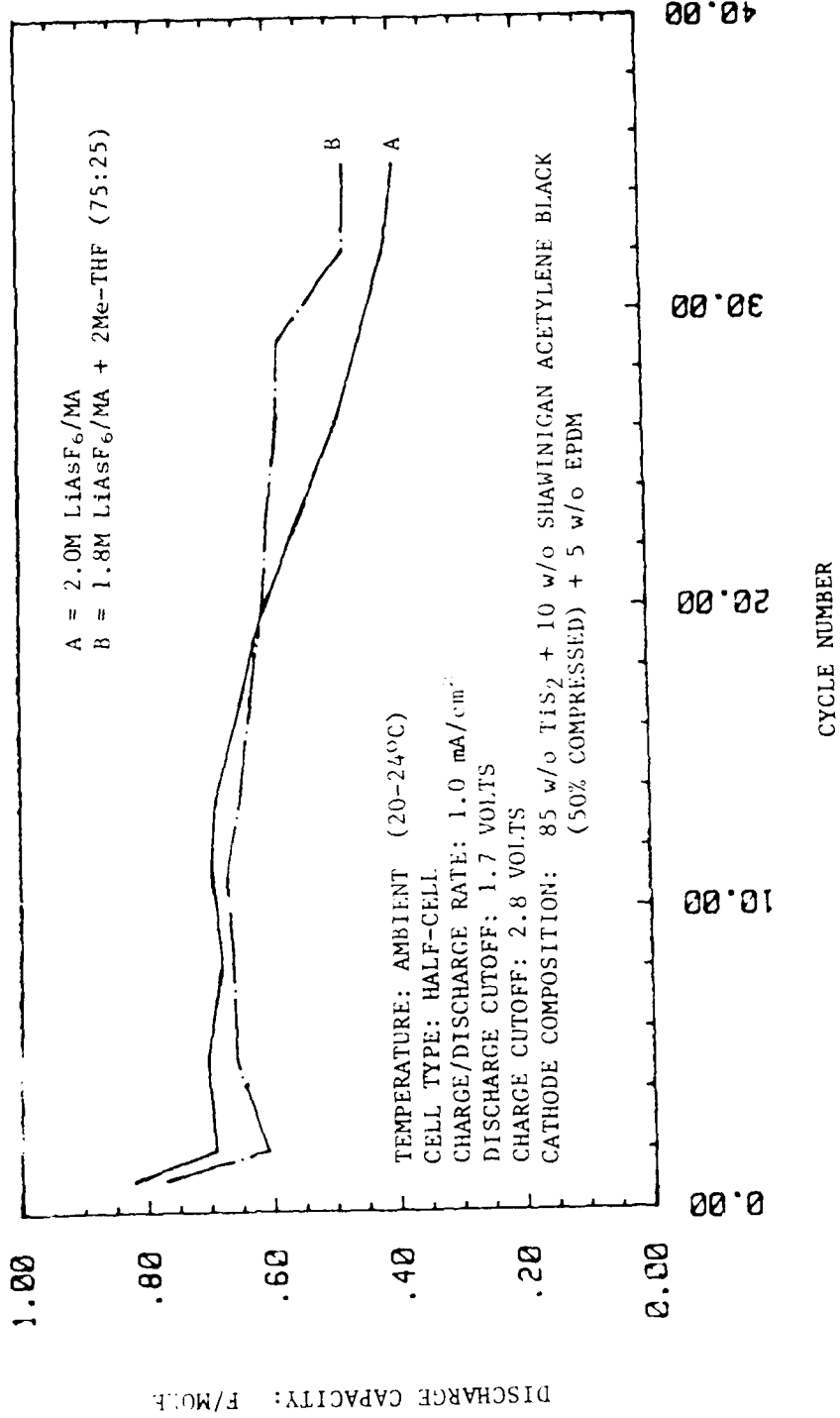


FIGURE 3-32. TiS<sub>2</sub> SCREENING STUDIES: CYCLE LIFE PERFORMANCE WITH AND WITHOUT 2-METHYL THF CO-SOLVENT

To better define the performance capabilities of  $\text{Li}_x\text{CoO}_2$ , additional cycle tests were carried out focusing on methyl acetate<sup>x</sup> electrolyte solutions. Dimethyl sulfite solutions were not considered for use with  $\text{Li}_x\text{CoO}_2$  because of their lower electrochemical stability at high oxidizing potentials.<sup>11</sup>

The majority of the cycle life tests were conducted in half-cells so as to eliminate any anode polarization effects in the methyl acetate solutions. The cathodes were manufactured by a cold pressing technique and contained 10 weight percent Shawinigan Acetylene Black (50 percent compressed) and 4 weight percent isotactic-polypropylene binder.

Because  $\text{Li}_x\text{CoO}_2$  cells do not exhibit a voltage deflection at end of charge, it is difficult to establish an upper voltage limit for this system. If the voltage is allowed to go too high, solution decomposition is inevitable. If the voltage limit is set too low, however, the charging capacity will be limited.

Therefore, various charging cutoff voltages were evaluated in the range of 4.5V to 4.85V. In all tests, a low charging current density of  $0.5 \text{ mA/cm}^2$  was employed so as to minimize polarization effects and maintain the charging voltages as low as possible.

Figure 3-33 shows the results for half-cells tested at a discharge rate of  $1.0 \text{ mA/cm}^2$ . As can be seen, all cells delivered an initial capacity of less than 0.6 F/mole and no additional capacity was obtained from the cell employing the higher stoichiometry material (i.e., Lot CML-CO-003,  $\text{Li}_{1.00}\text{Co}_{1.00}\text{O}_2$ ). All cells exhibited a significant loss in capacity after a few cycles accompanied by discoloration of the electrolyte solution.

Figure 3-34 shows the results for a half-cell and a 2-plate laboratory rick cell tested at a discharge rate of  $5 \text{ mA/cm}^2$ . The initial capacities were approximately the same as obtained at  $1 \text{ mA/cm}^2$  indicating that  $\text{Li}_x\text{CoO}_2$  does indeed possess good rate capabilities. However, a rapid decline<sup>x</sup> in capacity was again observed in these cells accompanied by discoloration of the electrolyte solution. The fact that the laboratory cell delivered four cycles before any loss in capacity was observed demonstrates that  $\text{Li}_x\text{CoO}_2$  does operate reversibly in the absence of solution decomposition.<sup>x</sup>

Although only limited testing has been completed with  $\text{Li}_x\text{CoO}_2$ , the results demonstrate that electrolyte decomposition remains a<sup>x</sup> key problem that must be resolved before this system can be practical. Although some improvement is indicated when the charging voltage is limited to 4.5V to 4.6V, the cycle life performance obtained is still disappointing. Therefore, in its present stage of development,  $\text{Li}_x\text{CoO}_2$  could not be considered a viable candidate for this program.

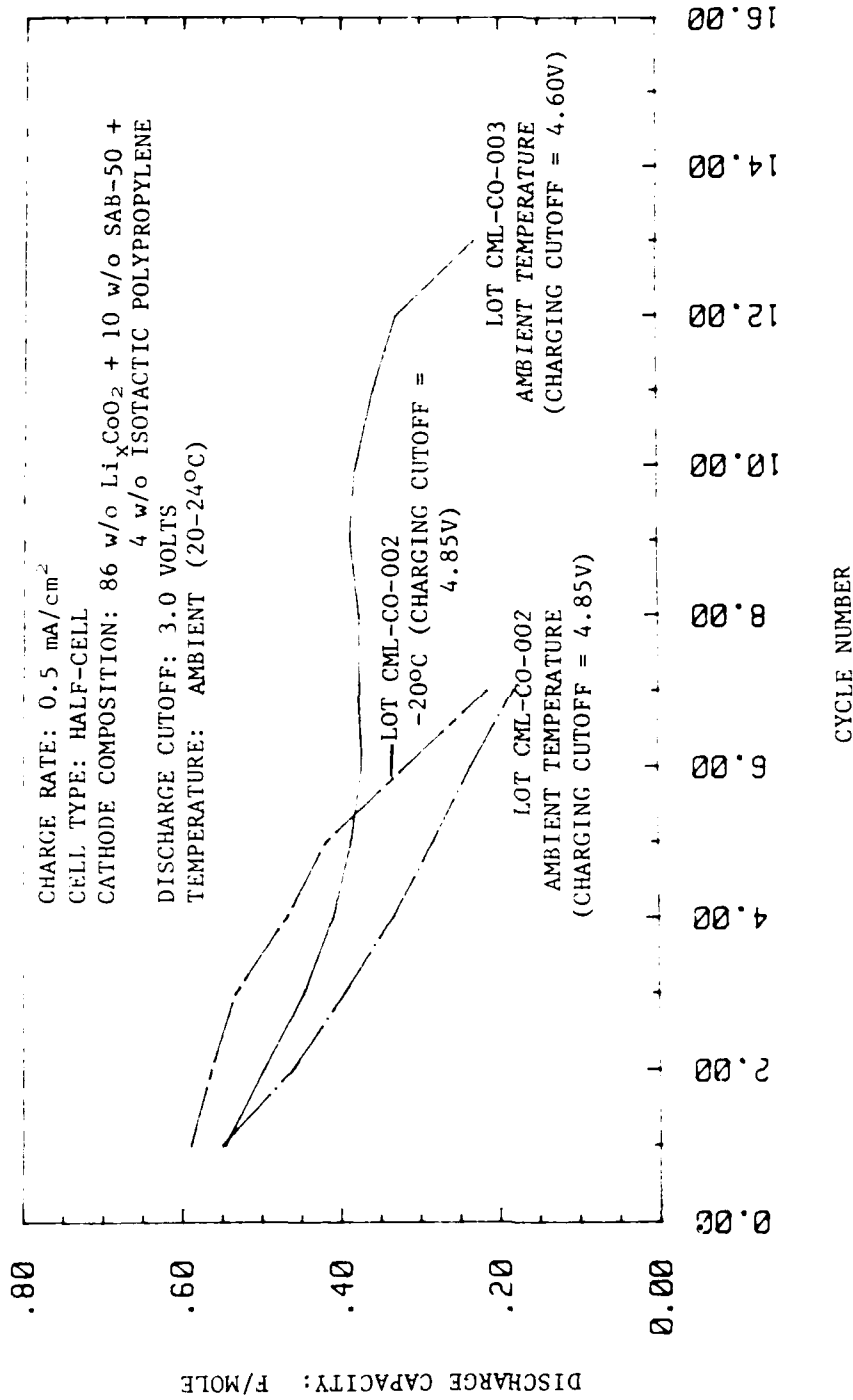
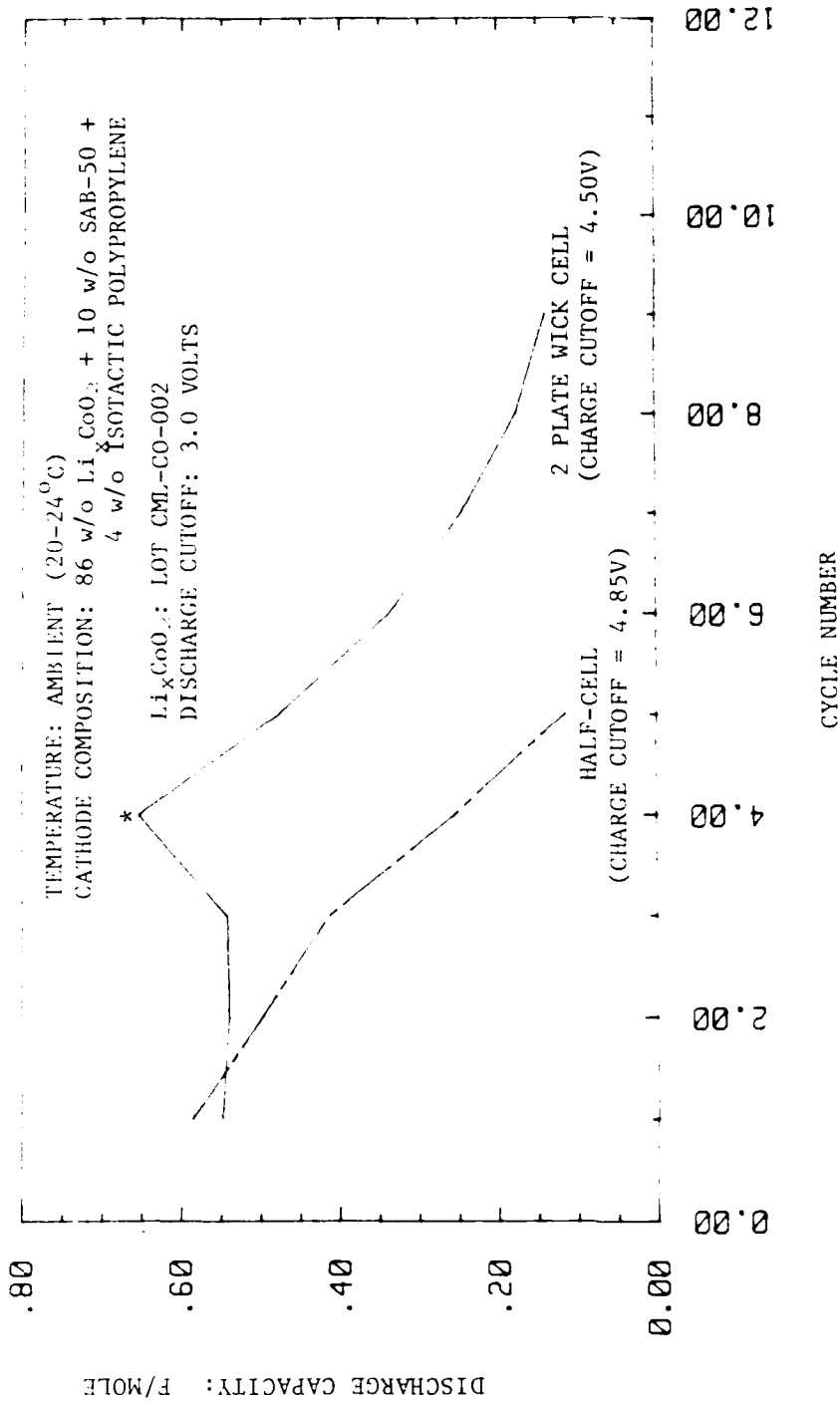


FIGURE 3-33. Li<sub>x</sub>CoO<sub>2</sub> SCREENING STUDIES: CYCLE LIFE PERFORMANCE WITH 2M LiAsF<sub>6</sub>/MA SOLUTIONS AT A DISCHARGE RATE OF 1.0 mA/cm<sup>2</sup>





\* THE FOURTH DISCHARGE OF THE LABORATORY CELL WAS INADVERTENTLY CONDUCTED AT A RATE OF 6.2 mA/cm<sup>2</sup> DUE TO A MALFUNCTION OF THE POWER SUPPLY. SURPRISINGLY, THIS RESULTED IN A HIGHER DISCHARGE EFFICIENCY FROM THE CELL.

FIGURE 3-34.  $\text{Li}_x\text{CoO}_2$  SCREENING STUDIES: CYCLE LIFE PERFORMANCE WITH 2M  $\text{LiAsF}_6/\text{MA}$  SOLUTIONS AT A DISCHARGE RATE OF 5 mA/cm<sup>2</sup>

## THERMAL STABILITY TESTS

Electrolyte Solutions

Although no separate tests were conducted in this program regarding the thermal stability of the individual electrolyte solutions themselves, an extensive data base has been developed at Honeywell on the elevated temperature stability of  $\text{LiAsF}_6/\text{MF}$  and  $\text{LiAsF}_6/\text{DMSI}$  solutions that can supplement our other screening test results involving selection of the electrolyte solution. Our work in this area has shown that both methyl formate and dimethyl sulfite solutions require contact with lithium metal for stability at elevated temperatures. Methyl formate solutions also require  $\text{LiBF}_4$ .<sup>8</sup> When these conditions are met, excellent stability is achieved, as summarized in Tables 3-9 and 3-10.

TABLE 3-9. AMPUL STORAGE TEST RESULTS FOR 2M  $\text{LiAsF}_6$  +  
0.4M  $\text{LiBF}_4/\text{MF}$  SOLUTIONS (HISTORICAL DATA)

Lithium Quantity, mg/ml	Electrolyte Water Level, ppm	Storage Temperature, °C				
		64	74	79	84	90
0.5	150	501	213	128	80	43
2.1	150	907	405	255	162	96
	300	824	299	184	115	64
3.7	50	1676	665	397	211	102
	150	1041	429	250	158	70
	300	911	177	188	125	63
6.2	150	1187	433	250	157	48
	300	906	293	200	121	71

- NOTES: 1. The above values represent days required for 50 percent of the ampuls in a test group to fracture.
2. Each test group contained 50 ampuls.
3. Ampul fracture is caused by gas-producing decomposition reactions of the electrolyte solution. Therefore, the time required for an ampul to fracture gives a direct indication of the rate that solution decomposition is occurring. The point at which 50 percent of the ampuls have fractured is used to define the average rate of decomposition for a particular test group.

TABLE 3-10. AMPUL STORAGE TEST RESULTS FOR 1.0M LiAsF<sub>6</sub>/DMSI SOLUTIONS (HISTORICAL DATA)

Lithium Quantity, mg/ml	Storage Temperature, °C		
	64	74	84
0.5	1559	532	179
2.1	2790	846	262
6.2	>3024	1475	323

NOTES: 1. The above values represent days required for 50 percent of the ampuls in a test group to fracture.

2. Each test group contained 50 ampuls.

3. Ampul fracture is caused by gas-producing decomposition reactions of the electrolyte solution. Therefore, the time required for an ampul to fracture gives a direct indication of the rate that solution decomposition is occurring. The point at which 50 percent of the ampuls have fractured is used to define the average rate of decomposition for a particular test group.

These historical results, therefore, demonstrate that methyl formate and dimethyl sulfite solutions offer suitable thermal stability for our rechargeable applications. Unfortunately, however, similar data are not available for methyl acetate solutions.

#### Cathode Materials

V<sub>2</sub>O<sub>5</sub>. Thermal stability tests with V<sub>2</sub>O<sub>5</sub> were conducted in methyl formate and methyl acetate solutions only. The physical appearance of the samples after storage are summarized in Table 3-11. At ambient temperature no changes were observed, while at 71°C, significant changes were observed in both solutions.

The results of the solution analyses are shown in Table 3-12. At ambient temperature, no solubility is indicated in either solution. At 71°C, V<sub>2</sub>O<sub>5</sub> was found to be insoluble in the 2.0M LiAsF<sub>6</sub> + 0.4M LiBF<sub>4</sub>/MF solution. With the 2.0M LiAsF<sub>6</sub>/MA solutions stored at elevated temperatures, the lithium metal was completely consumed and the ampuls were observed to contain significant pressure when they were opened. The V<sub>2</sub>O<sub>5</sub> had changed in color from orange to black and the solution contained approximately 800 ppm vanadium.

TABLE 3-11. V<sub>2</sub>O<sub>5</sub> THERMAL STABILITY TESTS--PHYSICAL APPEARANCE OF SAMPLES AFTER STORAGE INTERVAL

<u>Storage Temperature</u>	<u>Electrolyte Solution</u>	<u>Observations</u>
Ambient (20-24°C)	2M LiAsF <sub>6</sub> + 0.4M LiBF <sub>4</sub> /MF	Clear solution. Li shiny, no deposit.
Ambient (20-24°C)	2M LiAsF <sub>6</sub> /MA	Clear solution. Li shiny, no deposit.
71°C	2M LiAsF <sub>6</sub> + 0.4M LiBF <sub>4</sub> /MF	Clear solution. Heavy brown deposits on Li and V <sub>2</sub> O <sub>5</sub> surfaces.
71°C	2M LiAsF <sub>6</sub> /MA	Dark brown solution. Cannot see Li or V <sub>2</sub> O <sub>5</sub> .

TABLE 3-12. SOLUBILITY OF V<sub>2</sub>O<sub>5</sub> IN LITHIUM BATTERY ELECTROLYTES--BY AA ANALYSIS

<u>Electrolyte Solution</u>	<u>Storage Temperature</u>	<u>Solubility* (ppm, V)</u>
2M LiAsF <sub>6</sub> + 0.4M LiBF <sub>4</sub> /MF	Ambient (20-24°C)	< 2.5
2M LiAsF <sub>6</sub> /MA	Ambient (20-24°C)	< 2.5
2M LiAsF <sub>6</sub> + 0.4M LiBF <sub>4</sub> /MF	71°C	< 2.5
2M LiAsF <sub>6</sub> + 0.4M LiBF <sub>4</sub> /MF	71°C	< 2.5
2M LiAsF <sub>6</sub> /MA	71°C	985
2M LiAsF <sub>6</sub> /MA	71°C	665

\* AA resolution in these samples is 2.5 ppm for Vanadium.

X-ray diffraction data for the recovered cathode material samples are given in Tables 3-13 to 3-16. All results are in good agreement with the JCPDS standard except for the sample stored in 2.0M LiAsF<sub>6</sub>/MA at 71°C. The data for this latter sample indicate that the V<sub>2</sub>O<sub>5</sub> had been largely converted to δ-Li/V<sub>2</sub>O<sub>5</sub>.<sup>12</sup>

Based on these results, it is concluded that V<sub>2</sub>O<sub>5</sub> is chemically compatible with the 2.0M LiAsF<sub>6</sub> + 0.4 LiBF<sub>4</sub>/MF solution, but not with the 2.0M LiAsF<sub>6</sub>/MA solution. The formation of lithiated V<sub>2</sub>O<sub>5</sub> in the latter solution during elevated temperature storage was quite surprising and indicates that some type of reducing agent may have been generated in the solution.

### TiS<sub>2</sub>

Thermal stability tests with TiS<sub>2</sub> were conducted in methyl formate and methyl acetate solutions only. The physical appearance of the samples after storage are summarized in Table 3-17. No changes were observed in the samples maintained at room temperature. At 71°C, however, significant changes were observed, particularly with the 2M LiAsF<sub>6</sub>/MA solutions.

The results of the solution analysis for titanium concentration are shown in Table 3-18. No solubility is indicated in either solution at room temperature nor in the methyl formate solution stored at 71°C. The methyl acetate solutions at elevated temperatures contained approximately 170 ppm titanium indicating some solubility of TiS<sub>2</sub>. However, these solutions contained a fine suspension which could not be removed even by filtration. Therefore, it is not clear how much of the detected titanium came from dissolved material and how much was due to the suspended solids.

The x-ray results of stored TiS<sub>2</sub> were complex. Only the sample stored in 2.0M LiAsF<sub>6</sub>/MA at ambient temperature gave a normal TiS<sub>2</sub> pattern. All other samples exhibited numerous additional peaks indicating the presence of other phases in addition to TiS<sub>2</sub>, as shown in Tables 3-19 to 3-21.

Based on these results, TiS<sub>2</sub> has been found to be insoluble in methyl formate solutions and, possibly, slightly soluble in methyl acetate solutions. The chemical compatibility of TiS<sub>2</sub> in these solutions, however, is not conclusive due to the detection of additional phases in the stored samples.

### LITHIUM CYCLING EFFICIENCY MEASUREMENTS

All lithium cycling efficiencies were determined at strip and plate current densities of 1 mA/cm<sup>2</sup> at ambient temperature (20-24°C). Our objective in this task was to identify an ester-based electrolyte solution that could offer a lithium cycling efficiency of ≥ 91.6 percent, the value reported for a LiAsF<sub>6</sub>/methyl THF solution under test conditions similar to those that we were employing.<sup>13</sup> At the outset, we realized that it was unlikely that any of the pure solutions could achieve this level of performance. Therefore, our approach was to establish the baseline efficiency achievable with each solvent and then investigate the use of additives and other co-solvents as a means of further enhancing performance to the desired

TABLE 3-13. X-RAY DIFFRACTION DATA FOR  $V_2O_5$  STORED IN 2M  $LiAsF_6$  + 0.4M  $LiBF_4$ /MF AT AMBIENT TEMPERATURE (20-24°C)

hkl	d-spacing, Å		Relative Intensity, Percent	
	JCPDS Standard	Observed	JCPDS Standard	Observed
200	5.76	5.776	40	54
001	4.38	4.370	100	100
101	4.09	4.084	35	47
110	3.40	3.404	90	48
400	2.88	2.881	65	54
011	2.76	2.762	35	30
111	2.687	2.684	15	7
310	2.610	2.611	40	27
002	2.185	2.183	17	13
102	2.147	2.142	11	8
411	1.992	1.993	17	15
600	1.919	1.916	17	20
302	1.900	1.901	17	14
012	1.864	1.861	13	14
020	1.778	1.781	3	24
601	1.757	1.755	30	8
021	1.648	1.648	11	12
121	1.632	1.630	7	6
412	1.564	1.564	11	8
701	1.5396	1.5372	3	7
321	1.5149	1.5149	17	6
710	1.4925	1.4909	17	7
711	1.4090	1.4123	7	6

- NOTES:
1. Analysis conducted under helium flow.
  2. Observed relative intensity based on peak height rather than on integrated density.
  3. JCPDS Standard ( $V_2O_5$ ):  $a = 11.51\text{Å}$ ,  $b = 3.559\text{Å}$ ,  $c = 4.371\text{Å}$ , orthorhombic.

TABLE 3-14. X-RAY DIFFRACTION DATA FOR  $V_2O_5$  STORED IN 2M  $LiAsF_6/MA$  AT AMBIENT TEMPERATURE (20-24°C)

hkl	d-spacing, Å		Relative Intensity, Percent	
	JCPDS Standard	Observed	JCPDS Standard	Observed
200	5.76	5.783	40	47
001	4.38	4.385	100	100
101	4.09	4.095	35	32
110	3.40	3.409	90	88
400	2.88	2.885	65	69
011	2.76	2.767	35	32
111	2.687	2.691	15	11
310	2.610	2.616	40	32
002	2.185	2.189	17	15
102	2.147	2.153	11	10
411	1.992	1.996	17	17
600	1.919	1.920	25	27
302	1.900	1.901	17	12
012	1.864	1.865	13	10
020	1.778	1.782	3	32
601	1.757	1.757	30	12
021	1.648	1.651	11	10
321	1.5149	1.5153	17	15
710	1.4925	1.4929	17	14

- NOTES:
1. Analysis conducted in air.
  2. Observed intensity based on peak height rather than on integrated peak area.
  3. JCPDS Standard ( $V_2O_5$ ):  $a = 11.51\text{Å}$ ,  $b = 3.559\text{Å}$ ,  $c = 4.371\text{Å}$ , orthorhombic.

TABLE 3-15. X-RAY DIFFRACTION DATA FOR  $V_2O_5$  STORED IN 2M  $LiAsF_6$   
+ 0.4M  $LiBF_4/ME$  AT  $71^\circ C$ 

hkl	d-spacing, $\text{\AA}$		Relative Intensity, Percent	
	JCPDS Standard	Observed	JCPDS Standard	Observed
200	5.76	5.746	40	41
001	4.38	4.375	100	97
101	4.09	4.090	35	28
110	3.40	3.405	90	100
400	2.88	2.883	65	65
011	2.76	2.762	35	35
111	2.687	2.683	15	15
310	2.610	2.610	40	39
211	2.492	2.494	7	4
401	2.405	2.407	7	6
002	2.185	2.187	17	14
102	2.147	2.147	11	7
411	1.992	1.992	17	11
600	1.919	1.916	25	23
012	1.864	1.861	13	14
112	1.840	1.836	5	6
020	1.778	1.781	3	25
601	1.757	1.755	30	11
021	1.648	1.649	11	11
412	1.564	1.565	11	9
321	1.515	1.517	17	13
710	1.493	1.493	17	16
602	1.442	1.444	5	6
711	1.412	1.414	7	7

- NOTES:
1. Analysis conducted under helium flow.
  2. Observed intensity based on peak height rather than on integrated peak area.
  3. JCPDS Standard ( $V_2O_5$ ):  $a = 11.51\text{\AA}$ ,  $b = 3.559\text{\AA}$ ,  $c = 4.371\text{\AA}$ , orthorhombic.



TABLE 3-16. X-RAY DIFFRACTION DATA FOR  $V_2O_5$  STORED IN 2M LiAsF<sub>6</sub>/MA AT 71°C

hkl	d-spacing, Å		Relative Intensity, Percent	
	JCPDS Standard	Observed	JCPDS Standard	Observed
200	5.636	5.673	6	9
	-	4.372	-	5
010	4.971	4.997	100	100
110	4.548	4.564	8	13
210	3.728	3.739	6	9
001	3.389	3.401	10	17
101	3.245	3.255	12	27
310	2.997	2.998	8	17
400	2.818	2.820	8	20
301	2.517	2.520	4	10
020	2.485	2.483	4	12
	-	2.446	-	5
401	2.167	2.166	4	7
320	2.073	2.071	5	7
501	1.879	1.883	7	16
	-	1.810	-	12
511	1.757	1.760	8	11
002	1.694	1.694	3	4
	-	1.516	-	5
	-	1.481	-	6
	-	1.451	-	8

- NOTES:
1. Analysis conducted under helium flow.
  2. Observed intensity based on peak height rather than on integrated intensity.
  3. The standard pattern is for  $\delta$ -LiV<sub>2</sub>O<sub>5</sub> (Ref. 8) calculated values for orthorhombic cells: a = 11.272Å, b = 4.971Å, c = 3.389Å.

TABLE 3-17.  $TiS_2$  THERMAL STABILITY TESTS--PHYSICAL APPEARANCE OF SAMPLES AFTER STORAGE INTERVAL

<u>Storage Temperature</u>	<u>Electrolyte Solution</u>	<u>Observations</u>
Ambient (20-24°C)	2M $LiAsF_6$ + 0.4M $LiBF_4$ /MF	Clear solution. Li shiny, no deposit.
Ambient (20-24°C)	2M $LiAsF_6$ /MA	Clear solution. Li shiny, no deposit.
71°C	2M $LiAsF_6$ + 0.4M $LiBF_4$ /MF	Clear solution. Black Li metal.
71°C	2M $LiAsF_6$ /MA	Pale yellow solution. Heavy brown deposit on Li surface.

TABLE 3-18. SOLUBILITY OF  $TiS_2$  IN LITHIUM BATTERY ELECTROLYTES--BY AA ANALYSIS

<u>Electrolyte Solution</u>	<u>Storage Temperature</u>	<u>Solubility*</u> (ppm, Ti)
2M $LiAsF_6$ + 0.4M $LiBF_4$ /MF	Ambient (20-24°C)	< 5
2M $LiAsF_6$ /MA	Ambient (20-24°C)	< 5
2M $LiAsF_6$ + 0.4M $LiBF_4$ /MF	71°C	< 5
2M $LiAsF_6$ + 0.4M $LiBF_4$ /MF	71°C	< 5
2M $LiAsF_6$ /MA	71°C	130 **
2M $LiAsF_6$ /MA	71°C	203 **

\* AA resolution in these samples is 5 ppm for Titanium.

\*\* Very light suspension present in the sample.

TABLE 3-19. X-RAY DIFFRACTION DATA FOR  $\text{TiS}_2$  STORED IN  
 2M  $\text{LiAsF}_6/\text{MA}$  AT AMBIENT TEMPERATURE (20-24°C)

hkl	d-spacing, Å		Relative Intensity, Percent	
	JCPDS Standard	Observed	JCPDS Standard	Observed
001	5.69	5.746	55	100
100	2.95	2.961	2	1
002	2.85	2.858	2	5
101	2.62	2.627	100	26
102	2.05	2.054	45	21
003	1.90	1.903	2	3
110	1.70	1.711	25	7
111	1.63	1.641	8	2
103	1.60	1.606	16	9
201	1.427	1.428	10	8
202	1.309	1.311	8	3

- NOTES:
1. Analysis conducted under helium flow.
  2. Observed intensity based on peak height rather than on integrated peak area.
  3. JCPDS Standard ( $\text{TiS}_2$ ):  $a = 3.4049\text{Å}$ ,  $c = 5.6912\text{Å}$ , hexagonal.

TABLE 3-20. X-RAY DIFFRACTION DATA FOR  $\text{TiS}_2$  STORED  
IN 2M  $\text{LiAsF}_6$  + 0.4M  $\text{LiBF}_4/\text{MF}$  AT  $71^\circ\text{C}$

hkl	d-spacing, $\text{\AA}$		Relative Intensity, Percent	
	JCPDS Standard	Observed	JCPDS Standard	Observed
001	5.69	5.754	55	84
	-	5.293	-	9
	-	4.821	-	10
	-	4.143	-	12
	-	3.641	-	6
	-	3.555	-	11
	-	3.296	-	6
	-	3.124	-	4
	-	3.053	-	4
100	2.95	2.959	2	4
002	2.85	2.865	2	4
101	2.62	2.633	100	100
	-	2.214	-	7
	-	2.157	-	4
	-	2.128	-	3
102	2.05	2.058	45	1
	-	2.006	-	4
003	1.90	1.907	2	4
	-	1.875	-	4
	-	1.771	-	3
	-	1.741	-	3
110	1.70	1.707	25	28
111	1.63	1.635	8	7
103	1.60	1.600	16	15
	-	1.530	-	3
201	1.427	1.429	10	13
202	1.309	1.312	8	8

- NOTES:
1. Analysis conducted under helium flow.
  2. Observed intensity based on peak height rather than on integrated peak area.
  3. JCPDS Standard ( $\text{TiS}_2$ ):  $a = 3.4049\text{\AA}$ ,  $c = 5.6912\text{\AA}$ , hexagonal.

TABLE 3-21. X-RAY DIFFRACTION DATA FOR  $\text{TiS}_2$  STORED IN  
2M  $\text{LiAsF}_6/\text{MA}$  at  $71^\circ\text{C}$ 

hkl	d-spacing, $\text{\AA}$		Relative Intensity, Percent	
	JCPDS Standard	Observed	JCPDS Standard	Observed
001	5.69	5.765	55	48
	-	5.299	-	14
	-	4.809	-	15
	-	3.777	-	10
	-	3.555	-	34
	-	3.061	-	7
002	2.85	2.871	2	6
101	2.62	2.627	100	100
	-	2.344	-	14
	-	2.156	-	5
102	2.05	2.058	45	35
	-	2.032	-	40
110	1.70	1.708	25	36
111	1.63	1.636	8	11
103	1.60	1.605	16	18
201	1.427	1.432	10	24
202	1.309	1.313	8	9

- NOTES:
1. Analysis conducted under helium flow.
  2. Observed intensity based on peak height rather than on integrated peak area.
  3. JCPDS Standard ( $\text{TiS}_2$ ):  $a = 3.4049\text{\AA}$ ,  $c = 5.6912\text{\AA}$ , hexagonal.

levels. We also felt that solute concentration could have a significant impact on lithium cycling efficiency and therefore included this variable in our evaluations.

### Methyl Formate Solutions

Baseline Evaluations. The objectives of these initial tests were to determine the cycling efficiencies of 2M LiAsF<sub>6</sub>/MF solutions and to establish the effects of the following parameters on lithium cyclability:

- o LiBF<sub>4</sub>
- o Cell Configuration
- o Solution Deaeration with Argon
- o Substrate Material

The results are summarized in Table 3-22. It was found that neither substrate material nor solution deaeration had a significant effect on lithium cycling efficiency. Flooded cells, however, tended to give lower results than 2-plate wick cells. LiBF<sub>4</sub> was indicated to be somewhat detrimental, lowering the efficiency from approximately 77 percent to about 70 percent when added at a concentration of 0.4M. Typical voltage profiles for the solutions with and without LiBF<sub>4</sub> present are shown in Figures 3-35 and 3-36.

The precipitates formed during the cycling tests were collected and analyzed by infrared spectroscopy using KBr pellets. The resulting spectra are shown in Figures 3-37 and 3-38. The strong and broad peaks around 3400 cm<sup>-1</sup> and the sharp peak at 1620-1640 cm<sup>-1</sup> are attributed to moisture, apparently introduced during sample preparation and handling. Characteristic peaks due to AsF<sub>6</sub><sup>-</sup> were present in both spectra at 710-720 cm<sup>-1</sup> and around 400 cm<sup>-1</sup>. Also, in the spectrum of the material collected from the 2M LiAsF<sub>6</sub> + 0.4M LiBF<sub>4</sub>/MF solution, peaks were observed at 1080 and 520 cm<sup>-1</sup>, characteristic of the BF<sub>4</sub><sup>-</sup> anion. Table 3-23 summarizes the bands observed in each sample. These analyses indicate that both the solvent and solute are involved in the interaction with lithium during extensive cycling.

Based on these results, the wick cell was selected as the preferred cell configuration with methyl formate solutions. It was also evident that significant improvements were required in the lithium cycling efficiency if methyl formate solutions were to be practical in rechargeable applications.

Effects of Solute Concentration. Table 3-24 summarizes the lithium cycling efficiencies achieved in methyl formate solutions as a function of LiAsF<sub>6</sub> concentration over the range of 0.5M to 2M. The results, shown graphically in Figure 3-39, demonstrate that the lithium cycling efficiency increases significantly as the solute concentration is lowered.

Although 2M LiAsF<sub>6</sub>/MF solutions would be preferred in order to achieve maximum performance capabilities, methyl formate solutions are so conductive that even dilute solutions can offer reasonable conductivities. For example, a 0.5M LiAsF<sub>6</sub>/MF solution has a conductivity of 16.3 mMH0/cm at ambient

TABLE 3-22. LITHIUM CYCLING RESULTS IN METHYL FORMATE SOLUTIONS--BASELINE EVALUATIONS

Electrolyte Solution	Cell Configuration	Substrate Material	Solution Pre-treatment	Starting Working Electrode Capacity (mAh)	No. of Cycles	Lithium Efficiency Percent
2M LiAsF <sub>6</sub> /MF	Wick	Ni	deaerated	55.8	24	80
2M LiAsF <sub>6</sub> /MF	Wick	Ni	deaerated	51.7	17	74
2M LiAsF <sub>6</sub> /MF	Wick	S.S.	deaerated	53.0	20	78
2M LiAsF <sub>6</sub> /MF	Half-Cell	S.S.	none	58.8	15	66
2M LiAsF <sub>6</sub> /MF	Half-Cell	S.S.	none	54.3	16	71
2M LiAsF <sub>6</sub> /MF	Half-Cell	S.S.	none	56.0	4	67
2M LiAsF <sub>6</sub> + 0.4M LiBF <sub>4</sub> /MF	Wick	Ni	deaerated	52.0	15	71
2M LiAsF <sub>6</sub> + 0.4M LiBF <sub>4</sub> /MF	Wick	Ni	deaerated	51.5	14	69
2M LiAsF <sub>6</sub> + 0.4M LiBF <sub>4</sub> /MF	Wick	S.S.	none	54.5	15	69

Note: S.S. = 304 Stainless Steel



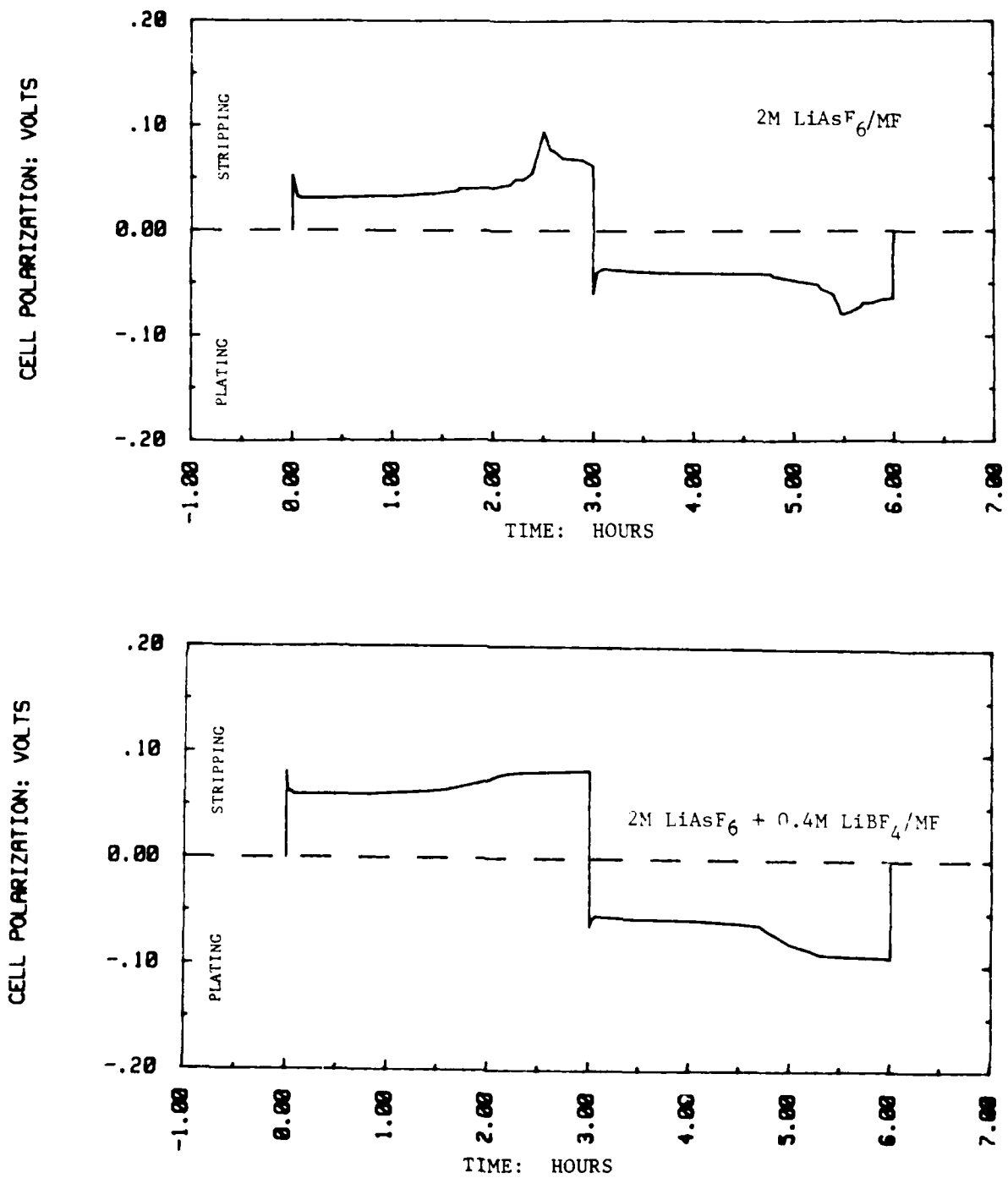


FIGURE 3-35. LITHIUM CYCLABILITY TESTS: TYPICAL VOLTAGE PROFILES FOR METHYL FORMATE SOLUTIONS IN WICK CELLS (THIRD CYCLE)

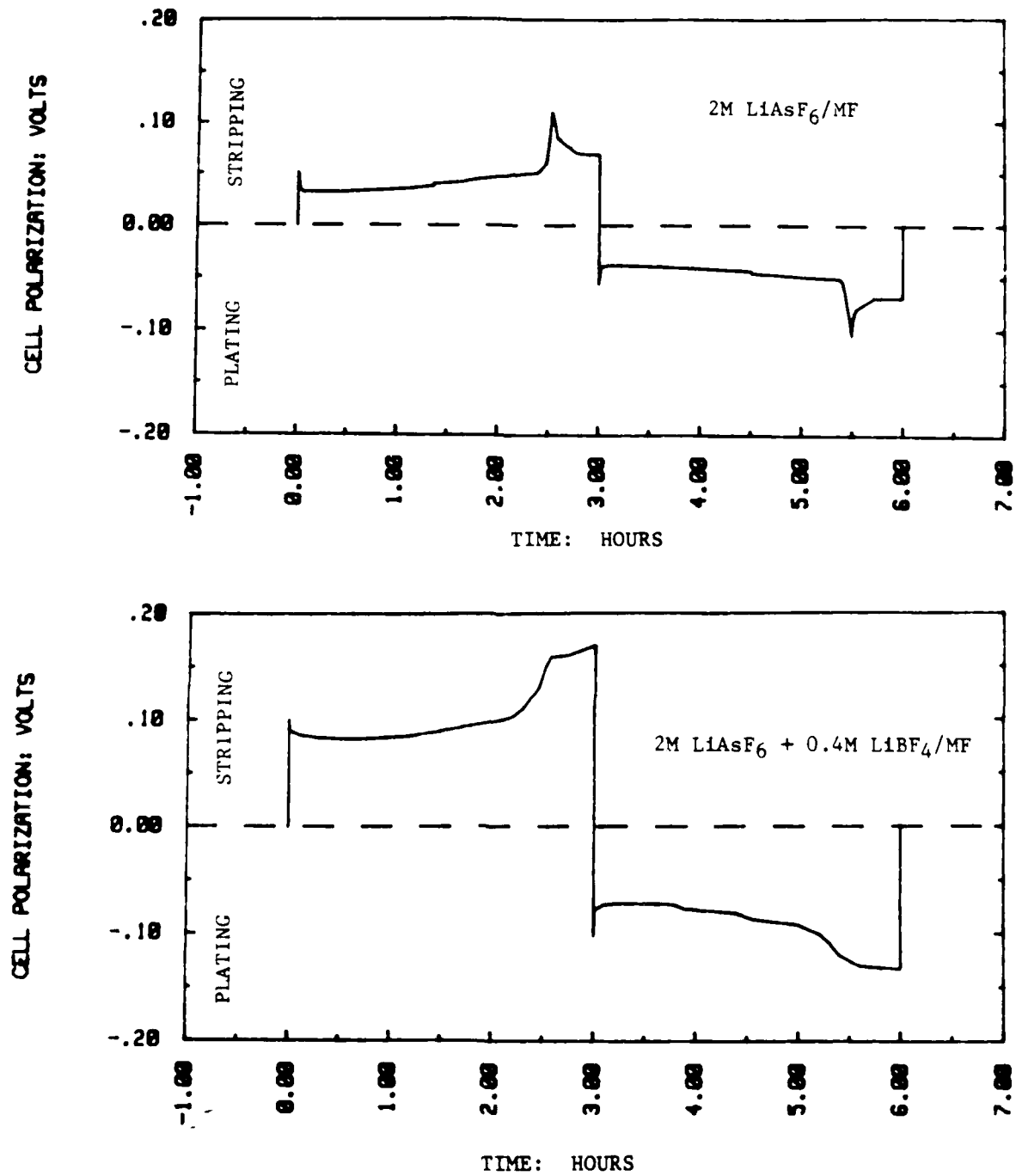


FIGURE 3-36. LITHIUM CYCLABILITY TESTS: TYPICAL VOLTAGE PROFILES FOR METHYL FORMATE SOLUTIONS IN WICK CELLS (TENTH CYCLE)

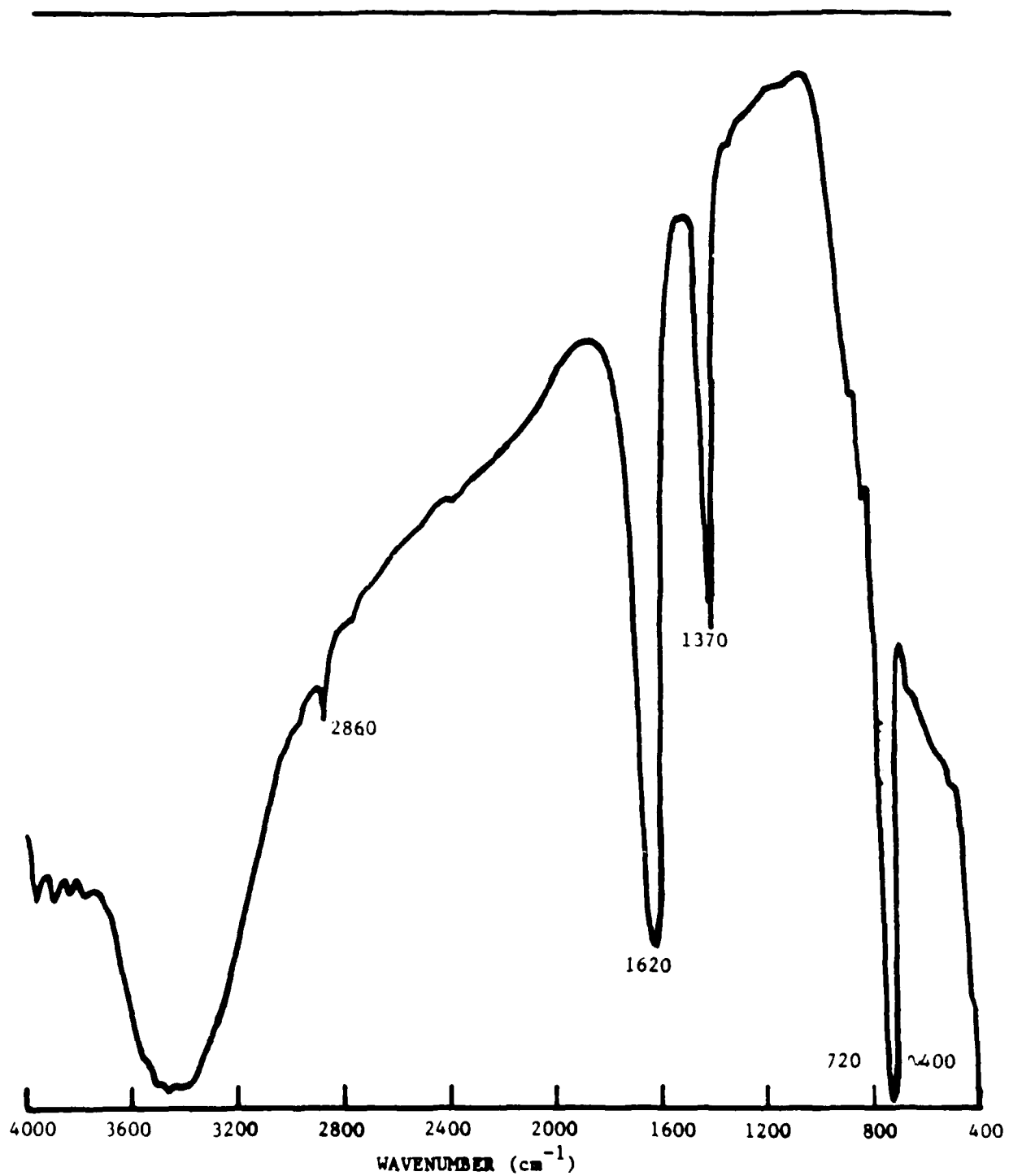


FIGURE 3-37. LITHIUM CYCLABILITY TESTS: IR SPECTRUM OF SOLID PRODUCT FROM 2M LiAsF<sub>6</sub>/MF CELL

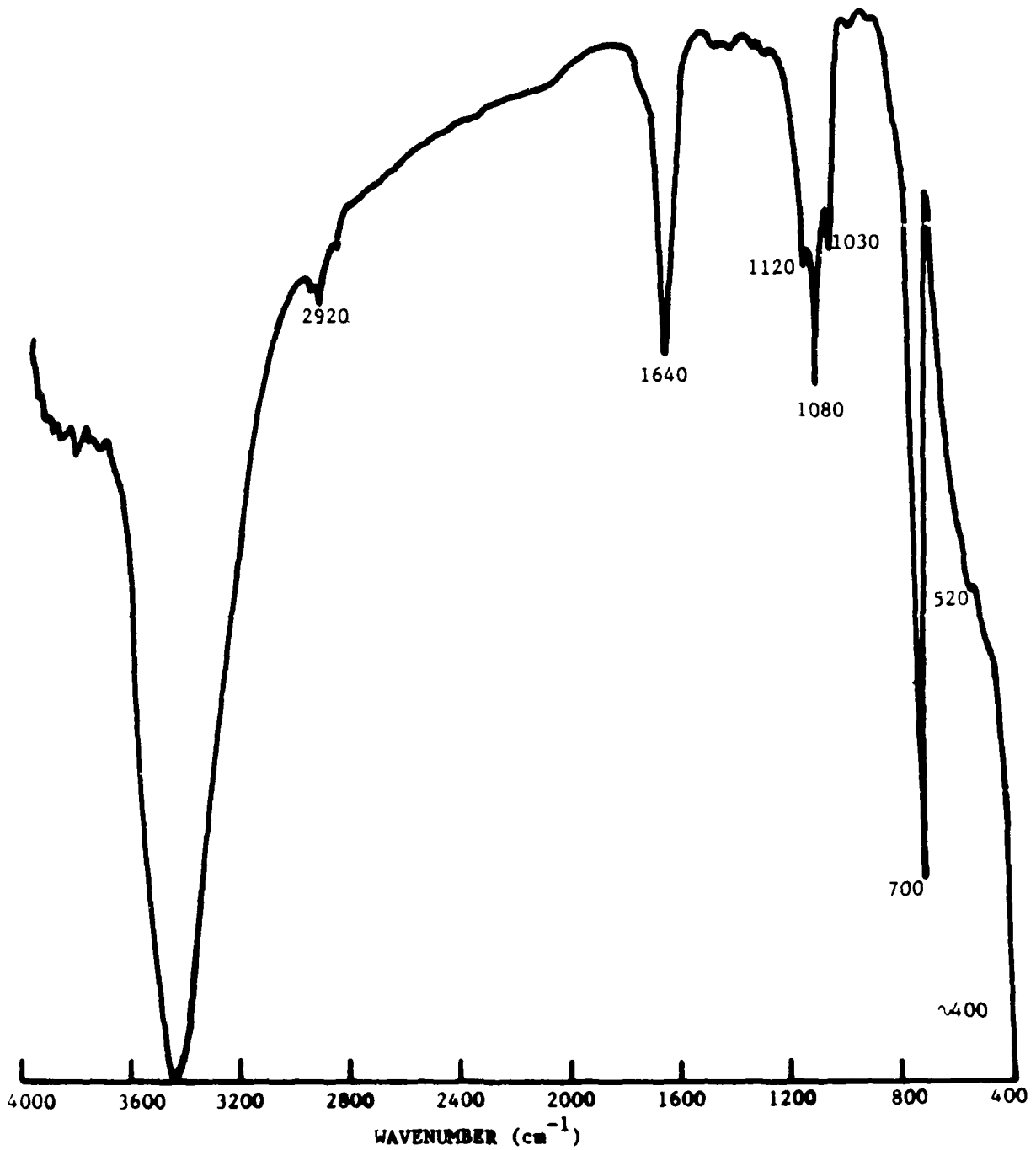


FIGURE 3-38. LITHIUM CYCLABILITY TESTS: IR SPECTRUM OF SOLID PRODUCT FROM 2M LiAsF<sub>6</sub> + 0.4M LiBF<sub>4</sub>/MF CELL

TABLE 3-23. LITHIUM CYCLABILITY TESTS: SUMMARY OF IR RESULTS FOR SOLID PRODUCT FROM METHYL FORMATE SOLUTIONS

<u>Electrolyte Solution</u>	<u>Bands Attributed To Organic Products (cm<sup>-1</sup>)</u>	<u>Bands Attributed To Solutes (cm<sup>-1</sup>)</u>	
2M LiAsF <sub>6</sub> /MF	2860	720	} AsF <sub>6</sub> <sup>-</sup>
	1370	~400	
2M LiAsF <sub>6</sub> + 0.4M LiBF <sub>4</sub> /MF	2960	700	} AsF <sub>6</sub> <sup>-</sup>
	2920	~400	
	2850		
	1120	1080	} BF <sub>4</sub> <sup>-</sup>
	1030	520	

TABLE 3-24. EFFECT OF LiAsF<sub>6</sub> CONCENTRATION ON LITHIUM CYCLING EFFICIENCY IN METHYL FORMATE (WICK CELL, NICKEL SUBSTRATE, DEAERATED)

<u>Electrolyte Solution</u>	<u>Starting Working Electrode Capacity, mAh</u>	<u>No. of Cycles</u>	<u>Lithium Efficiency Percent</u>
2M LiAsF <sub>6</sub> /MF*	53.7	20	77
1.0M LiAsF <sub>6</sub> /MF	58.3	23	78
0.5M LiAsF <sub>6</sub> /MF	49.6	32	87
2M LiAsF <sub>6</sub> + 0.4M LiBF <sub>4</sub> /MF*	51.8	14	70
1M LiAsF <sub>6</sub> + 0.2M LiBF <sub>4</sub> /MF	57.0	26	81
0.5M LiAsF <sub>6</sub> + 0.1M LiBF <sub>4</sub> /MF	51.1	28	85

\* Represents the average of two experiments. Individual results are given in Table 3-22.

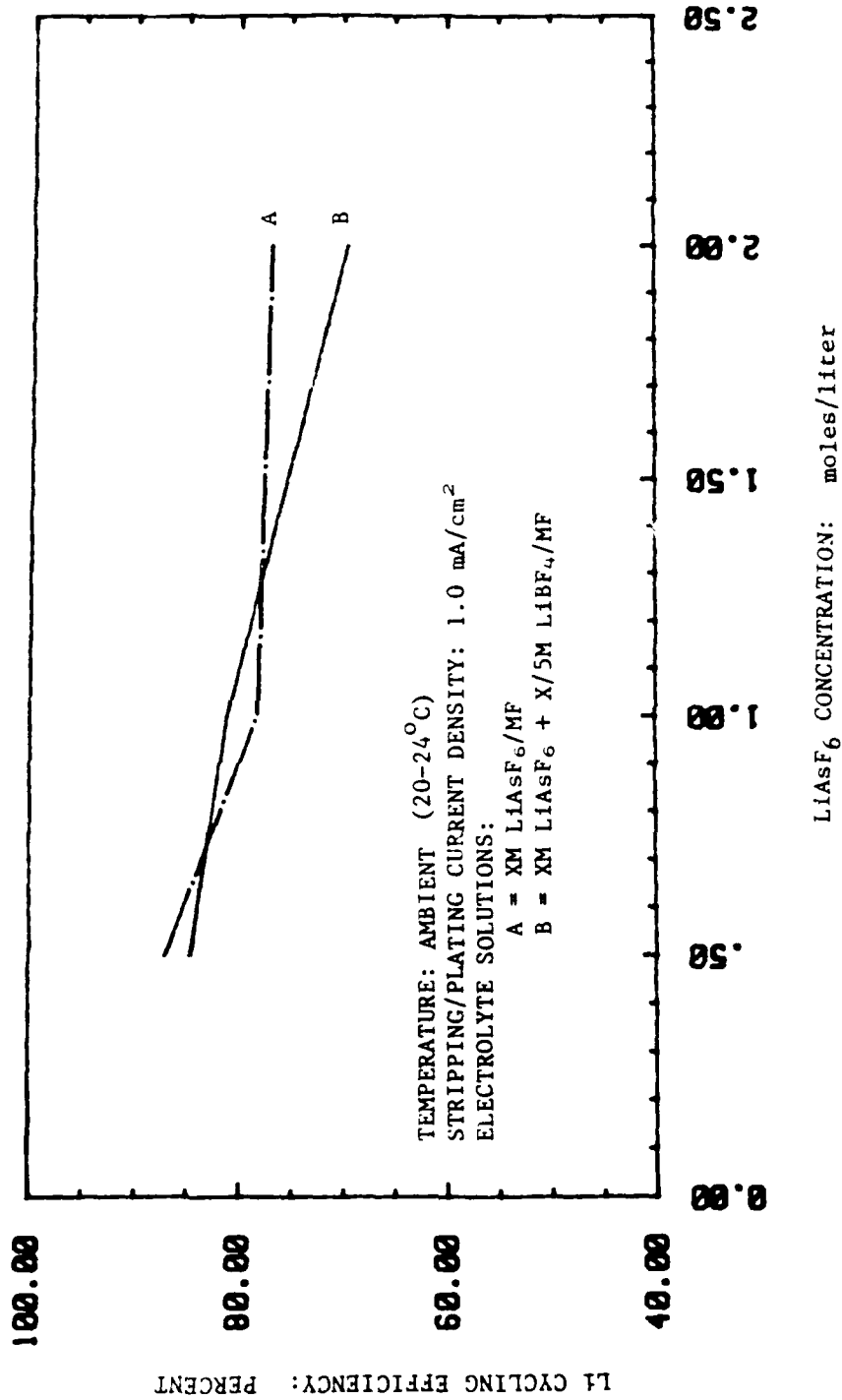


FIGURE 3-39. LITHIUM CYCLING EFFICIENCY VERSUS LiAsF<sub>6</sub> CONCENTRATION FOR METHYL FORMATE SOLUTIONS IN WICK CELLS

temperature. Therefore, lower solution concentrations could indeed be a viable means of improving the cyclability of lithium in methyl formate solutions without severely degrading performance.

Effects of Electrolyte Additives.<sup>9</sup> In an effort to improve the lithium cycling efficiency of concentrated methyl formate solutions, additives consisting of 2-methoxy-ethanol, 2-methyl-furan, and carbon dioxide ( $\text{CO}_2$ ) were evaluated. 2-methoxy-ethanol and 2-methyl-furan were selected based on their reported ability to enhance the lithium cycling efficiency in 2-methyl THF solutions.<sup>14,15</sup>

$\text{CO}_2$  was evaluated as a precursor to reduce the parasitic loss of plated lithium through the formation of an ionically conductive, protective film. The investigations included using  $\text{CO}_2$  both as an electrolyte additive and as a method to pretreat the lithium anode prior to exposure to the electrolyte solution.

The results for 2-methoxy-ethanol and 2-methyl furan are given in Table 3-25. As can be seen, these additives were both found to be detrimental, yielding significantly lower cycling efficiencies than the undoped solution.

Table 3-26 summarizes the results achieved with  $\text{CO}_2$ . Pretreatment of the working lithium electrodes was carried out by storing the electrodes in a sealed vessel with 20 psig  $\text{CO}_2$  pressure for 3, 24, or 120 hours. This technique was found to significantly improve the lithium cycling efficiency in the more concentrated solutions. Figure 3-40 illustrates this effect by comparing the results for solutions with and without pretreatment of the anode. Using this approach, efficiencies of 84 to 87 percent were achieved with a 1M  $\text{LiAsF}_6$  + 0.2M  $\text{LiBF}_4/\text{MF}$  solution.

In the tests employing  $\text{CO}_2$  as an electrolyte additive, solutions were first saturated with  $\text{CO}_2$  and then, following activation, the cells were pressurized with  $\text{CO}_2$  gas. As can be seen in Table 3-26, excellent results were achieved by this method. The lithium cycling efficiency of 93 percent obtained with a 2M  $\text{LiAsF}_6$  + 0.4M  $\text{LiBF}_4/\text{MF}$  solution exceeds the reported value for  $\text{LiAsF}_6/2\text{-methyl THF}$  solutions under similar experimental conditions.  $\text{CO}_2$  was also observed to decrease the anode polarization levels, as illustrated in Figures 3-41 and 3-42.

### Methyl Acetate Solutions

Baseline Evaluations. Table 3-27 summarizes the results for the baseline tests conducted with the 2M  $\text{LiAsF}_6/\text{MA}$  solutions. These results indicate a lithium cycling efficiency of approximately 70 percent for this solution with no significant effects noted for solution deaeration, substrate material, or cell configuration.

The infrared spectrum for the solid product formed during the cycle tests is shown in Figure 3-43, while the observed bands are summarized in Table 3-28. These results indicate that both the solute and solvent are involved in the reactions leading to the formation of the solid product.

TABLE 3-25. EFFECT OF ORGANIC ADDITIVES ON LITHIUM CYCLING EFFICIENCY IN METHYL FORMATE

<u>Electrolyte Solution</u>	<u>Additive</u>	<u>Additive Concentration, w/o</u>	<u>Starting Working Electrode Capacity, mAh</u>	<u>No. of Cycles</u>	<u>Lithium Efficiency Percent</u>
2M LiAsF <sub>6</sub> + 0.4M LiBF <sub>4</sub> /MF	None	-	51.8	14	70
2M LiAsF <sub>6</sub> + 0.4M LiBF <sub>4</sub> /MF	2-Methoxyethanol	2	42.7	7	51
2M LiAsF <sub>6</sub> + 0.4M LiBF <sub>4</sub> /MF	2-Methyl furan	2	45.7	6	34

- NOTES: 1. All tests were conducted in wick cells employing nickel substrates and all solutions were deaerated with argon prior to use.
2. The value for the undoped solution represents the average of two tests. See Table 3-22 for individual results.



TABLE 3-26. EFFECT OF CO<sub>2</sub> ON LITHIUM CYCLING EFFICIENCY IN METHYL FORMATE (WICK CELL, NICKEL SUBSTRATE)

<u>Electrolyte Solution</u>	<u>Solution Pretreatment</u>	<u>Working Electrode Pretreatment Time with CO<sub>2</sub>, Hr.</u>	<u>Cell CO<sub>2</sub> Over-pressure, psig</u>	<u>Starting Working Electrode Capacity, mAh</u>	<u>No. of Cycles</u>	<u>Lithium Efficiency Percent</u>
2M LiAsF <sub>6</sub> + 0.4M LiBF <sub>4</sub> /MF	deaerated	none	none	51.8	14	70
2M LiAsF <sub>6</sub> + 0.4M LiBF <sub>4</sub> /MF	deaerated	3	none	44.4	18	80
2M LiAsF <sub>6</sub> + 0.4M LiBF <sub>4</sub> /MF	deaerated	24	none	44.7	20	81
2M LiAsF <sub>6</sub> + 0.4M LiBF <sub>4</sub> /MF	deaerated	120	none	53.6	17	73
1M LiAsF <sub>6</sub> + 0.2M LiBF <sub>4</sub> /MF	deaerated	none	none	57.0	26	81
1M LiAsF <sub>6</sub> + 0.2M LiBF <sub>4</sub> /MF	deaerated	3	none	42.7	26	87
1M LiAsF <sub>6</sub> + 0.2M LiBF <sub>4</sub> /MF	deaerated	24	none	44.0	22	84
1M LiAsF <sub>6</sub> + 0.2M LiBF <sub>4</sub> /MF	deaerated	120	none	45.6	26	86
0.5M LiAsF <sub>6</sub> + 0.1M LiBF <sub>4</sub> /MF	deaerated	none	none	51.1	28	85
0.5M LiAsF <sub>6</sub> + 0.1M LiBF <sub>4</sub> /MF	deaerated	24	none	43.7	22	84
2M LiAsF <sub>6</sub> + 0.4M LiBF <sub>4</sub> /MF	purged with CO <sub>2</sub>	none	50	49.0	58	93
2M LiAsF <sub>6</sub> + 0.4M LiBF <sub>4</sub> /MF	purged with CO <sub>2</sub>	none	8	68.9	57	89

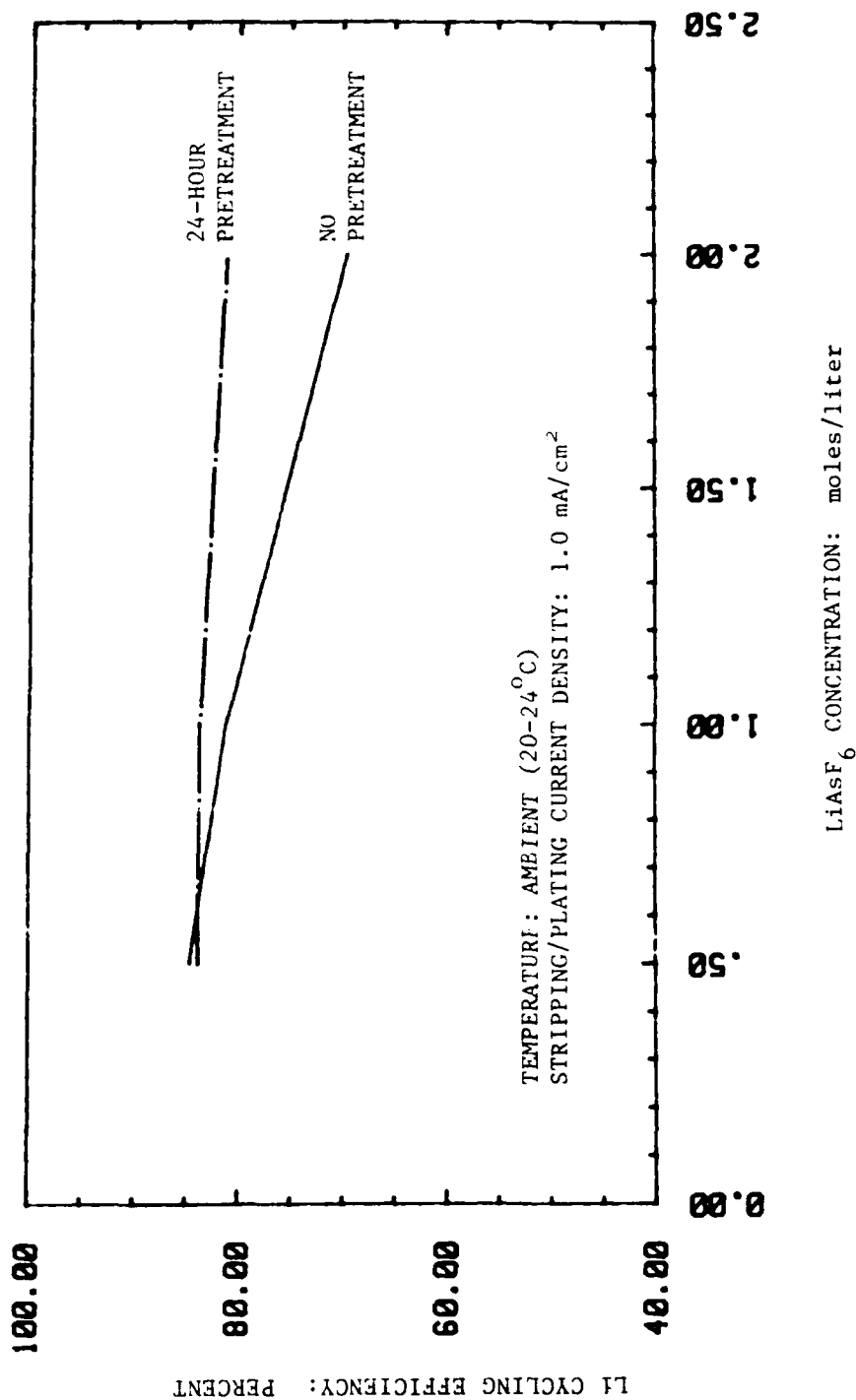


FIGURE 3-40. LITHIUM CYCLING EFFICIENCIES FOR XM LiAsF<sub>6</sub> + X/5M LiBF<sub>4</sub>/MF SOLUTIONS WITH AND WITHOUT CO<sub>2</sub> PRETREATMENT OF THE WORKING ELECTRODES

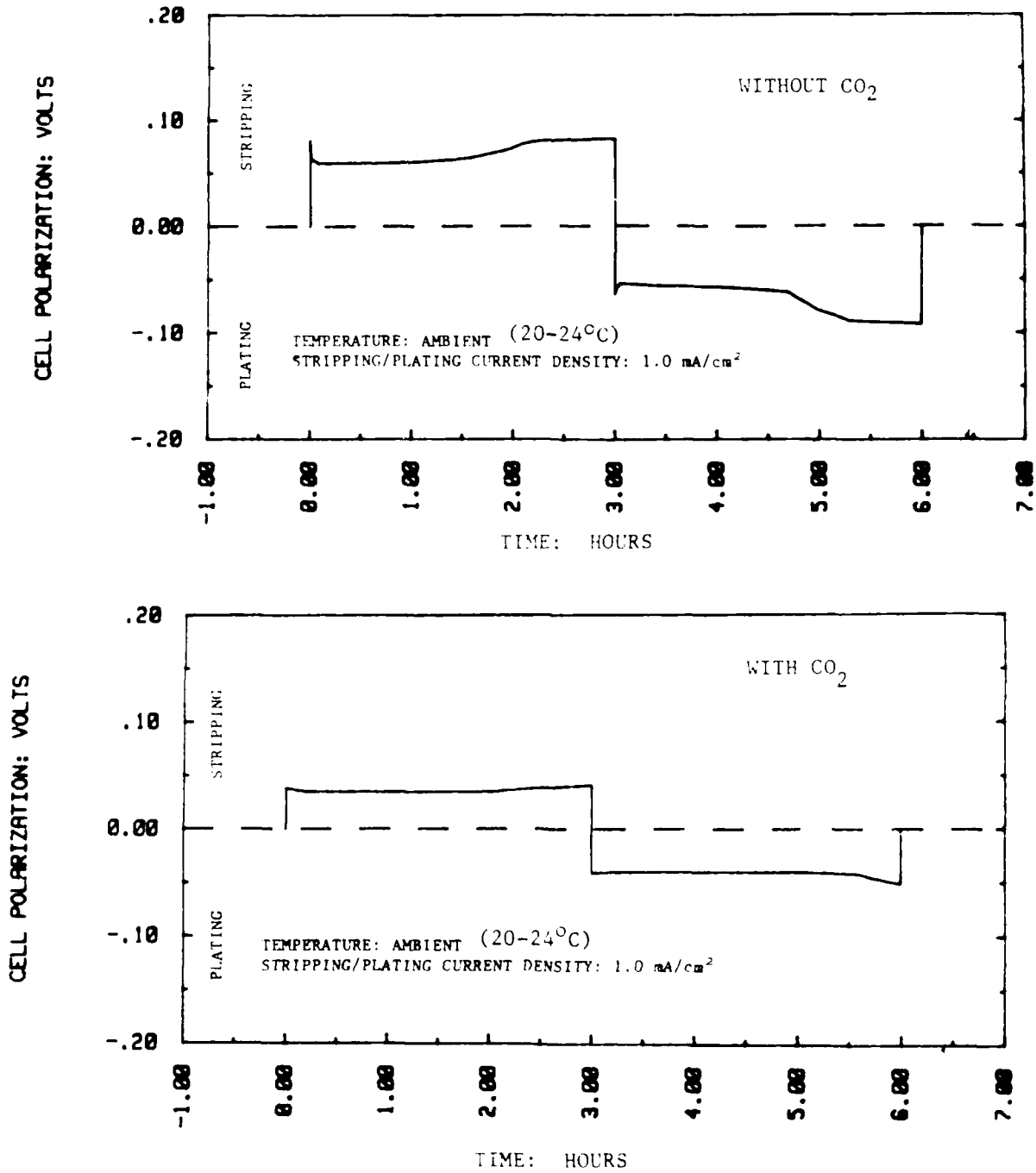


FIGURE 3-41. LITHIUM CYCLABILITY TESTS: TYPICAL VOLTAGE PROFILES FOR 2M LiAsF<sub>6</sub> + 0.4M LiBF<sub>4</sub>/MF SOLUTIONS IN WICK CELLS WITH AND WITHOUT CO<sub>2</sub> ADDED TO SOLUTION (THIRD CYCLE)

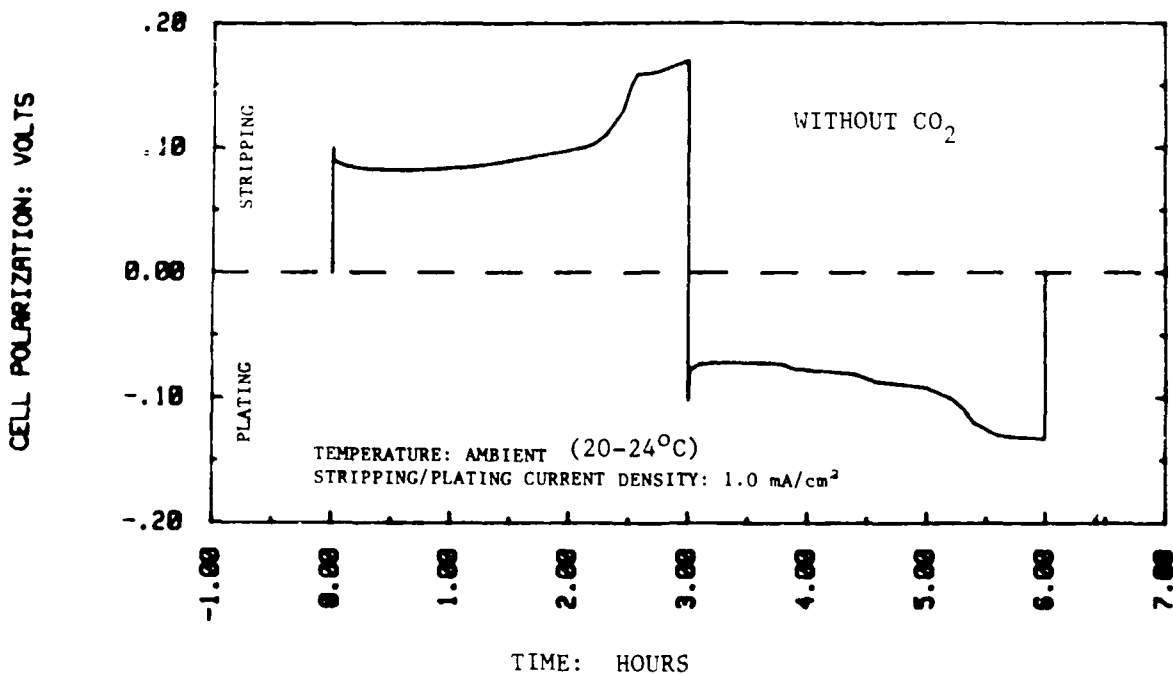
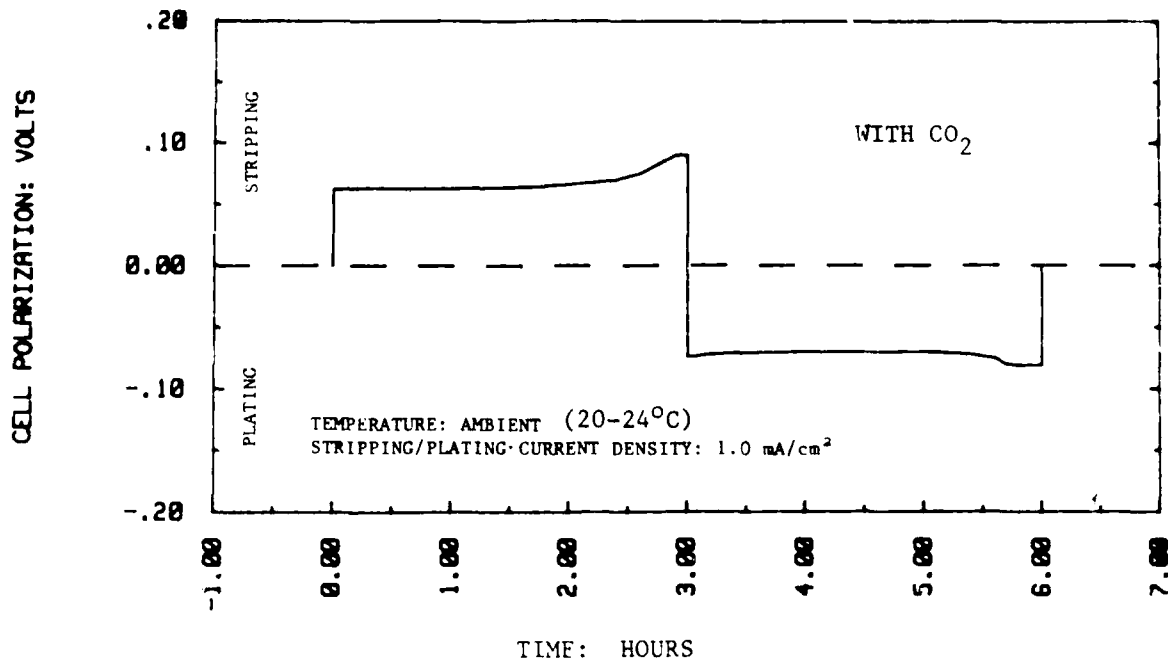


FIGURE 3-42. LITHIUM CYCLABILITY TESTS: TYPICAL VOLTAGE PROFILES FOR 2M LiAsF<sub>6</sub> + 0.4M LiBF<sub>4</sub>/MF SOLUTIONS IN WICK CELLS WITH AND WITHOUT CO<sub>2</sub> ADDED TO SOLUTION (TENTH CYCLE)

TABLE 3-27. LITHIUM CYCLING RESULTS IN METHYL ACETATE SOLUTIONS--BASELINE EVALUATIONS

<u>Electrolyte Solution</u>	<u>Cell Configuration</u>	<u>Substrate Material</u>	<u>Solution Pre-treatment</u>	<u>Starting Working Electrode Capacity, mAh</u>	<u>No. of Cycles</u>	<u>Lithium Efficiency Percent</u>
2M LiAsF <sub>6</sub> /MA	wick	Ni	deaerated	51.6	14	69
2M LiAsF <sub>6</sub> /MA	half-cell	304 Stainless Steel	none	57.6	15	71

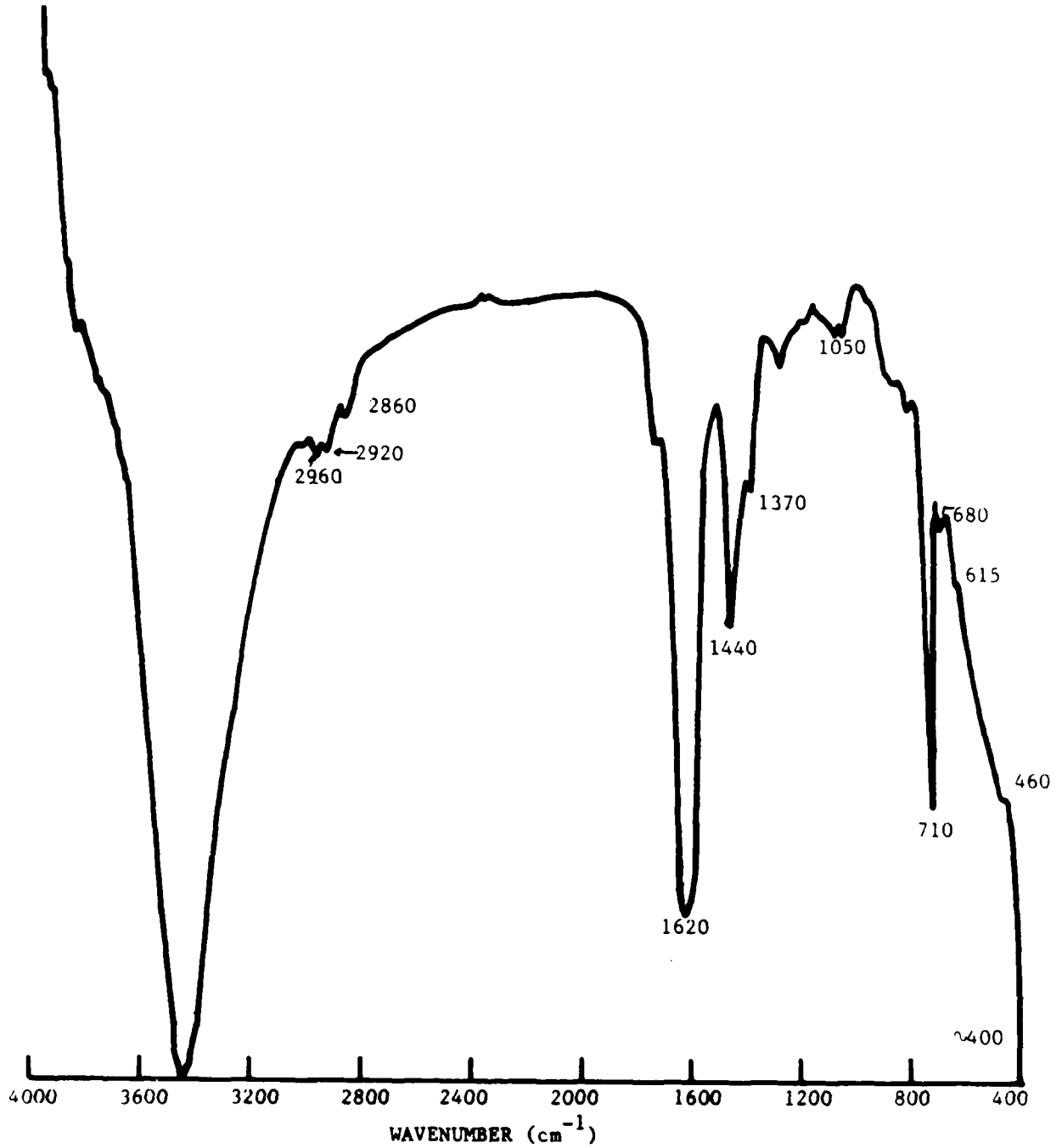


FIGURE 3-43. IR SPECTRUM OF SOLID REACTION PRODUCT FORMED ON LITHIUM CYCLED IN 2M LiAsF<sub>6</sub>/MA

TABLE 3-28. LITHIUM CYCLABILITY TESTS: SUMMARY OF IR RESULTS FOR SOLID PRODUCT FROM 2M LiAsF<sub>6</sub>/MA SOLUTIONS

<u>Bands Attributed To Organic Products (cm<sup>-1</sup>)</u>	<u>Bands Attributed To Solutes (cm<sup>-1</sup>)</u>
2960	710
2920	} AsF <sub>6</sub> <sup>-</sup>
2860	
1440	
1370	
1050	
680	
615	
460	

Effects of Solute Concentration. Table 3-29 summarizes the lithium cycling efficiencies achieved in LiAsF<sub>6</sub>/MA solutions over the concentration range of 0.5M to 3M. As can be seen, the trend is just the opposite of that observed with methyl formate solutions in that the efficiency increases with increasing soluble concentration. The results also indicate that there is a difference attributed to cell configuration at lower concentrations with wick cells yielding lower efficiencies. Figure 3-44 shows the effects of solute concentration on lithium cycling efficiency for both cell configurations.

Effects of Ether Co-Solvents.<sup>9</sup> In an effort to improve the lithium cycling efficiency of methyl acetate solutions, blended solvent mixtures containing ether co-solvents were evaluated. The two co-solvents investigated were 1,2-DME and THF. These tests were conducted using 2-plate wick cells.

The results are summarized in Table 3-30. As can be seen, no improvements were achieved with any of the blended solvents evaluated.

Effects of Electrolyte Additives.<sup>9</sup> Another approach investigated to improve the lithium cycling efficiency of methyl acetate solutions was the use of electrolyte additives. The additives evaluated were 2-methoxy-ethanol and 2-methyl-furan. Tests were conducted with both MA and MA + THF mixtures. Pretreatment of the anode with CO<sub>2</sub> was also investigated in these studies. These tests also employed 2-plate wick cells.

Table 3-31 summarizes the results for the investigations involving 2-methoxy-ethanol and 2-methyl-furan. As can be seen, no improvements in lithium cycling efficiency were achieved with these additives.

TABLE 3-29. EFFECT OF  $\text{LiAsF}_6$  CONCENTRATION ON LITHIUM CYCLING EFFICIENCY IN METHYL ACETATE

<u>Electrolyte Solution</u>	<u>Cell Configuration</u>	<u>Substrate Material</u>	<u>Solution Pre-treatment</u>	<u>Starting Working Electrode Capacity, mAh</u>	<u>No. of Cycles</u>	<u>Lithium Efficiency Percent</u>
3M $\text{LiAsF}_6$ /MA	wick	Ni	deaerated	55.9	18	73
2M $\text{LiAsF}_6$ /MA	wick	Ni	deaerated	51.6	14	69
1M $\text{LiAsF}_6$ /MA	wick	Ni	deaerated	46.7	8	51
0.5M $\text{LiAsF}_6$ /MA	wick	Ni	deaerated	48.2	6	36
2M $\text{LiAsF}_6$ /MA	half-cell	304 SS	none	57.6	15	71
1M $\text{LiAsF}_6$ /MA	half-cell	Ni	none	54.5	11	60
0.5M $\text{LiAsF}_6$ /MA	half-cell	Ni	none	66.3	11	49

TABLE 3-30. EFFECT OF ETHER CO-SOLVENTS ON LITHIUM CYCLING EFFICIENCY IN METHYL ACETATE

<u>Co-Solvent</u>	<u>Co-Solvent Concentration, w/o</u>	<u>Starting Working Electrode Capacity, mAh</u>	<u>No. of Cycles</u>	<u>Lithium Efficiency, Percent</u>
None	-	51.6	14	69
Tetrahydrofuran	2	56.9	13	62
Tetrahydrofuran	11	54.5	10	53
Tetrahydrofuran	17	45.3	9	59
Tetrahydrofuran	25	48.4	11	63
Tetrahydrofuran	50	47.9	9	56
1,2-Dimethoxyethane	11	59.1	8	39
1,2-Dimethoxyethane	17	40.5	8	59
1,2-Dimethoxyethane	25	45.0	10	63
1,2-Dimethoxyethane	50	40.4	7	52

- NOTES: 1. All tests were conducted in wick cells employing nickel substrates for the working electrodes.
2. All solutions were deaerated with argon prior to use.



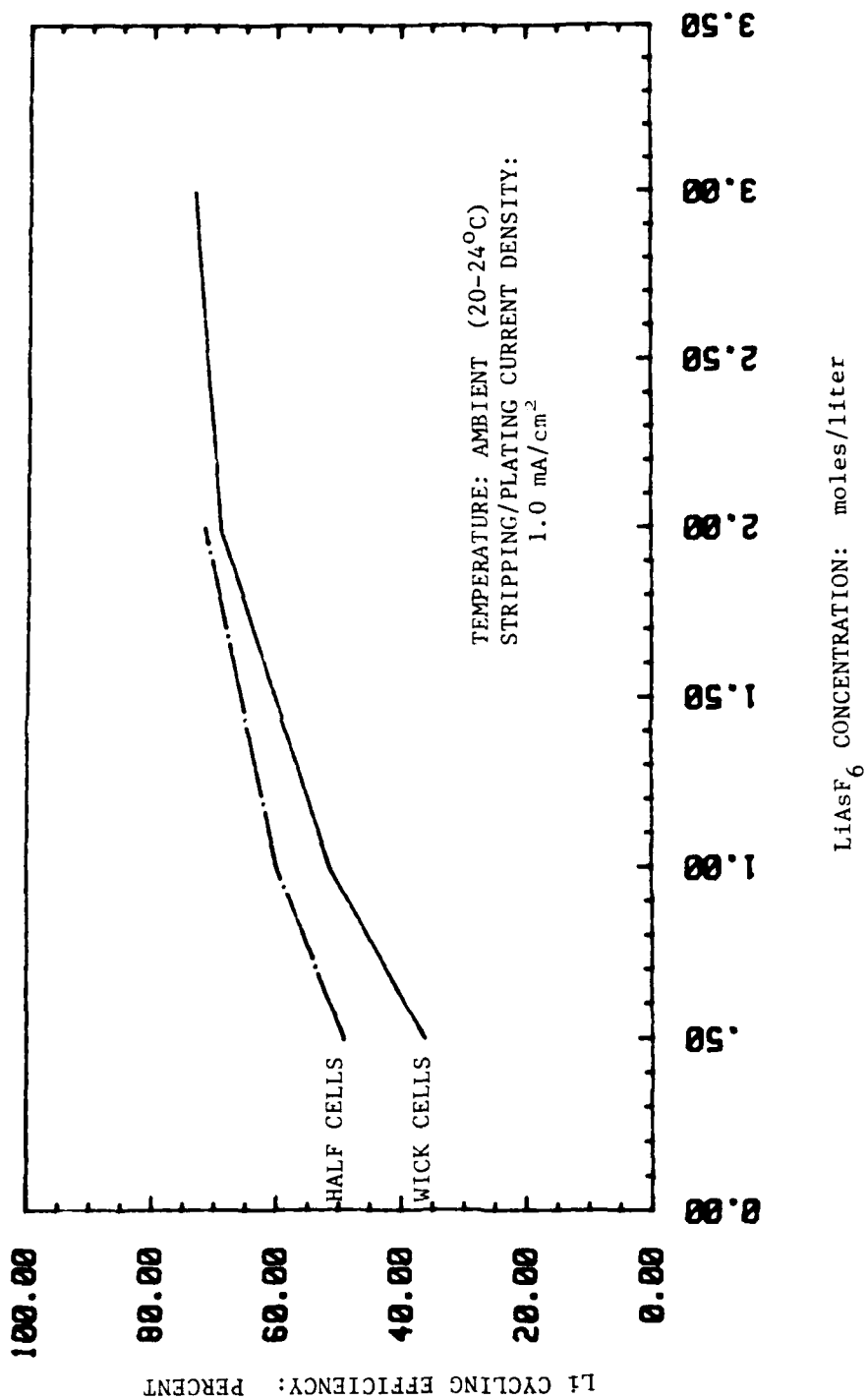


FIGURE 3-44. LITHIUM CYCLING EFFICIENCY VERSUS LiAsF<sub>6</sub> CONCENTRATION FOR METHYL ACETATE SOLUTIONS

TABLE 3-31. EFFECT OF ORGANIC ADDITIVES ON LITHIUM CYCLING EFFICIENCY IN METHYL ACETATE

<u>Electrolyte Solution</u>	<u>Additive</u>	<u>Additive Concentration v/o</u>	<u>Starting Working Electrode Capacity, mAh</u>	<u>No. of Cycles</u>	<u>Lithium Efficiency Percent</u>
2M LiAsF <sub>6</sub> /MA	none	-	51.6	14	69
2M LiAsF <sub>6</sub> /MA	2-methoxyethanol	0.3	49.5	11	62
2M LiAsF <sub>6</sub> /MA	2-methoxyethanol	2.0	59.3	15	65
2M LiAsF <sub>6</sub> /MF	2-methyl furan	2.0	55.9	9	67
2M LiAsF <sub>6</sub> /MA + THF (50:50)	none	-	47.9	9	56
2M LiAsF <sub>6</sub> /MA + THF (50:50)	2-methoxyethanol	0.3	46.3	8	50
2M LiAsF <sub>6</sub> /MA + THF (50:50)	2-methoxyethanol	1.0	51.7	10	55
2M LiAsF <sub>6</sub> /MA + THF (50:50)	2-methoxyethanol	2.5	47.4	4	<10
2M LiAsF <sub>6</sub> /MA + THF (50:50)	2-methoxyethanol	5.0	40.6	3	<10
2M LiAsF <sub>6</sub> /MA + THF (50:50)	2-methyl furan	0.3	46.6	9	57
2M LiAsF <sub>6</sub> /MA + THF (50:50)	2-methyl furan	1.0	50.6	9	54
2M LiAsF <sub>6</sub> /MA + THF (50:50)	2-methyl furan	2.5	41.4	10	66
2M LiAsF <sub>6</sub> /MA + THF (50:50)	2-methyl furan	5.0	51.2	14	69

- NOTES: 1. All tests were conducted in wick cells employing nickel substrates for the working electrodes.
2. All solutions were deaerated with argon prior to use.

The results for CO<sub>2</sub> pretreatment of the lithium surface are given in Table 3-32. As before, the pretreatment process consisted of storing the lithium working electrodes in a sealed vessel with 20 psig CO<sub>2</sub> pressure for 3, 24, and 120 hours. In the methyl acetate solutions, however, pretreatment of the lithium surface with CO<sub>2</sub> was found to have no beneficial effect. No further improvements were pursued due to the incompatibility of methyl acetate solutions and V<sub>2</sub>O<sub>5</sub> cathode material at elevated temperatures.

#### Dimethyl Sulfoxide Solutions

Baseline Evaluations. Initial testing was conducted using 1M LiAsF<sub>6</sub>/DMSI solutions. Half-cell tests yielded a lithium cycling efficiency of 81 percent for this solution. However, satisfactory results could not be achieved in wick cells due to severe polarization and noisy voltage/time profiles. This could be explained by cell configuration. In the laboratory cell, formation of pale grey precipitates was observed on the Lithium surface of the working electrodes. In the half-cell, loose, solid products formed at the working electrode can easily fall to the bottom of the cell tube thus minimizing passivation effects.

Figure 3-45 shows the infrared spectrum for the solid product collected after the cycle tests while Table 3-33 summarizes the observed bands. As with the other solutions, both solvent and solute are indicated to be involved in the formation of the solid product.

TABLE 3-32. EFFECT OF ELECTRODE PRETREATMENT WITH CO<sub>2</sub> ON LITHIUM CYCLING EFFICIENCY IN METHYL ACETATE

<u>Storage Time for Working Electrode in CO<sub>2</sub> Atmosphere, h</u>	<u>Starting Working Electrode Capacity, mAh</u>	<u>No. of Cycles</u>	<u>Lithium Efficiency, Percent</u>
0	51.6	14	69
3	50.2	9	51
24	55.2	15	67
120	50.4	13	66

- NOTES: 1. All tests were conducted in wick cells employing nickel substrates for the working electrodes.
2. All solutions were deaerated with argon prior to use.

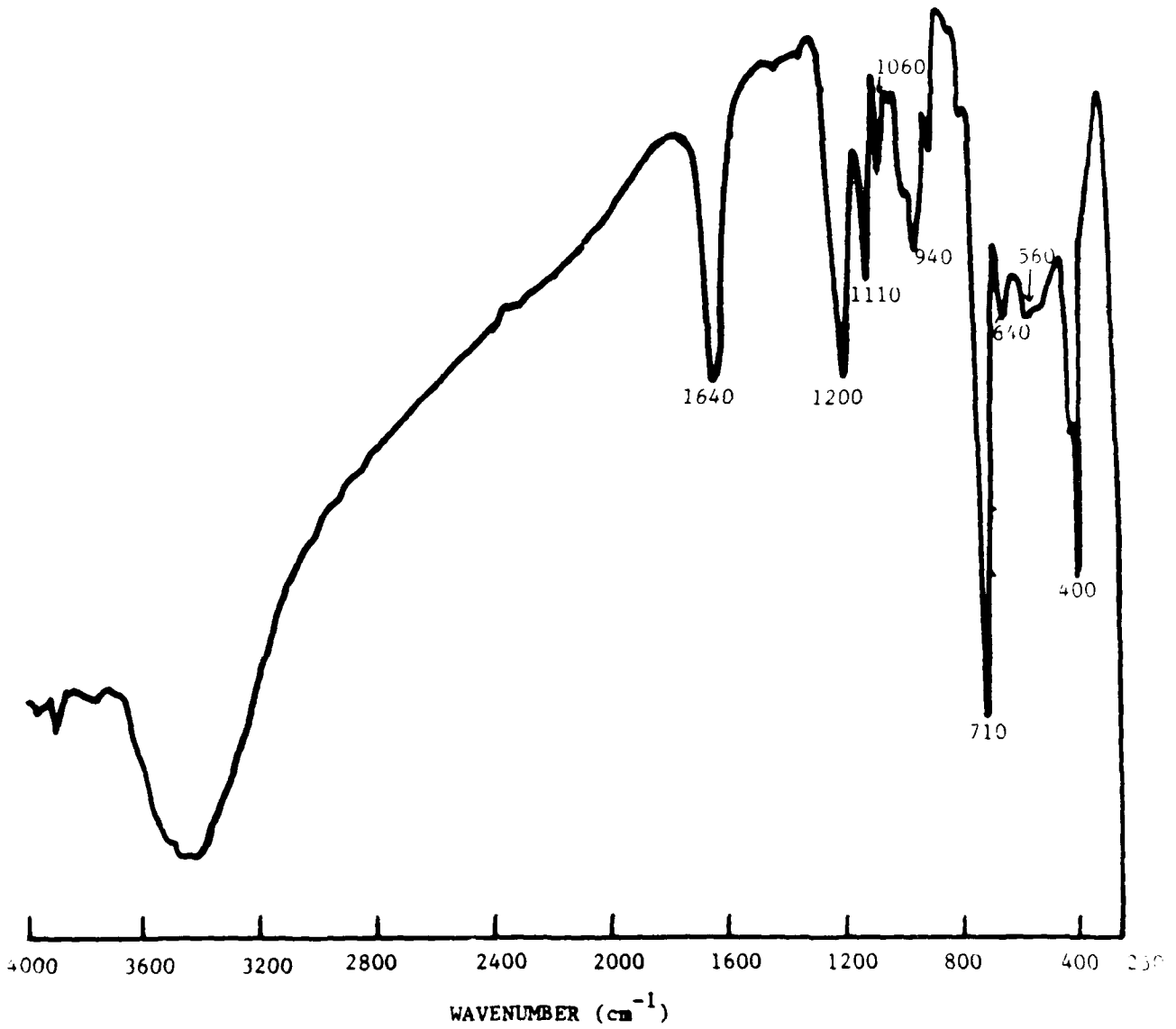


FIGURE 3-45. IR SPECTRUM OF SOLID REACTION PRODUCT FORMED ON LITHIUM CYCLED IN 1M LiAsF<sub>6</sub>/DMSI

TABLE 3-33. LITHIUM CYCLABILITY TESTS: SUMMARY OF IR RESULTS FOR SOLID PRODUCT FROM 1M  $\text{LiAsF}_6$ /DMSI SOLUTIONS

<u>Bands Attributed To Organic Products (<math>\text{cm}^{-1}</math>)</u>	<u>Bands Attributed To Solutes (<math>\text{cm}^{-1}</math>)</u>
1200	710 } $\text{AsF}_6^-$
1110	400 }
1060	
940	
640	
560	

Effects of Solute Concentration. Table 3-34 summarizes the effects of  $\text{LiAsF}_6$  concentration on the lithium cycling efficiency in DMSI solutions over the range of 0.5M to 2M. These tests were all conducted using half-cells. The results, which are graphed in Figure 3-46, indicate that the maximum lithium cycling efficiency occurs at a  $\text{LiAsF}_6$  concentration near 1M.

#### SCREENING STUDIES SUMMARY

The objective of the screening studies was to identify the cathode material/electrolyte solution combination offering the optimum performance capabilities for a rechargeable lithium cell technology. Based on the results obtained, the following system was selected.

- o Cathode Material:  $\text{V}_2\text{O}_5$
- o Electrolyte Solution: 2M  $\text{LiAsF}_6$  + 0.4M  $\text{LiBF}_4$ /MF doped with  $\text{CO}_2$

This system offers good cycle life performance with little capacity degradation combined with good thermal stability and high lithium cycling efficiencies. In addition, the high conductivity of the methyl formate solution offers the capabilities needed to achieve enhanced rate capabilities and low temperature performance over existing rechargeable lithium technologies.

Results for the other candidate materials evaluated are summarized below.

#### $\text{LiAsF}_6$ /Methyl Acetate Solutions

$\text{LiAsF}_6$ /methyl acetate solutions offer good conductivities and were therefore very attractive for consideration in rechargeable cell applications.

TABLE 3-34. EFFECT OF  $\text{LiAsF}_6$  CONCENTRATION ON LITHIUM CYCLING EFFICIENCY IN DIMETHYL SULFITE (HALF-CELL, NO SOLUTION PRETREATMENT)

<u>Electrolyte Solution</u>	<u>Substrate Material</u>	<u>Starting Working Electrode Capacity, mAh</u>	<u>No. of Cycles</u>	<u>Lithium Efficiency Percent</u>
2M $\text{LiAsF}_6$ /DMSI	Ni	54.1	19	76
1M $\text{LiAsF}_6$ /DMSI	304 SS	45.0	19	81
0.5M $\text{LiAsF}_6$ /DMSI	Ni	57.8	19	74

The major deficiency identified with these solutions was their low lithium cycling efficiencies. The maximum efficiency achieved was only 73 percent and no improvements were realized with any of the additives or co-solvents evaluated. In addition, methyl acetate solutions were found to be unstable with  $\text{V}_2\text{O}_5$  at elevated temperatures. Methyl acetate solutions, therefore, were found to be clearly inferior to the methyl formate solutions.

#### $\text{LiAsF}_6$ /Dimethyl Sulfite Solutions

Because of the limited testing done, the capabilities of dimethyl sulfite for rechargeable applications have not been fully defined. However, the results do indicate that dimethyl sulfite is not suitable for use with high voltage systems as evidenced by the apparent electrolysis reactions observed during charging of  $\text{V}_2\text{O}_5$  cells.

#### $\text{TiS}_2$

Poor cycle life performance was obtained with  $\text{TiS}_2$  using methyl formate solutions, apparently due to solvent cointercalation.<sup>2</sup> With methyl acetate solutions, much improved performance was achieved. With these solutions, it has been found that capacity degradation decreases as the solute concentration increases. Over 200 cycles have been achieved using a 3M  $\text{LiAsF}_6$ /MA solution. These concentrated solutions, however, are highly viscous which severely limits their rate capabilities and low temperature performance. In addition, the low lithium cycling efficiencies offered by methyl acetate solutions are not sufficient for long cycle life applications. Therefore, the  $\text{TiS}_2$ /methyl acetate system does not offer the performance capabilities needed for this program.

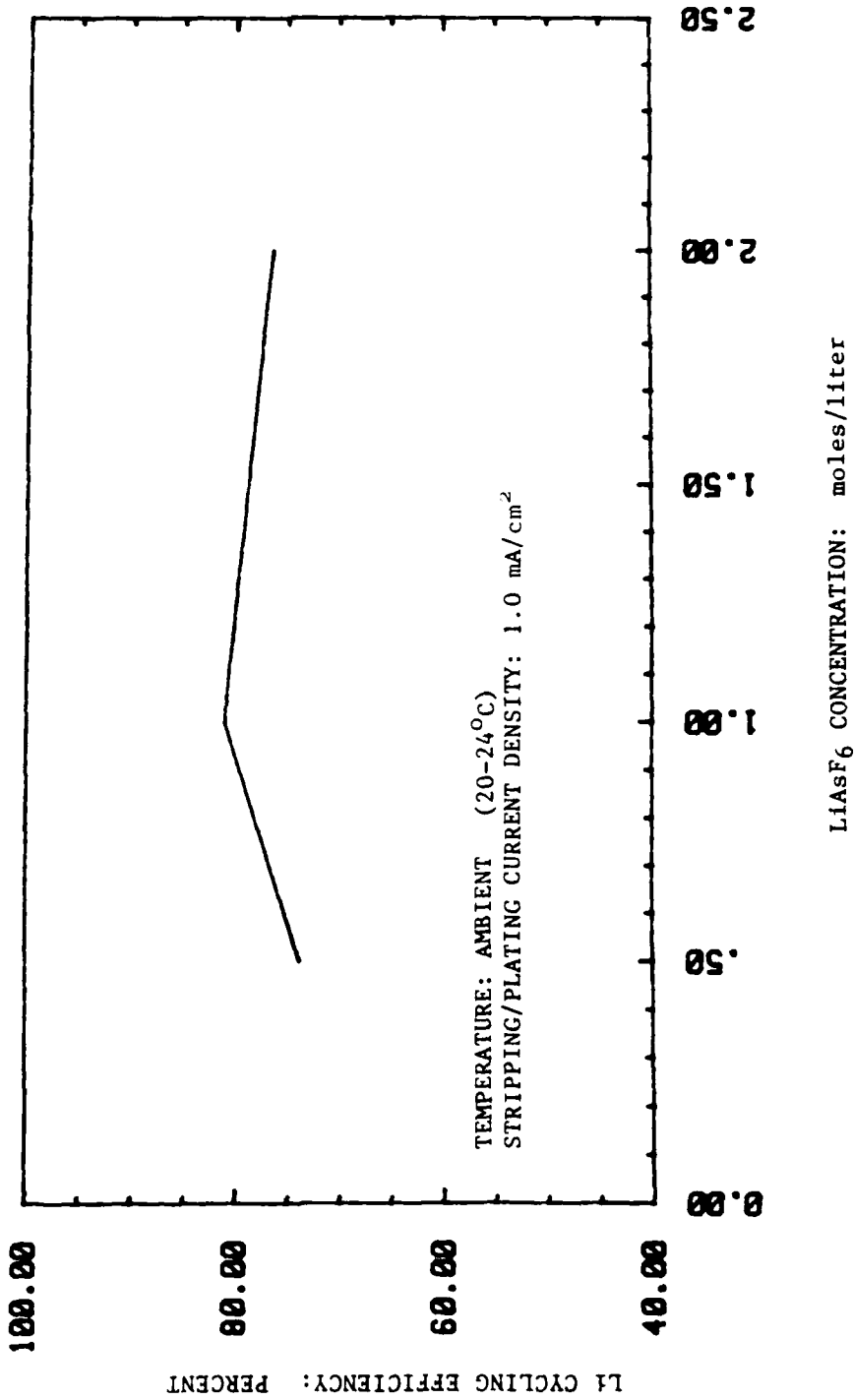


FIGURE 3-46. LITHIUM CYCLING EFFICIENCY VERSUS LiAsF<sub>6</sub> CONCENTRATION FOR DIMETHYL SULFITE SOLUTIONS (HALF-CELL RESULTS)

Li<sub>x</sub>CoO<sub>2</sub>

The major problem encountered with this cathode material was electrolyte decomposition at the high potentials required during charging. Methyl acetate solutions yielded better performance than methyl formate solutions but significant capacity degradation was still observed in early cycle life. In addition, the maximum discharge efficiencies typically achieved were only about 60 percent.

In spite of the disappointing results obtained in these preliminary evaluations, we still feel that Li<sub>x</sub>CoO<sub>2</sub> is an attractive high energy density cathode material. In the absence of electrolyte decomposition, Li<sub>x</sub>CoO<sub>2</sub> was indicated to operate reversibly and, even at an efficiency of only 60 percent, could yield an active material energy density of about 670 Wh/kg. Thus, with proper development, Li<sub>x</sub>CoO<sub>2</sub> could indeed be a viable rechargeable technology. However, we felt that the magnitude of effort required to fully develop this system was beyond the scope of this program and, therefore, were forced to discontinue work with Li<sub>x</sub>CoO<sub>2</sub>.

V<sub>2</sub>S<sub>5</sub>

Our preliminary investigations showed V<sub>2</sub>S<sub>5</sub> to be unstable with ester-based solutions. Although detailed analyses were not conducted, we believe that V<sub>2</sub>S<sub>5</sub> decomposes to VS<sub>2</sub> in these solutions. Because of this apparent inherent instability, V<sub>2</sub>S<sub>5</sub> was dropped from consideration early in the program.

V<sub>2</sub>O<sub>5</sub> CATHODE PROCESSING STUDIESIntroduction

Cathode processing is a critical part in the development of a practical rechargeable lithium technology. To achieve efficient operation and long cycle life capabilities, the physical properties of manufactured cathodes are extremely important. Cathodes must be porous to allow for adequate distribution of the electrolyte solution within the electrode structure. At the same time, however, cathodes must be rugged and flexible so that they can be easily handled during cell manufacture and so that they do not deteriorate during extensive cycling.



To achieve ruggedness and flexibility, binders are essential. However, binders must be identified that can provide the desired physical properties without degrading performance. Conductive diluents are also necessary to achieve good rate capabilities and low temperature operability. Conductive diluents also improve efficiency during extended cycling by helping to maintain good particle-to-particle contact throughout the volume of the cathode.

Cathode processing methods must be developed that are tailored to the specific properties of each cathode material and binder type. To ensure a rapid development cycle, it is imperative that these processing methods be production-oriented, suitable for scale-up with respect to both electrode size and electrode quantity.

Once  $V_2O_5$  had been selected in the screening studies, effort focused on developing suitable cathode manufacturing processes for this material. The objective of this work was to identify a production-oriented manufacturing technique that could produce rugged, flexible cathodes that operate efficiently over a wide range of temperatures and discharge rates without significant degradation in capacity over cycle life.

#### Process Evaluations

Evaluation of manufactured cathodes considered both mechanical properties and electrochemical performance. Table 3-35 summarizes the cathode compositions employed along with the mechanical properties of the finished electrodes. In most processes, Shawinigan Acetylene Black (50 percent compressed) was employed as the conductive diluent. For the roll milled electrodes, however, Vulcan XC-72R carbon was used because our experience in manufacturing carbon electrodes has shown this carbon to be the easiest to roll mill. The roll milled electrodes also employed a different grade of  $V_2O_5$  than the cathodes made by other processes. This  $V_2O_5$  was obtained from our G2666 cell production line and is manufactured in Germany by Metallurg. The roll milling process requires a relatively large amount of material to make a single cathode pad. Therefore, for these initial investigations, it was decided to employ the Metallurg material and conserve the  $V_2O_5$  that had been specially synthesized and characterized in-house for later studies. All other processes, however, employed  $V_2O_5$  that had been prepared in-house (Lot CML-V2-001).

From a mechanical standpoint, the cold pressed, Teflonated cathodes were the least desirable, offering little in the way of ruggedness or flexibility. Sintering, however, was found to greatly improve the properties of the cold pressed electrodes. At the other extreme, roll milled cathodes were found to be extremely rugged and totally flexible.

Performance evaluation of the manufactured electrodes was conducted through limited cycle life tests in 2-plate wick cells at a charge/discharge rate of  $1.0 \text{ mA/cm}^2$ . A  $2M \text{ LiAsF}_6 + 0.4M \text{ LiBF}_4/\text{MF}$  solution was employed in all tests.

TABLE 3-35. CATHODE DESCRIPTIONS FOR  $V_2O_5$  CATHODE PROCESSING STUDIES

<u>Cathode Process</u>	<u>Ruggedness</u>	<u>Flexibility</u>	<u>Initial Discharge Performance</u>	<u>Cycle Performance</u>
Cold Pressing with Teflon Binder	Poor	Poor	Excellent	Excellent
Cold Pressing and Sintering with Teflon Binder	Good	Good	Good	Good
Cold Pressing with Isotactic Polypropylene Binder	Fair	Fair	Good	Good
Pasting with EPDM Binder	Excellent	Good	Poor	Poor
Roll Milling with Teflon Binder	Excellent	Excellent	Good	Fair

NOTE: Performance evaluations based on limited cycle-life tests at a charge/discharge rate of 1.0 mA/cm<sup>2</sup>.

The cycle life results are shown in Figure 3-47. It was found that the cold pressed, Teflonated electrodes yielded the best performance. Their average efficiency over 10 cycles was 87.3 percent (based on a theoretical capacity of 1 F/mole) and little degradation of capacity was observed over cycle life. The sintered electrodes also performed relatively well as did the pressed electrodes employing isotactic-polypropylene binder. The pasted electrodes performed poorly while the roll milled electrodes yielded intermediate performance.

The results in Figure 3-47 show that all processes evaluated exhibited little degradation in capacity after the second cycle. In general, therefore, the primary effect of cathode processing on performance of  $V_2O_5$  cathodes appears to be in the magnitude of capacity loss between the first and second discharge. Stated in another way, these results indicate that capacity decline in early cycle life is an effect of the mechanical properties of the cathode and not due to degradation of the cathode material. This is very significant in that it suggests that this loss in capacity in the first few cycles can be controlled, and possibly eliminated through optimization of the cathode manufacturing process.

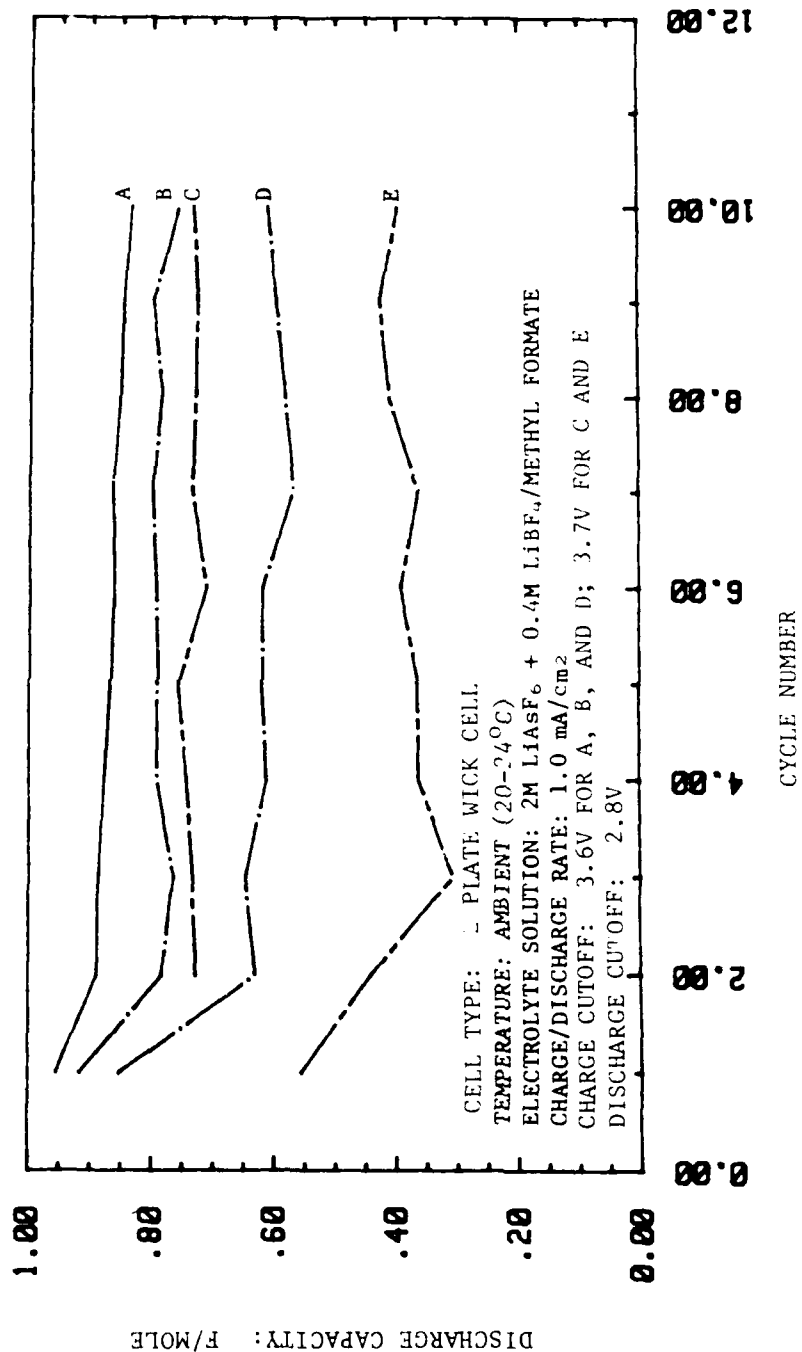


FIGURE 3-47. Li/V<sub>2</sub>O<sub>5</sub> CELL CYCLE LIFE PERFORMANCE FOR VARIOUS CATHODE MANUFACTURING PROCESSES

- A = COLD PRESSED, TEFLON BINDER
- B = COLD PRESSED, ISOTACTIC POLYPROPYLENE BINDER
- C = COLD PRESSED AND SINTERED, TEFLON BINDER
- D = ROLL MILLED, TEFLON BINDER
- E = PASTED, EPDM BINDER

Summary

Based on the results of the evaluations of the five cathode processing methods, it is concluded that the following two processes offer the best combination of mechanical and performance properties:

- o Roll Milled Electrodes
- o Cold Pressed and Sintered Teflonated Electrodes

Roll milled cathodes are, by far, the best from a mechanical standpoint and are also suited to scale-up. Although their initial performance was somewhat disappointing, the results suggested that through proper optimization, these performance deficiencies could be overcome. Therefore, roll milling was selected as the process of choice. However, in the event that the performance of roll milled cathodes could not be improved to the necessary level, sintered electrodes would then be employed.

V<sub>2</sub>O<sub>5</sub> ROLL MILLED CATHODE OPTIMIZATION STUDIESIntroduction

To improve the performance of roll milled V<sub>2</sub>O<sub>5</sub> cathodes, investigations were conducted in an effort to identify and optimize the key parameter(s) that control the performance of these electrodes. The parameters evaluated included carbon type, carbon content, binder content, and V<sub>2</sub>O<sub>5</sub> particle size.

Because of the relatively large quantities of V<sub>2</sub>O<sub>5</sub> needed to manufacture the numerous lots of roll milled cathodes, these studies were also carried out using the Metallurg grade of V<sub>2</sub>O<sub>5</sub> from our G2666 cell production line.

These initial optimization studies were conducted in 2-plate wick cells employing a charge/discharge rate of 1.0 mA/cm<sup>2</sup>. The electrolyte solution was 2.0M LiAsF<sub>6</sub> + 0.4M LiBF<sub>4</sub>/MF and all testing was done at ambient temperature.

Evaluation Tests

Table 3-36 summarizes the physical properties of the manufactured cathodes along with their cycle life performance results.

Effects of Carbon Type. In the initial investigations of roll milled cathodes, Vulcan XC-72R carbon was used as the conductive diluent because our experience had shown it to be well suited to the roll milling process. However, this carbon had not been used previously with V<sub>2</sub>O<sub>5</sub> so its effect on performance was not known. Therefore, additional cathodes were manufactured and tested with Shawinigan Acetylene Black (SAB) as the conductive diluent. Both 50 and 100 percent compressed grades were evaluated.

TABLE 3-36. ROLL MILLED  $V_2O_5$  CATHODE DESCRIPTIONS AND CYCLE PERFORMANCE SUMMARY

Conductive Diluent	XC-72R	SAB-50	SAB-100	XC-72R	XC-72R	XC-72R	XC-72R	XC-72R	XC-72R	XC-72R	XC-72R
$V_2O_5$ Supplier	Metallurg	Metallurg	Metallurg	Metallurg	Metallurg	Metallurg	Metallurg	Metallurg	Metallurg	Metallurg	Metallurg
$V_2O_5$ Content, w/o	80	80	80	85	87	89	90	75	65	65	85
Teflon Binder Content, w/o	10	10	10	5	3	1	5	5	5	5	5
Cond. Diluent Content, w/o	10	10	10	10	10	10	5	20	30	30	10
Nominal Cathode Thickness, inches	0.027	0.024	0.025	0.026	0.025	0.025	0.028	0.024	0.031	0.031	0.019
Nominal Cathode Density, g/cc	1.04	1.21	1.22	1.16	1.05	1.09	1.33	0.91	0.77	0.77	1.12
Ruggedness	Excellent	Excellent	Excellent	Excellent	Excellent	Excellent	Excellent	Excellent	Excellent	Excellent	Excellent
Flexibility	Excellent	Excellent	Excellent	Excellent	Excellent	Excellent	Excellent	Excellent	Excellent	Excellent	Excellent
Capacity Delivered on First Discharge, F/Mole	0.85	0.75	0.72	0.87	0.93	0.82	0.85	0.72	0.77	0.77	0.91
Average Discharge Capacity For Cycles 2-9, F/Mole	0.61	0.62	0.54	0.64	0.62	0.62	0.70	0.50	0.51	0.51	0.78

In these studies, the carbon and Teflon contents were both maintained at 10 weight percent. The manufactured electrodes were all found to be rugged and completely flexible, although the cathodes containing the 50 percent compressed acetylene black were difficult to process.

Figure 3-48 compares the cycle life performance obtained with the three carbon types. The cells containing the Shawinigan Acetylene Black were limited to a maximum depth of discharge of 75 percent which only affected the first discharge since the capacity delivered on subsequent cycles was below this value. Equivalent performance was obtained with XC-72R and Shawinigan 50 percent compressed carbons while cathodes incorporating Shawinigan 100 percent compressed carbon delivered somewhat lower capacity over cycle life.

These results show that, at the 10 percent binder level, no significant improvement in performance is achieved with the Shawinigan Acetylene Blacks as conductive diluents. Therefore, due to its superior processing characteristics, Vulcan XC-72R remained the carbon of choice for roll milled cathodes.

#### Effects of Binder Content<sup>16</sup>

Because binders are inert, insulating materials, they can often lower the electrical conductivity of manufactured electrodes and thus degrade performance. In general, therefore, it is desirable to maintain the binder concentration as low as possible, particularly with low conductivity cathode materials such as  $V_2O_5$ .

To investigate the effects of binder content on cell performance, roll milled cathodes were evaluated having Teflon contents of 10, 5, 3, and 1 weight percent. All electrodes contained 10 weight percent of Vulcan XC-72R carbon as the conductive diluent. It was found that, even at one percent binder level, the rolled electrodes exhibited excellent mechanical properties.

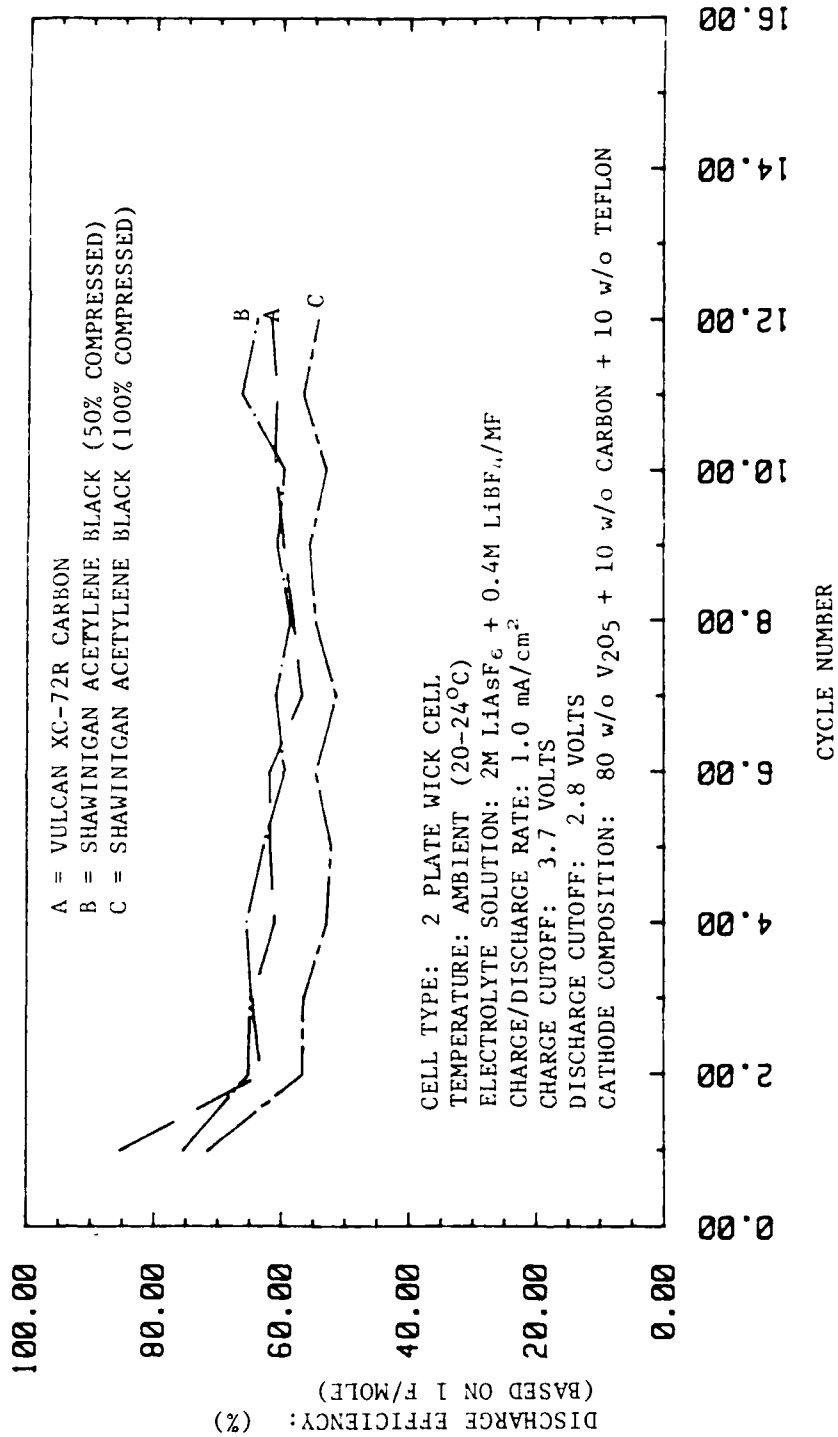


FIGURE 3-48. EFFECTS OF CARBON TYPE ON THE PERFORMANCE OF ROLL MILLED V<sub>2</sub>O<sub>5</sub> CATHODES

The cycle results are shown in Figure 3-49. Surprisingly, no significant difference in cell performance was observed indicating that binder content is not critical over the range of 1-10 weight percent.

Although no improvement in performance was obtained, the ability to manufacture rugged, flexible cathodes with binder contents as low as 1 weight percent is significant. Any reduction in binder or conductive diluent will result in a corresponding increase in energy density since the cathode will contain a higher percentage of active material.

#### Effects of Carbon Content

The effects of carbon content were evaluated using cathodes containing 5, 10, 20 and 30 weight percent XC-72R carbon. In these tests, the Teflon binder content was fixed at 5 weight percent.

The cycle results are shown in Figure 3-50. Again, the results were somewhat surprising. With  $V_2O_5$  having low electrical conductivity, it was expected that increasing the carbon content of the cathodes would be beneficial. Instead, it was found that the performance dropped significantly with the higher carbon loadings. In addition, the results show that no loss in performance occurs when the carbon content is reduced to 5 weight percent which also offers benefits with respect to increasing the energy density of  $V_2O_5$  cathodes.

#### Effects of $V_2O_5$ Particle Size<sup>16</sup>

To determine the effects of  $V_2O_5$  particle size on performance, cathodes were manufactured using Lot CML-V2-003  $V_2O_5$ . As discussed previously, this material was manufactured from ground ammonium metavanadate in an effort to reduce the particle size of  $V_2O_5$ . The cathodes contained 10 weight percent Vulcan XC-72R carbon and 5 weight percent Teflon binder. Figure 3-51 compares the particle size distribution of Lot CML-V2-003 with that of Metallurg grade of  $V_2O_5$ . As can be seen, there is a distinct difference in these materials, particularly at the extremes of the distribution.

Limited cycle life performance results for the two grades of  $V_2O_5$  are compared in Figure 3-52. As can be seen, a significant improvement in performance was achieved with the cell incorporating the fine particle size  $V_2O_5$  indicating that particle size is a key factor affecting performance of roll milled cathodes.

#### Summary

The results of these studies have shown that significant improvements in the performance of roll milled cathodes can be achieved using finer particle size  $V_2O_5$ . Therefore, roll milled cathodes have been selected for use in the prototype hardware cells to be developed in Phase II of this program. Final optimization of these cathodes will be conducted in the early stages of Phase II, encompassing both higher discharge rates and low temperature operation.



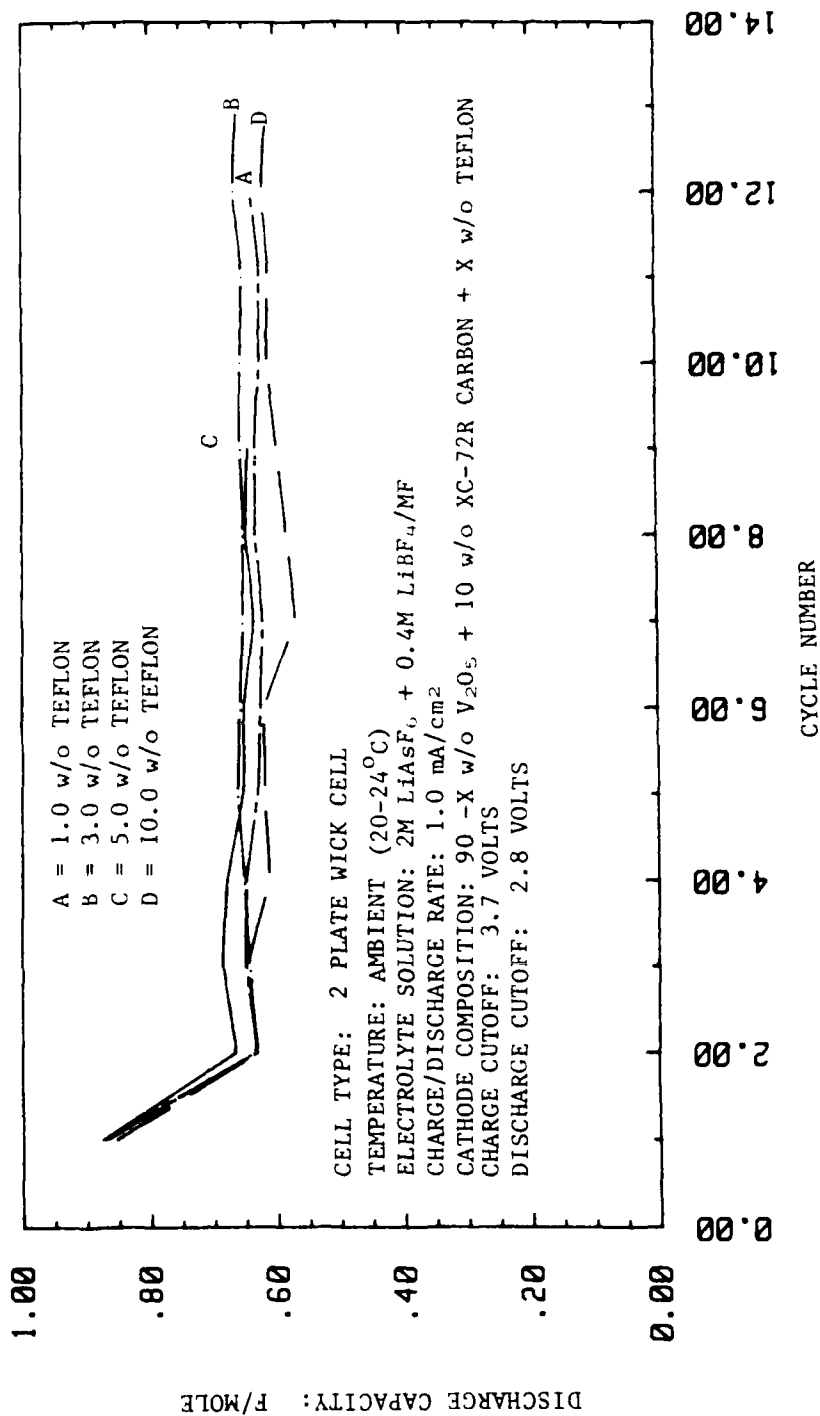


FIGURE 3-49. EFFECTS OF TEFLON BINDER CONTENT ON THE PERFORMANCE OF ROLL MILLED V<sub>2</sub>O<sub>5</sub> CATHODES

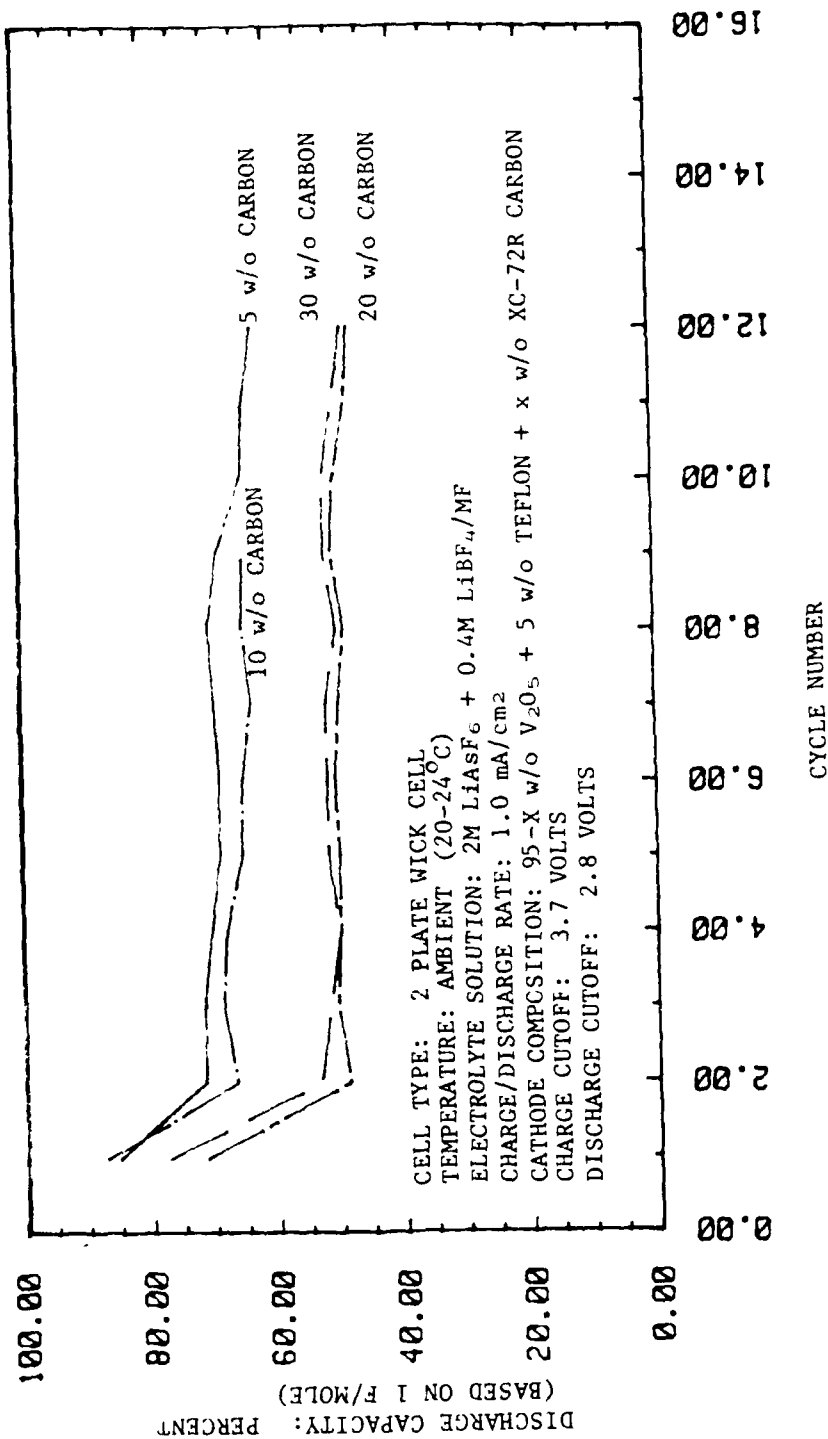


FIGURE 3-50. EFFECTS OF CARBON CONTENT ON THE PERFORMANCE OF ROLL MILLED V<sub>2</sub>O<sub>5</sub> CATHODES

**PARTICLE SIZE ANALYSIS OF V2O5**

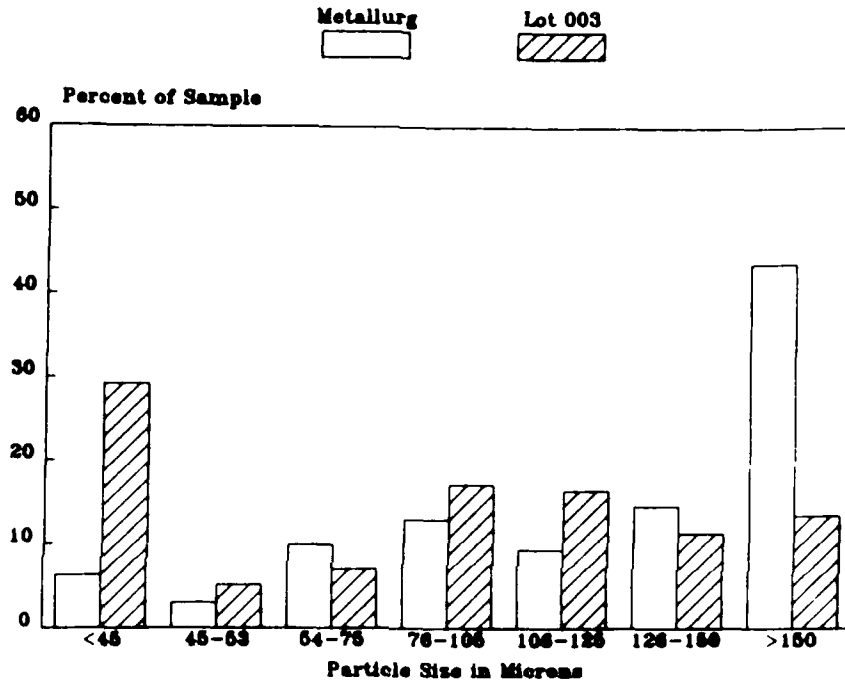


FIGURE 3-51. PARTICLE SIZE DISTRIBUTIONS FOR THE METALLURG V2O5 VERSUS THAT FOR V2O5 MANUFACTURED FROM GROUND AMMONIUM METAVANADATE (LOT CML-V2-003)

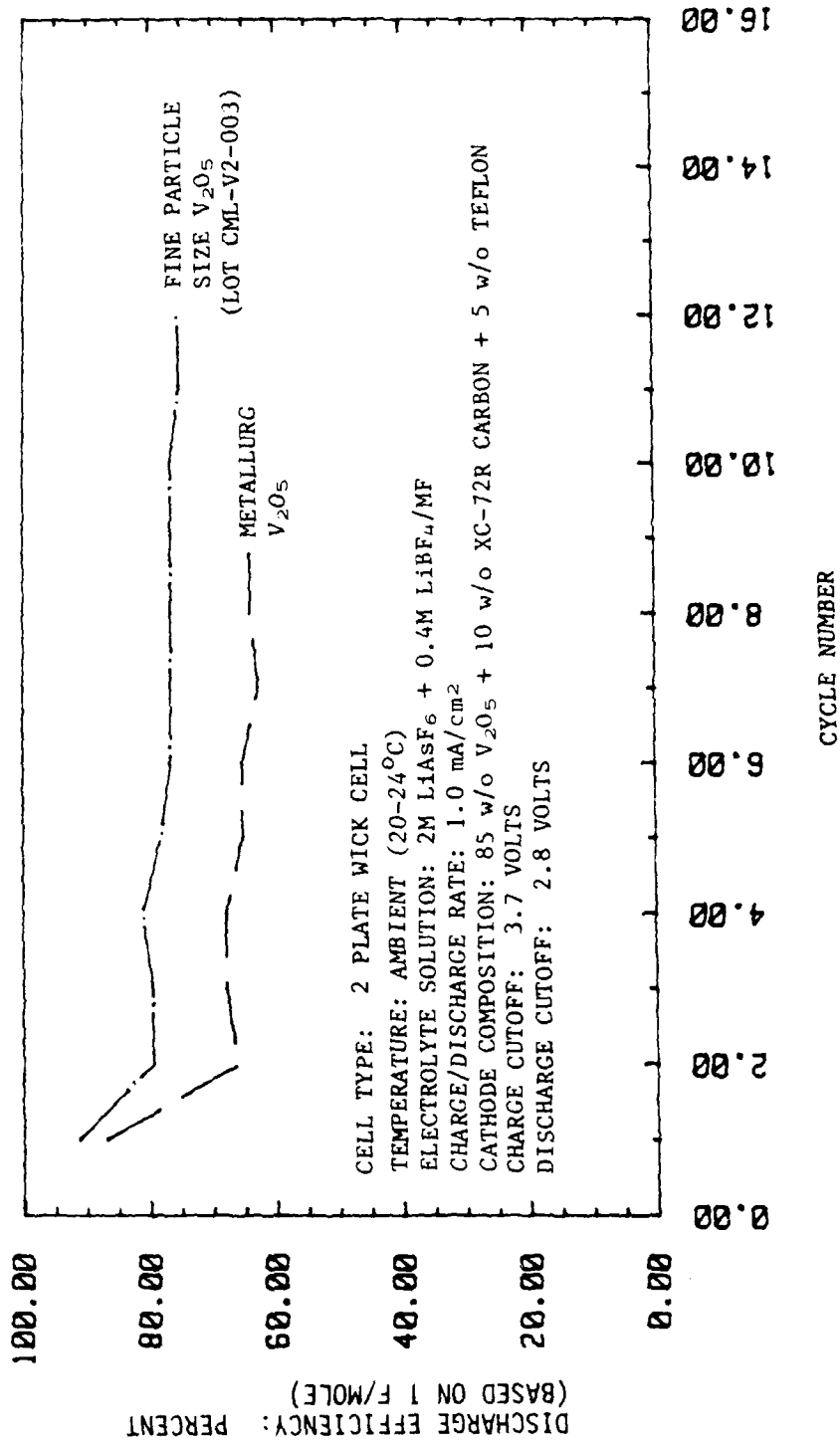


FIGURE 3-52. EFFECTS OF V<sub>2</sub>O<sub>5</sub> PARTICLE SIZE ON THE PERFORMANCE OF ROLL MILLED CATHODES

$V_2O_5$  PERFORMANCE DEMONSTRATION

Once the cathode technology had been established, additional tests were conducted to evaluate the performance of the rechargeable  $Li/V_2O_5$  system versus the performance guidelines of the program. In particular, we wanted to demonstrate that the selected system could indeed achieve 100 cycles without significant degradation in capacity and to begin to explore the effects of higher rates of discharge on extended cycle life performance. We also wanted to verify that  $CO_2$  was not detrimental to cell performance since, to this point,  $CO_2$  had only been evaluated in anode studies and not in complete cells. All tests were conducted using 2-plate wick cells incorporating roll milled cathodes composed of 85 w/o  $V_2O_5$ , 10 w/o Vulcan XC-72R carbon, and 5 w/o Teflon binder.

Figure 3-53 shows the results for extended cycle life tests at a discharge rate of  $1 \text{ mA/cm}^2$  (approximately C/7 rate). The results for two cells tested at ambient temperature are shown; one with  $CO_2$  and one without  $CO_2$ . For the first 87 cycles, these two cells performed similarly, thus demonstrating that  $CO_2$  has no detrimental effects on cell performance. On the 87th cycle, the cell without  $CO_2$  was inadvertently overdischarged resulting in a rapid decline in capacity in subsequent cycles. During the 105th cycle, the charge cutoff was increased from 3.7V to 3.9V which significantly improved the output although the cell never recovered to its original level. The cell containing  $CO_2$  delivered an average capacity of 0.8 F/mole through 110 cycles after which the capacity declined rapidly. Capacity loss in this cell was attributed to depletion of the anode. The calculated lithium cycling efficiency, based on 110 cycles, was 93 percent, identical to the results achieved in the lithium cycling experiments with the  $CO_2$ -doped solution. The cell tested at  $-20^\circ\text{C}$  yielded an average capacity of 0.6 F/mole over 160 cycles.

Figure 3-54 shows the extended cycle life results for a cell tested at a discharge rate of  $5 \text{ mA/cm}^2$  (C/1.3 rate). A total of 205 cycles were achieved at an average capacity of 0.55 F/mole. During the extended testing, this cell was also inadvertently overdischarged due to an equipment problem. On the 28th cycle, the cell was discharged to a total depth of 1.82 F/mole, thus representing a fairly severe overdischarge abuse. Significantly, however, no substantial loss in performance occurred as a result of the overdischarge.

Table 3-37 lists the average voltages and active material energy densities realized at various points throughout the cycle life tests described above. The results of these tests serve to demonstrate the extended cycle life capabilities of the  $Li/V_2O_5$  system, showing that the 100 cycle deep discharge goal can indeed be achieved with this technology. We have also demonstrated that long cycle life performance can be achieved at low temperatures and at moderate rates of discharge, although further improvements in operating efficiency are needed under these operating conditions. We believe, however, that these improvements can be readily achieved through further optimization of the cathode structure.

One of the key concerns with insertion-type cathode materials is their susceptibility to structural damage during overdischarge resulting in loss of

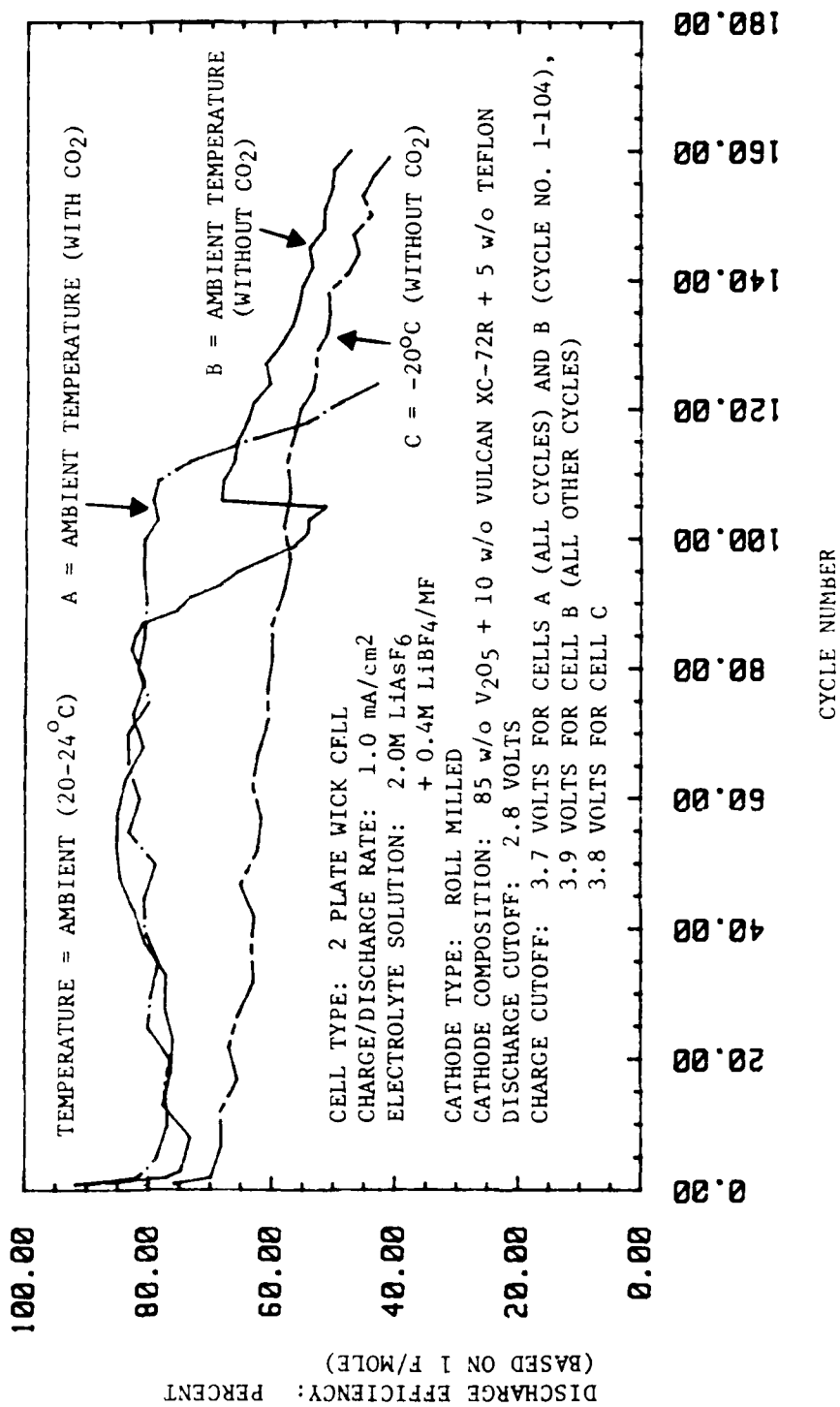


FIGURE 3-5j. DEMONSTRATION OF THE EXTENDED CYCLE LIFE CAPABILITIES OF THE RECHARGEABLE Li/V<sub>2</sub>O<sub>5</sub> SYSTEM

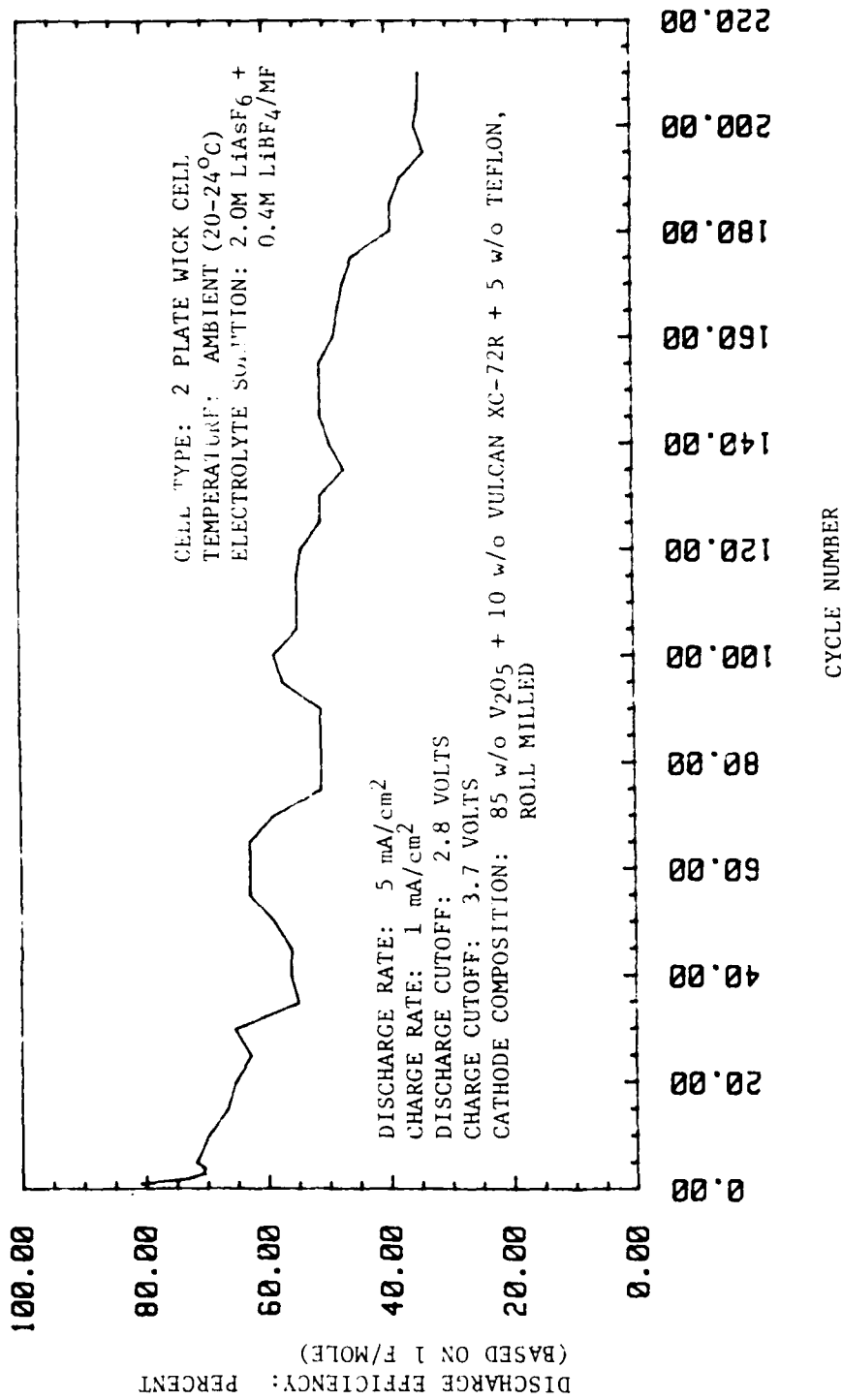


FIGURE 3-54. EXTENDED CYCLE LIFE PERFORMANCE OF Li/V<sub>2</sub>O<sub>5</sub> SYSTEM AT THE DISCHARGE RATE OF 5 mA/cm<sup>2</sup>

TABLE 3-37. PERFORMANCE SUMMARY FOR Li/V<sub>2</sub>O<sub>5</sub> LABORATORY CELLS TESTED UNDER EXTENDED CYCLE LIFE CONDITIONS

Cycle No.	Discharge Rate mA/cm <sup>2</sup>	Test Temperature °C	Delivered Capacity, F/Mole	Average Voltage, V	Delivered* Energy Density, Wh/Kg	Notes
1	1	Ambient (20-24°C)	0.89	3.23	410	Without CO <sub>2</sub> (Cell B in Figure 3-53)
2	1	"	0.75	3.21	347	
10	1	"	0.76	3.22	348	
50	1	"	0.83	3.21	380	
86	1	"	0.82	3.22	378	
1	1	Ambient (20-24°C)	0.91	3.22	417	With CO <sub>2</sub> (Cell A <sup>2</sup> in Figure 3-53)
2	1	"	0.81	3.20	372	
10	1	"	0.76	3.15	342	
50	1	"	0.78	3.19	357	
100	1	"	0.80	3.19	366	
1	1	-20	0.75	3.07	331	Without CO <sub>2</sub> (Cell C in Figure 3-53)
2	1	"	0.67	3.15	305	
10	1	"	0.65	3.15	296	
50	1	"	0.59	3.11	264	
100	1	"	0.58	3.09	256	
1	5	Ambient (20-24°C)	0.83	3.01	359	Without CO <sub>2</sub> (Cell in Figure 3-54)
2	5	"	0.74	3.01	321	
10	5	"	0.72	3.01	309	
50	5	"	0.70	3.12	312	
100	5	"	0.60	3.09	268	

\* The above energy densities are based on active materials only.

reversibility. Although we have not yet done a systematic investigation, the inadvertent overdischarges that occurred during our extended cycle life tests indicate that the Li/V<sub>2</sub>O<sub>5</sub> technology can sustain significant overdischarge beyond 1 F/mole without catastrophic loss of performance. This area will be more fully evaluated in Phase II so as to establish appropriate operating boundaries for this system.



## CHAPTER 4

## CONCLUSIONS

At the onset of this program, the room-temperature lithium rechargeable technology faced performance limitations with respect to rate capability and low temperature operability. To overcome these performance deficiencies, this program undertook the development of four high energy density cathode materials ( $V_2O_5$ ,  $TiS_2$ ,  $V_2S_5$ , and  $LiCoO_2$ ) in conjunction with the use of ester-based electrolyte solutions because of their superior solution conductivity.

An electrolyte formulation composed of  $2M LiAsF_6 + 0.4 LiBF_4$ /methyl formate saturated with  $CO_2$  was successfully developed with the following demonstrated capabilities:

- o Solution Conductivity--43 mmh $\cdot$ cm at room temperature and 13 mmho/cm at  $-40^\circ C$ . This solution at  $-40^\circ C$  is still three times more conductive than the more commonly used ether-based solution at ambient temperature.
- o 93% Lithium Efficiency--this lithium efficiency enables the use of methyl formate-based solution in practical hardware. In the case of  $Li/V_2O_5$  cell, cyclability up to 50 cycles can be projected at the 100% depth of discharge based on  $Li/V_2O_5$  ratio of 3:1.

Of the four cathode materials studied ( $V_2O_5$ ,  $TiS_2$ ,  $V_2S_5$ , and  $LiCoO_2$ ),  $V_2O_5$  emerged to be the best overall performer:

- o Cyclability surpassing 100 cycles--cycled cell capacity can be held at a level corresponding to 80 percent cathode discharge efficiency throughout the life of the cell before reaching the lithium depletion point. To a large extent, the ability to achieve this high level of cathode utilization is due to our focused development of the cathode processing technology. Particle size of the  $V_2O_5$  was found to be key to enhanced cell performance and electrode integrity was critical to achieving cyclability without degrading cell capacity.

$Li/V_2O_5$  laboratory cell produces 366 Wh/kg (or 166 Wh/lb) at the 100th cycle when tested at room temperature. Using this value, practical energy densities of 50 Wh/lb and 60 Wh/lb can be projected for "D" cell and No. 6 size cell, respectively.

- o Discharge current density surpassing  $5 \text{ mA/cm}^2$ --this allows addressing application of the  $\text{Li/V}_2\text{O}_5$  technology in missions requiring rate capability up to  $C/1.3$ .

The other three cathode materials were dropped from further development because of their general incompatibility with ester-based solutions. Specifically, severe cointercalation was observed between  $\text{TiS}_2$  and methyl formate which adversely affect cycle performance. Discharge capacity was severely degraded even on the first cycle for  $\text{V}_2\text{S}_5$  cathode in methyl formate-based solution. Finally, although  $\text{LiCoO}_2$  was demonstrated to be reversible and offered to be a high cell potential cathode, the high cell potential needed to charge this cathode system decomposed the solvent during charge.

In closing, Phase I of this program successfully selected a rechargeable technology ( $\text{Li/V}_2\text{O}_5$ ) that is ready for transitioning to a more hardware development phase. Phase I demonstrated overall performance capabilities of the  $\text{Li/V}_2\text{O}_5$  technology at the laboratory cell level, and the objective of Phase II is to demonstrate the stated capabilities of  $\text{Li/V}_2\text{O}_5$  cell at the hardware level via a 30 Ah cell.

## REFERENCES

1. Ebner, W.B. and Lin, H.W., "High Cycle Life Rechargeable Lithium - Organic Electrolyte Cell," Third Quarterly Report, Contract DAAK20-84-C-0412 (LABCOM), Honeywell Inc., Oct 1985.
2. Winn, D.A., "Titanium Disulphide: A Solid Solution Electrode," Mat. Res. Bull., 11, 1976, p. 559.
3. Yamamoto, T., Kikkawa, S. and Koizumi, M., "Effect of Nonstoichiometry and Solvent on Discharge Property of Li/TiS<sub>2</sub> Battery," J. Electrochem. Soc., 131, 1984, p. 1343.
4. Rao, B.M.L. and Shropshire, J.A., "Effect of Sulfur Impurities on Li/TiS<sub>2</sub> Cells," J. Electrochem. Soc., 128, 1981, p. 942.
5. Whittingham, M.S. and Panella, J.A., "Formation of Stoichiometric Titanium Disulfide," Mat. Res. Bull., 16, 1981, p. 37.
6. Mizushima, K., Jones, P.C., Wiseman, P.J., and Goodenough, J.B., "Li<sub>x</sub>CoO<sub>2</sub> (0 < x < 1): A New Cathode Material for Batteries of High Energy Density," Mat. Res. Bull., 15, 1980, p. 783.
7. Deshpande, S.L. and Bennion, D.N., "Lithium Dimethyl Sulfite Graphite Cell," J. Electrochem. Soc., 125, 1978, p. 687.
8. Ebner, W.B. and Walk, C.R., "LiAsF<sub>6</sub> - Methyl Formate Electrolyte Solutions," Proceedings of the 27th Power Sources Symposium, 21-26 Jun 1976, p. 48.
9. Honeywell Internal Development Program.
10. Jacobson, A.J. and Rich, S.M., "Electrochemistry of Amorphous V<sub>2</sub>S<sub>5</sub> in Lithium Cells," J. Electrochem. Soc., 147, 1980, p. 779.
11. Lin, H.W. and Ebner, W.B., "High Cycle Life Rechargeable Lithium - Organic Electrolyte Cells," Second Quarterly Report, DAAK20-84-C-0412 (LABCOM), Honeywell Inc., Aug 1985.

REFERENCES (Cont.)

12. Murphy, D.N., Christian, P.A., DiSalvo, F.J. and Waszczak, J.V., "Lithium Incorporation by Vanadium Pentoxide," Inorganic Chemistry, 18, 1979, p. 2800.
13. Foos, J.S. and Rembetsy, L.M., "Lithium Cycling in Sulfolane-Based Electrolytes," Extended Abstracts, 83-2, Electrochem. Soc., Fall Meeting, Washington, D.C., 9-14 Oct 1983, p. 117.
14. Glugla, P.G., "Lithium Cycling Behavior in 2-Methyltetrahydrofuran With Alcohol Additives," J. Electrochem. Soc., 130, 1983, p. 113.
15. Abraham, K.M., Foos, J.S. and Goldman, J.L., "Long Cycle-Life Secondary Lithium Cells Utilizing Tetrahydrofuran," J. Electrochem. Soc., 131, 1984, p. 2197.
16. Ebner, W.B. and Lin, H.W., "High Cycle Life Rechargeable Lithium - Organic Electrolyte Cells," Fourth Quarterly Report, Contract DAAK20-84-C-0412 (LABCOM), Honeywell Inc., Feb 1986.

## DISTRIBUTION

	<u>Copies</u>		<u>Copies</u>
Defense Technical Information Center Cameron Station Alexandria, VA 22314	12	Naval Civil Engineering Lab Attn: Alan Inouye (Code L43) Port Hueneme, CA 93043-5003	1
Office of Naval Technology Attn: Code 232 (Dr. A. J. Faulstich) 800 N. Quincy Street Arlington, VA 22217-5000	2	Commander, Naval Weapons Support Center Attn: J. Marusek (Code 30512) Crane, IN 47522	1
Institute for Defense Analyses R&E Support Division 400 Army-Navy Drive Arlington, VA 22202	1	Naval Underwater Systems Center Attn: J. Moden (Code SB332) Newport, RI 02840	1
Commander Space and Naval Warfare Systems Command Washington, DC 20363-5100	1	David W. Taylor Naval Ship R&D Center Attn: W.J. Levendahl (Code 2703) Annapolis Laboratory Annapolis, MD 21402	1
Office of Naval Research Attn: Code 1113 (Dr. R.J. Nowak) 800 N. Quincey Street Arlington, VA 22217-5000	2	Air Force of Scientific Research Attn: R.A. Osteryoung Directorate of Chemical Science 1400 Wilson Boulevard Arlington, VA 22209	1
Naval Ocean Systems Center Attn: Code 922 Dr. S. Spazk (Code 6343) San Diego, CA 92152	1 1	Air Force Aero Propulsion Laboratory Attn: W.S. Bishop (Code AFAPL/POE-1) J.Lander (Code AFAPL/POE-1) Wright-Patterson AFB, OH 45433	1 1
Naval Coastal Systems Center Attn: R. Johnson (Code 410T) T. Sherman (Code 4210) Panama City, FL 32407	1 1	Office of Chief of Research and Development Department of the Army Attn: Dr. S.J. Magram Energy Conversion Branch Room 410, Highland Building Washington, DC 20315	1
Mare Island Naval Shipyard Attn: S.G. Marsh (Code 280.39/0204) Ocean Engineering Department Vallejo, CA 94592	1	U.S. Army Research Office Attn: B.F. Spielvogel P.O. Box 12211 Research Triangle Park, NC 27709	1

U.S. Army Electronics Command		California Institute of Technology	
Attn: Dr. M. Salomon (Code SLCET-PR)	1	Attn: Dr. R. Somoano	1
Dr. W.K. Behl (Code SLCET-PR)	1	Dr. H. Frank	1
Dr. M. Binder (Code SLCET-PR)	1	G. Halpert	1
Fort Monmouth, NJ 07703		Jet Propulsion Laboratory	
		4800 Oak Grove Drive	
Army Material and Mechanical Research Center		Pasadena, CA 91103	
Attn: J.J. DeMarco	1	Sandia Laboratories	
Watertown, MA 02172		Attn: Dr. S. Levy	1
		Albuquerque, NM 87115	
USA Mobility Equipment R&D Command		ESB Research Center	
Attn: J. Sullivan (Code DRXFB)	1	Attn: Library	1
(Code DRME-EC)	1	19 W. College Avenue	
Electrochemical Division		Yardley, PA 19067	
Fort Belvoir, VA 22060			
Department of Energy		EIC-Corporation	
Attn: Dr. A. Landgrebe		Attn: Dr. K.M. Abraham	1
(Code MS E-463)	1	111 Downey Street	
Energy Research and Development Agency		Norwood, MA 02062	
Division of Applied Technology		Boeing Aerospace Company	
Washington, DC 20545		Attn: S. Gross	1
		C.J. Johnson	1
NASA Headquarters		P.O. Box 3999	
Attn: Dr. J. H. Ambrus	1	Seattle, WA 98124	
(Code RTS-6)	1		
Washington, DC 20546		Moli Energy Ltd.	
		Attn: Dr. J.A. Stiles	1
Central Intelligence Agency		3958 Myrtle Street	
Attn: Dr. T.X. Mahy	3	Burnaby, B.C. Canada V5C 4G2	
c/o OTS			
Washington, DC 20505		Library of Congress	
		Attn: Gift and Exchange Div.	4
NASA Goddard Space Flight Center		Washington, DC 20540	
Attn: T. Hennigan (Code 716.2)	1		
Greenbelt, MD 20771			
Bell Laboratories			
Attn: Dr. J.J. Auburn	1		
Dr. J. Broadhead	1		
600 Mountain Avenue			
Murray Hill, NJ 07974			

Eagle-Picher Industries, Inc. Attn: D.R. Cottingham J.Dines Electronics Division, Couples Department P.O. Box 47 Joplin, MO 64801	1 1	Duracell Int., Inc. Attn: Dr. A.N. Dey Duracell Research Center 37 A St. Needham, MA 02194	1
Foote Mineral Company Attn: H.R. Grady Exton, PA 19341	1	Power Conversion, Inc. 70 MacQuesten Parkway S. Mount Vernon, NYH 10550	1
Gould, Inc. Attn: S.S. Nielsen G.R. Ault 40 Gould Center Rolling Meadows, IL 60008	1 1	Union Carbide Battery Products Division Attn: R.A. Powers P.O. Box 6116 Cleveland, OH 44101	1
GTE Laboratory Attn: Dr. F. Dampier 520 Winter Street Waltham, MA 02154	1	Wilson Greatbatch, Ltd. Attn: Library 1000 Wehrle Drive Clarence, NY 14030	1
Honeywell, Inc. Attn: Library W.B. Ebner Defense Systems Group Power Sources Center 104 Rock Road Horsham, PA 19044	1 1	Yardney Electric Corporation Attn: Library A. Beachielli 82 Mechanic Street Pawcatuck, CT 02891	1 1
Lockheed Missiles and Space Company, Inc. Attn: Library Lockheed Palo Alto Research Laboratory 3251 Hanover Street Palo Alto, CA 94304	1	Battery Engineering Inc. Attn: Dr. N. Marincic Dr. C.R. Schlaikjer 1636 Hyde Park Avenue Hyde Park, MA 02136	1 1
Ballard Research Inc. Attn: Dr. A.C. Harkness 1164 15 St. W North Vancouver, B.C. Canada V7P 1M9	1	Eveready Battery Co. Attn: Dr. G.E. Blomgren 25225 Detroit Road P.O. Box 45035 Westlake, OH 44145	1
Duracell Int., Inc. Attn: B. McDonald Battery Division South Broadway Tarrytown, NY 10591	1		

RAY-O-VAC Attn: R. Foster Udell 101 East Washington Avenue Madison, WI 53703	1	Electrochimica Corporation Attn: Dr. M. Eisenberg 20 Kelly Court Menlo Park, CA 94025	1
TRW Systems Attn: Ed Moon, Rm. 2251 Bldg. O-1 One Space Park Redondo Beach, CA 90278	1	Electrochemistry Consultants Attn: Dr. B.B. Owens 4707 Lyndale Avenue North Minneapolis, MN 55430	1
ALTUS Corporation Attn: G.L. Griffin 1610 Crane Court San Jose, CA 95112	1	Electrochem Industries Attn: Dr. W.D.K. Clark 10,000 Wehrle Drive Clarence, NY 14031	1
SAFT America, Inc. Attn: Dr. R.J. Staniewicz 107 Beaver Court Cockeysville, MD 21030	1	Internal Distribution: E231 E232 R33 R33 (P. Smith) E35 (GIDEP) C72W (Johnson) E22 (Johnston)	2 15 25 20 1 1 1
EG&G Idaho Inc. Attn: G.L. Henriksen P.O. Box 1625 Idaho Falls, ID 83415	1		
General Dynamics Attn: W. Pickwick Mail Stop 493-01-02 P.O. Box 1804 Warren, MI 48090	1		
Combustion Engineering Inc. Attn: D.N. palmer J.E. Brule 1000 Prospect Hill Road Department 9452-510 P.O. Box 500 Windsor, CT 06095-0500	1 1		
W.R. Grace & Co. Attn: Dr. M. Anderman Dr. J.T. Lundquist 7379 Route 32 Columbia, MD 21044	1 1		
Energy Conversion (ECO) Attn: Dr. F.M. Walsh 225 Needham Street Newton, MA 02164	1		